ISAS-INTERNATIONAL SCHOOL
FOR ADVANCED STUDIES

INVARIANTS OF N-DIMENSIONAL PL-MANIFOLDS FROM THE (RE)COUPLING OF ANGULAR MOMENTA

Thesis submitted for the degree of

"Doctor Philosophiæ

CANDIDATE

Gaspare Carbone

SUPERVISOR

Professor M. Carfora

CO-SUPERVISOR

Professor A. Marzuoli

International School for Advanced Studies

SISSA-ISAS

October 2000

TO MY FATHER

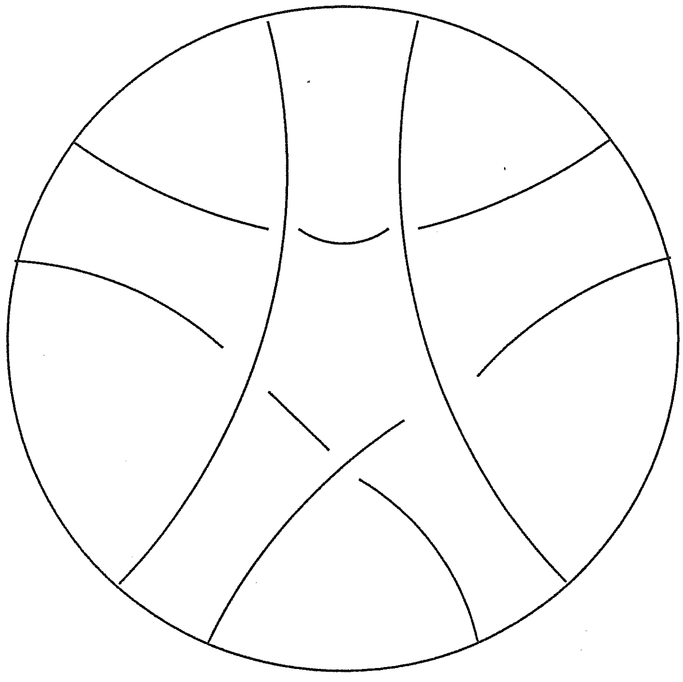

INVARIANTS OF N-DIMENSIONAL PL-MANIFOLDS FROM THE (RE)COUPLING OF ANGULAR MOMENTA

Gaspare Carbone-Ph.D. Thesis

Supervisor: M. Carfora

Co-Supervisor: A. Marzuoli

Abstract.

In this thesis we present classes of state sum models involving triangulations of d-dimensional compact manifolds based on recouplings of angular momenta of SU(2) (and of its q-counterpart $U_q(sl(2))$, q a root of unity). Such classes are arranged in hierarchies depending on the dimensionality of the skeleton of the dual lattice associated with each triangulation, and include all known closed models, namely the Ponzano-Regge state sum and the Turaev-Viro invariant in dimension $d = 3$, the Crane-Yetter invariant in $d = 4$. In general, the recoupling coefficient associated with a d-simplex turns out to be a $\{3(d-2)(d+1)/2\}j$ symbol, or its q-analog. Each of the state sums can be further extended to compact triangulations $(T^d, \partial T^d)$ of a PL-pair $(M^d, \partial M^d)$, where the triangulations of the boundary manifolds are not keeped fixed. In both cases we find out the algebraic identities which translate complete sets of topological moves, thus showing that all state sums are actually independent of the particular triangulations chosen. Then, owing to Pachner's theorems, it turns out that classes of PL-invariant models can be defined in any dimension d.
The continuum theories corresponding to such PL-invariant models are also analyzed. In particular, the classical $SU(2)$ $\{3(d-2)(d+1)/2\}j$-hierarchy for closed manifolds turns out to correspond to a pure BF theory in each dimension d.
Finally, focusing the attention on the Turaev-Viro invariant, we introduce suitable techniques in order to deal with link observables in such a context. As a byproduct of this analysis we find out a quite efficient way for computing explicitly the quantum invariant itself in a number of cases.

Index

1 **Introduction.** **7**

2 **Discretization methods and PL-manifolds.** **13**

3 **An outlook of Racah-Wigner algebra.** **27**

3.1 Wigner D-functions. 27

3.2 Clebsh-Gordan coefficients and 3jm-symbols. 29

3.3 6j symbols. 32

3.4 3nj-symbols. 34

3.5 The graphical method. 35

4 **Invariants of closed M^d from colorings of $(d-1)$-simplices.** **41**

4.1 Definition of the invariant $Z_\chi[M^d]$. 41

4.2 $Z_\chi[M^2]$ and its invariance. 45

4.3 The TQFT associated with $Z_\chi[M^d]$. 47

5 **Invariants of $(M^d, \partial M^d)$ induced by Z_χ^{d-1}.** **50**

5.1 The invariant $Z[(M^3, \partial M^3)]$. 50

5.2 The invariant $Z[(M^4, \partial M^4)]$. 56

5.3 $Z^d[(M^d, \partial M^d)]$ and its equivalence under elementary boundary operations. 61

6 **Invariants of closed M^d from colorings of $(d-2)$-simplices.** **77**

6.1 $Z[M^d]$ and its equivalence under bistellar moves. 77

6.2 Derivation of associated TQFTs. 82

6.2.1 A proof by means of the Freidel-Krasnov discretization method. 83

6.2.2 A proof by means of a generalization of the Ooguri approach. 92

7 Observables in Turaev-Viro model and explicit computation of $Z_{TV}[M^3]$. 106

7.1 Observable and link invariants. 106

7.2 Dehn surgery. 111

7.3 Reformulation of the Turaev–Viro invariant. 113

7.3.1 $S^2 \times S^1$. 114

7.3.2 S^3. 115

7.3.3 The lens space $L(2,1)$ 116

7.3.4 The lens space $L(3,1)$ 117

7.3.5 The lens space $L(n,1)$ 118

7.3.6 Explicit computation of the invariant for the lens space $L(p,h)$ 119

8 Appendices. 125

8.1 Quantum extension. 125

8.2 Explicit calculus of $Z_\chi[M^2]$. 127

8.3 Relations proving the invariance of
$Z[(M^4, \partial M^4)]$ under shellings. 128

8.4 Some remarks on $SU(2)$. 132

8.5 Construction of the auxiliary 2-torus surface. 133

8.6 $Z^3[L(4,1)]$ and $Z^3[L(5,2)]$ reduction. 135

Bibliography 137

Chapter 1

Introduction.

The search for combinatorial invariants of compact d-dimensional manifolds (especially in $d = 3, 4$) plays a key role both in topological lattice field theories and in quantum gravity discretized according to Regge's prescription [1]. From a historical point of view, the typical examples of this class of models in dimension three are provided in [2] and in [3] (further developments can be found in [4], [5], [6], [7] and in [8] for what concerns in particular a categorical approach to the subject).

As a matter of fact, all the papers quoted above deal essentially with state sum invariants for a closed 3 or 4-dimensional manifold. The interest in dealing with a d-dimensional compact pair $(M^d, \partial M^d)$ (where ∂M^d is the $(d-1)$-dimensional boundary manifold of M^d) relies on the fact that in typical physical situations we have to consider probability amplitudes between different $(d-1)$-dimensional Riemannian geometries which represent the boundary of an d-dimensional (pseudo)Riemannian manifold. (We notice in particular that invariants for PL-pairs appear also in the loop quantum gravity approach, see *e.g.* [9], [10] and references therein).

Borrowing the language from the Euclidean functional integral approach to the quantization of gravity, we have to evaluate quantities such as $< (N_1, h_1) \mid \mathcal{O} \mid (N_2, h_2) > / < (N_1, h_1) \mid (N_2, h_2) >$, where (N_1, h_1) and (N_2, h_2) are $(d-1)$-dimensional manifolds equipped with fixed Riemannian metrics h_1 and h_2 respectively, and $\mathcal{O}$ is some observable. The symbol $< \mid >$ denotes a functional integration over (a suitable class of) d-dimensional Riemannian metrics, up to diffeomorphisms, interpolating between (N_1, h_1) and (N_2, h_2). If we are interested in studying either the topological sector of quantum gravity or just a topological model, the requirement of taking fixed geometries on the boundaries appears to be much too restrictive. Indeed, a topological d-dimensional field theory, when *restricted* to a $(d-1)$-dimensional boundary, keeps on taking its topological character (namely, it is independent from the metric on the boundary as well), and thus topological (or PL) invariants of pairs $(M^d, \partial M^d)$ induce necessarily invariants on the boundary components. On the other hand, we shall see how it is possible to extend classes of PL invariants for closed manifolds in order to get associated invariants for pairs. Namely, we shall find out a sort of holography principle regulating the relations between PL invariants in contiguous dimensions.

The general setting of this plan can be summarized as follows:

- *step 1)* Given a (suitable defined) PL-invariant state sum $Z[M^{d-1}]$ for a closed $(d-1)$-dimensional PL-manifold M^{d-1}, we extend it to a state sum for a pair $(T^d, \partial T^d \equiv T^{d-1})$. This is achieved by assembling in a suitable way the *squared roots* of the symbols associated with the fundamental blocks in $Z[M^{d-1}]$ in order to pick up the recoupling symbol to be associated with the d-dimensional simplex; the dimension of the $SU(2)$-labelled (or the q-colored) $(d-2)$-simplices is keeped fixed when passing from T^{d-1} to $T^d \supset T^{d-1}$.

- *step 2)* The state sum for $(T^d, \partial T^d)$ gives rise to a PL-invariant $Z[(M^d, \partial M^d)]$ owing to the fact that we can exploit a set of topological moves, the *elementary shellings* of Pachner [11] (the algebraic identities associated with such moves in $d = 3$ were established in [12] and [13]).

- *step 3)* From the expression of $Z[(M^d, \partial M^d)]$ we can now extract a state sum for a *closed* triangulation T^d. The proof of its PL-invariance relies now on the algebrization in any dimension d of the *bistellar moves* introduced in [14]. The procedure turns out to be consistent with known results in dimension 3 (see [2], [3] and [7]) and in dimension 4 (see [6] and [15]), and provides us with a PL-invariant $Z[M^d]$ where each d-simplex in T^d is represented by a $\{3(d-2)(d+1)/2\}j$ recoupling coefficient of $SU(2)$ (or by the corresponding q-analog).

The scheme we have outlined above gives us an algorithmic procedure for generating (different kinds of) invariants for closed manifolds in contiguous dimensions, namely $Z[M^{d-1}] \to Z[M^d]$.

Furthermore, the (multi)–hierarchic structure underlying these classes of invariants is sketched below as an array:

$$\begin{array}{rcccccc}
\textit{dimension}: & 2 & 3 & 4 & \dots & d & d+1 \\
 & Z^2_\chi & Z^3_{PR} & & & & \\
 & & Z^3_\chi & Z^4_{CY} & & & \\
 & & & Z^4_\chi & \ddots & & \\
 & & & & \ddots & \ddots & \\
 & & & & & Z^d_\chi & Z^{d+1} \\
 & & & & & & Z^{d+1}_\chi
\end{array}$$

The quantities $Z^d_\chi \equiv Z_\chi[M^d]$ on the first diagonal of the array, which we referred to in *step 1)*, are invariants depending upon the Euler characteristic of the closed manifold M^d; they can be defined both in the classical case of $SU(2)$ and in the case $q \neq 1$,(in this last case the notation $Z^d_\chi(q)$ should be more suitable). They are obtained in any dimension d by labelling the $(d-1)$-simplices of the triangulations with the ranks of $SU(2)$ representations, $j = 0, 1/2, 1, 3/2, \dots$ (see *Appendix 8.1* for the general definition in the q-case). Notice that these invariants are in fact trivial in dimension $d = 2n+1$ since here we are dealing exclusively with manifolds.

The hierarchy on the second diagonal of the array includes classical PL-invariants $Z^d \equiv Z[M^d]$ involving products of $\{3(d-2)(d+1)/2\}j$ symbols of $SU(2)$ as we said in *step 3)*. In this case the labelling j have to be assigned to the $(d-2)$-simplices of each triangulation (namely edges in $d = 3$, triangles in $d = 4$, and so on). Thus we recover the Ponzano–Regge model Z^3_{PR} and the Ooguri–Crane–Yetter invariant $Z^4_{CY}(q = 1)$; the other invariants are new. A similar remark holds true also in the q-deformed context, where the hierarchy would be rewritten in terms of the counterparts $Z^d(q) \equiv Z[M^d](q)$ (and in particular we found the Turaev–Viro invariant in $d = 3$, see [3]).

Coming back to the relations between invariants lying in the same row of the array, they can be further analyzed in view of the extension of each $Z[M^d]$ to $Z[(M^d, \partial M^d)]$. Thus the first row can be read as a PR-model with Z^2_χ on its boundary, the second row as a CY-model with Z^3_χ on its boundary, while the other rows display new invariants for PL-pairs in each dimension.

As a consequence of the above remarks, the whole table (together with a similar q-table) can be reconstructed row by row just from the explicit form of the invariant Z^d_χ. Then, in a sense, it is not surprising that the invariant Z^4_{CY}, having on its boundary $Z^3_\chi = const.$ for any choice of ∂M^4, turns out to be simply the discretized version of a combination of signature and Euler characteristic of M^4 (see [16]). On the other hand, the invariants Z^3, which are generated by non–trivial Z^2_χ, are related to Reidmeister torsion (see *e.g.* [17]).

The proper way to investigate the nature of the invariants in $d = 2n$ and $d = 2n + 1$ is by no doubts the search for explicit correspondences with some $TQFT$s. For what concerns again the three dimensional case, the relation between either Z^3 or $Z^3(q)$ and the generating functional of a suitable a suitable $TQFT$ has been extensively discussed by Turaev in [18], [17], by Roberts in [16], [19], [20], by Beliakova and Durhuus (by means of the spin network formalism) in [21], by Mizoguchi and Tada (by considering the perturbative development of the quantum 6j–symbols around the value $q = 1$) in [4], and by Kauffman and Lins (by using the Temperly–Lieb recoupling theory) in [22]. The four dimensional case corresponding to the invariant $Z^4(q)$ has been addressed by Roberts in [19] and by Broda in [23] [24] [25]. It turns out that, in both these dimensions and for the quantum case, the associated TQFT is a BF theory with a cosmological constant term, the parameter Λ of which is equal to $1/k$ in $d = 3$, and to $1/k^2$ in $d = 4$, where k is the deformation parameter of the quantum group. Then in the limit $k \to \infty$ we obtain in a quite straightforward way that the *classical* invariants in $d = 3, 4$ actually correspond to *pure* BF theory. A short list of references about the general setting of BF theories and about their connections with related fields should include at least [26], [27], [28], [29] [30], [31], [32], [33], [34], [35], [36] .

In order to address the problem of the correspondence between our classical PL invariant models and (pure) BF theories in higher dimensional cases, we realize that two different approaches can indeed be used. Firstly, we may start from the discretized procedure of BF theories proposed by Freidel and Krasnov in [37], and then, by using the machinery of angular momentum theory, recover the symbol associated with a d-simplex in the spin model. The second possibility relies on the generalization in any dimension d of the Ooguri procedure established in [5] to address the three dimensional case.

Similar remarks and (possibly) similar methods apply also to our quantum invariants, which should be discretized versions of BF theories with suitable constraint terms in each dimension. We are currently investigating such issues, see [38].
The strong evidence about the existence of a direct correspondence between combinatorial and continuum models in any dimension opens new perspectives in both classes of theories. As a further example of fruitful interplay among different approaches in geometric topology, in the final part of the thesis we will analyze in detail the structure of the Turaev-Viro invariant.

The thesis is organized as follows.
In the following two chapters we collect all we need about PL topology (Chapter 2) and the (re)coupling theory of angular momenta of $SU(2)$ (Chapter 3).
The content of Chapters 4, 5 and Section 6.1 is based on the papers quoted in [12], [13] and [39]. In particular, in Chapter 4 we define the PL invariants Z^d_χ which appear in the first diagonal of the array displayed above, and we evaluate their expressions in the q-deformed case. The corresponding TQFT is also considered. In Chapter 5 we discuss the classical invariants for pairs $(M^d, \partial M^d)$, having Z^{d-1}_χ on their boundary manifolds (the quantum counterparts can be easily found as indicated in Appendix 8.1). In Section 6.1 we show that the state sums for closed manifolds generated by the previous ones are actually PL invariants (collected in the second diagonal of our array).
The content of Section 6.2 will appear in [38] and concerns the correspondence between our classical PL invariants and pure BF theories following the arguments outlined before.
In Chapter 7 (based on [40]) we introduce observables and links in the Turaev-Viro model. After a brief review on surgery operations on 3-manifolds, we are able to rewrite the state sum in terms of Heegard splittings. In this way we obtain a new diagrammatical representation of the state sums associated to lens spaces and we give their explicit expressions in terms of $3nj$ symbols.
Finally, in Chapter 8 we collect some appendices containing technical details.

Acknowledgements

I want to thank my Supervisors Mauro Carfora and Annalisa Marzuoli. I would have never completed this thesis without their guidance, their encouragement and their help to draft the manuscript.

Chapter 2

Discretization methods and PL-manifolds.

In this chapter we collect some basic definitions and theorems on Piecewise-Linear (PL) topology (we refer the reader to e.g. [41], [42] for more details on the general part concerning simplicial complexes, polyhedra, dual complexes and so on). In particular, we focus our attention on the issue of combinatorial (or PL) equivalence of d dimensional compact simplicial PL manifolds which will be extensively addressed in connection with the search for new PL-invariants from the (re)coupling of angular momenta. Recent result due to Pachner (see [43]) provide us with a general framework to deal with such kind of questions. This is achieved by exploiting suitable sets of topological operations on simplices, namely the bistellar moves in the case of closed manifolds and the elementary shellings in the case of manifolds with a non-empty boundary.

By a p-simplex $\sigma^p \equiv (x_0, x_1, \dots, x_p)$ with vertices $x_0, x_1, \dots, x_p$ we mean the subspace of $\mathbb{R}^d (d > p)$ defined by $\sigma^p \doteq \sum_{i=1}^{p} \lambda_i x_i$, where $(x_0, x_1, \dots, x_p)$ are $(p+1)$ points in general position in $\mathbb{R}^d$ with $\sum_i \lambda_i = 1$ and $\lambda_i \geq 0, \forall i$.

Definition 1 *Let σ^p and τ^q be simplices in $\mathbb{R}^d$ with distinct vertices and such that the totality of these vertices is at most $(d+1)$ and they are in general position in $\mathbb{R}^d$. Then such vertices span a simplex, $\sigma^p \star \tau^q$, the join of σ^p and τ^q, defined as the $(p+q+1)$-simplex obtained by taking the convex hull in $\mathbb{R}^d$, viz.:*

$$\sigma^p \star \tau^q \;\doteq\; conv(\sigma^p \cup \tau^q). \tag{2.1}$$

A *face* of a p-simplex σ^p is any simplex the vertices of which are a subset of those of σ^p.

Definition 2 *A finite simplicial complex T (or, more precisely, the geometrical realization of an abstract simplicial complex) is a finite collection of simplices in $\mathbb{R}^d$ such that:* i) *if $\sigma^p \in T$, then so are all of its faces;* ii) *if $\sigma^p, \tau^q \in T$ then $\sigma^p \cap \tau^q$ is either a (common) face or is empty.*
T has dimension d if d is the maximum dimension of its faces. The faces of maximal dimension, σ^d, are called facets of T.

Definition 3 *If T_1 and T_2 are simplicial complexes, then the join of T_1 with T_2 is defined according to:*

$$T_1 \star T_2 \doteq \{\sigma_1 \star \sigma_2 \ s.t. \ \sigma_1 \in T_1, \sigma_2 \in T_2\} \tag{2.2}$$

where $\sigma_1 \star \sigma_2$ is given in Definition 1. In particular, the join of a complex T with the empty simplex gives $T \star \{\emptyset\} = T$, while the join of T with the empty complex gives $T \star \emptyset = \emptyset$. (Notice that in the following also the join of a complex T with a simplex τ will be denoted by $T \star \tau$ for short).

A simplicial complex is *pure* provided that all its facets have the same dimension.
The *boundary complex* of a pure simplicial d-complex T is denoted by ∂T and it is the subcomplex of T the facets of which are the $(d-1)$-faces of T which are contained in only one facet of T. The set of the interior faces of T is denoted by $int(T) \doteq T \setminus \partial T$.
If σ is a simplex, then by $\mathcal{B}(\sigma)$ we mean the complex made up by all the faces of σ, except σ itself. Moreover

$$\mathcal{F}(\sigma) \doteq \mathcal{B}(\sigma) \cup \{\sigma\} \tag{2.3}$$

is the complex made up by σ and all its proper faces.

Given a (finite) simplicial complex T, consider the set theoretic union $|T| \subset \mathbb{R}^d$ of all simplices from T, namely

$$|T| \doteq \cup_{\sigma \in T} \sigma. \tag{2.4}$$

Introduce on the set $|T|$ a topology that is the strongest of all topologies in which the embedding of each simplex into $|T|$ is continuous (the set $A \subset |T|$ is closed iff $A \cap \sigma^p$ is closed in σ^p for any $\sigma^p \in T$). The topological space $|T|$ is the underlying *polyhedron*, geometric carrier of the simplicial complex T; the polyhedron $|T|$ is said to be triangulated by the simplicial complex T. More generally, a *triangulation* of a topological space M is a simplicial complex T together with a homeomorphism $|T| \to M$.

Definition 4 *A simplicial map $f : T_1 \to T_2$ between two simplicial complexes T_1, T_2 is a continuous map $f : |T_1| \to |T_2|$ between the corresponding underlying polyhedra which takes p-simplices to p-simplices for all p.*
The map f is a simplicial isomorphism if $f^{-1} : T_1 \to T_2$ is also a simplicial map.

A *subdivision* T' of T is a simplicial complex such that: *i)* $|T'| \cong |T|$, where $\cong$ denotes a homeomorphism between topological spaces; *ii)* each p-simplex of T' is contained in a p-simplex of T, for every p. A property of a simplicial complex T which is invariant under subdivisions is a *combinatorial* (or *Piecewise Linear*) property of T. More precisely:

Definition 5 *A PL-homeomorphism*

$$f \, : \, T_1 \longrightarrow T_2 \tag{2.5}$$

between two simplicial complexes (of the same dimension) is a map which is a simplicial isomorphism for some subdivisions T_1' and T_2' of T_1 and T_2 respectively.

Definition 6 *A PL-manifold of dimension d is a polyhedron $M \cong |T|$, each point of which has a neighborhood, in M, PL-homeomorphic to an open set in $\mathbb{R}^n$.*

PL-manifolds are realized by simplicial manifolds under the equivalence relation generated by PL-homeomorphisms according to the following:

Definition 7 *Two PL-manifolds* $M_1 \cong |T_1|$ *and* $M_2 \cong |T_2|$ *are PL-homeomorphic, or*

$$M_1 \cong_{PL} M_2 \tag{2.6}$$

if there exists a map $g : M_1 \to M_2$ *which is both a homeomorphism and a simplicial isomorphism, in the sense of Definition 5.*

In what follows we shall use the notation

$$T \longrightarrow M \cong |T| \tag{2.7}$$

to denote a *particular triangulation* of the closed PL-manifold M and, when dealing with a PL-pair $(M, \partial M)$, we shall write:

$$(T, \partial T) \longrightarrow (M, \partial M) \cong (|T|, |\partial T|) \tag{2.8}$$

where the triangulation on ∂M is the unique triangulation induced on it by the chosen triangulation T in M. The extension of Definitions 5, 6 and 7 to PL-pairs is quite straightforward and can be found *e.g.* in [42]. Recall also (see *e.g.* [44]) that a sufficient condition for characterizing a triangulated space as a PL-manifold follows from the:

Theorem 1 *A simplicial d-complex* K *is a (simplicial) PL-manifold of dimension d if, for all p-simplices* $\sigma^p \in K$*, the link of* σ^p*,* $link(\sigma^p; K)$*, has the topology of the boundary of the standard* $(d-p)$*-simplex, namely if:* $link(\sigma^p; K) \cong \mathbb{S}^{d-p-1}$ *(the* $(d-p-1)$*-dimensional sphere).*

In the above statement, $link(\sigma^p; K)$ is the union of all faces τ of all simplices in the star of σ satisfying $\sigma \cap \tau = \emptyset$ (the star of σ in K is simply the union of all simplices of which σ is a face).

The point that we are going to examine now concerns PL-equivalence of polyhedra. Notice that Definition 7 turns out to be quite difficult to be handled with in practice, since one should go over and over through subdivisions in order to find out isomorphic triangulations. The issue of *combinatorial equivalence* was first addressed by Alexander in [45].

Definition 8 *Let $T \to M$ be a triangulation of a PL d-manifold and let $\emptyset \neq A \in T$ such that $link(A;T) = \mathcal{B}(B) \star \mathcal{L}$, where $B \neq \emptyset$ is a simplex not contained in T. Then the transformation*

$$k_{(A,B)}T := (T \backslash A \star \mathcal{B}(B) \star \mathcal{L}) \cup \mathcal{B}(A) \star B \star \mathcal{L}$$

is a stellar exchange where $\star$ is the join .

In the case of $dimB = 0$, i.e. $B = \{b\}$ is a new vertex, the operations $k_{(A,B)} =: \sigma_{(A,B)} =: \sigma_A$ are called stellar subdivisions. Here $A \in \partial T$ or $A \in int(T)$ respectively, depending on whether $\mathcal{L}$ is a ball or a sphere. Conversely, $k^{-1}_{(A,B)} = \sigma_B^{-1}$ is an inverse stellar subdivision in the case of $dimA = 0$. The definition of stellar subdivision and their inverses are still applicable to arbitrary simplicial complexes.

Alexander proved the following theorem (which indeed holds true for more general complexes too):

Theorem 2 *For any polyhedron M which is dimensionally homogeneous (viz., its underlying simplicial complex is pure) any two triangulations of M can be transformed one into the other by a finite sequence of stellar subdivisions and their inverse transformations.*

The stellar subdivisions, typically known also as *Alexander's transformations* (or moves), are not elementary, in the sense that each one of them involves a variable number of d-simplices of the triangulation T we are considering. Thus, being interested in transformations between different triangulations of a PL-manifold M, one should implement Alexander's moves over a lot of local arrangements of simplices which cannot be factorized into simpler blocks. On the other hand, owing to Theorem 2, PL-manifolds are mapped homeomorphically into PL-manifolds, and moreover all admissible triangulations of a given M are related to each other by a suitable sequence of Alexander's moves. The way out from this situation is to look for a different set of moves, which are both elementary (*i.e.* they involve just a fixed number of simplices in any dimension d) and equivalent to Alexander's transformations, namely topology–preserving and ergodic (*i.e.* they must span all the possible triangulations of a given M). A set of moves that shares these requirements for the case of *closed* d-dimensional PL-manifolds has been found by Pachner: the *bistellar elementary operations* (see [14] and also Appendix A of [46] for an account on this subject in connection with simplicial quantum gravity models in $d = 3, 4$).

Definition 9 *Let $T \to M$ be a triangulation of a PL d-manifold, such that, for $\emptyset \neq A \in T$ and $B \neq \emptyset$ a simplex not contained in T, we have $dimA + dimB = d$ (i.e. $\mathcal{L} = \{\emptyset\}$ in Def. (8)). Then $k_{(A,B)} =: \chi_{(A,B)} =: \chi_A$ is a bistellar k-operation if $dimA = k$.*

Obviously we have $\chi^{-1}_{(A,B)} = \chi_{(B,A)}$. The corresponding equivalence relation between the triangulations is denoted by '$\approx_{bst}$'. If $dimB \geq 1$, $B = \rho \star B'$, then $\chi_{(A,B)}$ is uniquely determined by ρ and by the facet $F =: A \star B'$ of M.

The statement of the main theorem in [43] can be rewritten in our notation as:

Theorem 3 *Let $T_1 \to M_1$, $T_2 \to M_2$ be triangulations of compact d-dimensional manifolds respectively. Then M_1 and M_2 are PL-homeomorphic if and only if T_1 and T_2 are equivalent under bistellar moves*

$$|T_1| \cong_{PL} |T_2| \iff (T_1) \approx_{bst} (T_2)$$

Pachner has introduced also a set of moves which are suitable in the case of compact d-dimensional PL-manifolds with a non–empty boundary, the *elementary shellings* (see [11] and [43]). As the term "elementary shelling" suggests, this kind of operation involves the cancellation of one d-simplex (facet) at a time in a given triangulation $(T, \partial T) \to (M, \partial M)$ of a PL-pair of dimension d. In order to be deleted, the facet must have some of its faces lying in the boundary ∂T. Moreover, using Definition 1, we may decompose a facet of this kind (considered now as a complex) into the join of two suitable faces belonging to it. This decomposition is obviously not unique, although in each dimension d there are only a finite number of possibilities of carrying it out (up to a relabelling of the faces of a given dimension).

Definition 10 *Let $(T, \partial T) \to (M, \partial M)$ be a triangulation of a PL-pair of dimension d and let σ^d be a facet decomposed according to:*

$$\sigma^d = \tau \star \sigma^r \tag{2.9}$$

where τ is a face of σ^d of dimension $p \geq 0$ such that $\tau \in int(T)$, and the second factor represents a face of σ^d of dimension $r \geq 0$ with the following property:

$$\mathcal{B}(\tau) \star \sigma^r \subseteq \partial T, \tag{2.10}$$

where $\mathcal{B}(\tau)$ is the complex made up by all the faces of τ except τ itself.

Then an elementary r-shelling of $(T, \partial T)$ is defined according to:

$$\varrho_{-\sigma^d}\,(T, \partial T) \doteq (T, \partial T) \setminus \{\mathcal{F}(\tau) \star \sigma^r\} \equiv (\tilde{T}, \partial\tilde{T}) \tag{2.11}$$

where $\mathcal{F}(\tau)$ is given in (2.3).

Notice that the dimension p of τ is given, in terms of d and r, by $p = d - r - 1$; moreover, if τ is a 0-simplex then $\mathcal{B}(\tau) = \emptyset$ and the remark at the end of Definition 3 has to be kept in mind.

The inverse operation amounts to add a new facet to $(\tilde{T}, \partial\tilde{T})$ along some faces in $\partial\tilde{T}$, and can be simply defined as:

$$\varrho_{+\sigma^d}\,(\tilde{T}, \partial\tilde{T}) \doteq (\varrho_{-\sigma^d})^{-1}\,(\tilde{T}, \partial\tilde{T}) \tag{2.12}$$

If we set $\varrho^+ \equiv \varrho_{+\sigma^d}$ and $\varrho^- \equiv \varrho_{-\sigma^d}$ for some facet (or missing facet) σ^d, we can establish an equivalence relation between triangulations according to:

Definition 11 *Two triangulations $(T, \partial T)$ and $(\tilde{T}, \partial\tilde{T})$ are said to be equivalent under elementary shellings if, and only if, they are connected by a finite number of elementary boundary operations, namely:*

$$(T, \partial T) \approx_{sh} (\tilde{T}, \partial\tilde{T}) \iff (\tilde{T}, \partial\tilde{T}) = \varrho_k^{\pm} \cdots \varrho_1^{\pm}\,(T, \partial T) \tag{2.13}$$

where $\varrho^{\pm}$ are defined in (2.12) and (2.11) respectively and k is an integer.

Remark 1

It may happen that there exists one face $\tau \in int(T)$ and different faces, say σ_1^r and σ_2^r, with both $\mathcal{B}(\tau) \star \sigma_1^r$ and $\mathcal{B}(\tau) \star \sigma_2^r$ in ∂T and such that $\sigma^d = \tau \star \sigma_1^r$, $\sigma^d = \tau \star \sigma_2^r$ for a fixed σ^d. However, for each σ^r belonging to ∂T, there exists at most one $\tau \in int(T)$ such that: *i)* $\tau \star \sigma^r$ is a facet; *ii)* $\mathcal{B}(\tau) \star \sigma^r \subseteq \partial T$. Hence the elementary operation $\varrho_{-\sigma^d}$ defined in (2.11) in uniquely determined by σ^r, and the set of the possible elementary shellings (performed on a single facet) is equal to the dimension d of the facet itself, since $r = 0, 1, \ldots, d-1$.□

The statement of the main theorem in [43] can be rewritten in our notation as:

Theorem 4 *Let $(T_1, \partial T_1) \to (M_1, \partial M_1)$ and $(T_2, \partial T_2) \to (M_2, \partial M_2)$ respectively be triangulations of compact d-dimensional manifolds with boundary. Then $(M_1, \partial M_1)$ and $(M_2, \partial M_2)$ are PL-homeomorphic if, and only if, $(T_1, \partial T_1)$ and $(T_2, \partial T_2)$ are equivalent under elementary shellings, namely:*

$$|(T_1, \partial T_1)| \cong_{PL} |(T_2, \partial T_2)| \iff (T_1, \partial T_1) \approx_{sh} (T_2, \partial T_2) \tag{2.14}$$

where $|(T_1, \partial T_1)| \cong (M_1, \partial M_1)$, $|(T_2, \partial T_2)| \cong (M_2, \partial M_2)$ and the equivalence $\approx_{sh}$ is explained in Definition 11.

Notice that in one direction ($\Leftarrow$) the result is quite straightforward and moreover, as a particular application, we may consider different triangulations $(T, \partial T), (\tilde{T}, \partial\tilde{T})$ of the same PL-pair $(M, \partial M)$.

Pachner has also proved a weaker version of the above result in [11], namely

Theorem 5 *Let $(T_1, \partial T_1) \to (M_1, \partial M_1)$ and $(T_2, \partial T_2) \to (M_2, \partial M_2)$ be triangulations of PL, compact d-dimensional pairs. Then:*

$$|(T_1, \partial T_1)| \cong_{PL} |(T_2, \partial T_2)| \iff (T_1, \partial T_1) \approx_{sh,bst} (T_2, \partial T_2) \tag{2.15}$$

where the equivalence $\approx_{sh,bst}$ is both under elementary shellings and under bistellar operations on d-simplices in $int(T_1)$ or $int(T_2)$.

Remark 2

The advantage of having to deal with elementary shellings is quite evident (although we shall use also Theorem 5 when handling our combinatorial invariants). Moreover, there exists a correspondence between bistellar moves in dimension d and elementary shellings in dimension $(d-1)$;

more precisely, each shelling realizes a particular type of bistellar on the boundary, and remembering that in the d dimensional case we have d shellings (and d inverse shellings) and exactly d bistellar on the $d-1$ dimensional boundary (including their inverse), it can be shown that the above correspondence is in fact one to one. We shall return on this point when dealing with our PL invariants in Chapters 5 and 6. In this respect, notice that Theorem 4 represents exactly the counterpart of Theorem 3 for closed $(d-1)$-PL-manifolds.□

In order to deal with the different sets of moves introduced above, we are going now to simplify our previous notations. If we denote by n_d the number of d-simplices $\in T^d$ involved in a given *bistellar operation*, then such a move will be represented with the notation

$$[n_d \rightarrow (d+1)-(n_d-1)]^{\mathbf{d}}_{bst} \tag{2.16}$$

Here the action of the move is made manifest since n_d d-simplices (glued together to form a PL ball) are transformed into new PL ball made up by $(d+1-(n_d-1))$ σ^d. The two configurations have the same boundary PL sphere, and the entire set of allowed moves in dimension d is found for $n_d = 1, 2, \ldots, d+1$.

Both for the *elementary shellings* (2.11), and for their inverse operations suitable notations read:

$$[n_{d-1} \rightarrow d-(n_{d-1}-1)]^{\mathbf{d}}_{sh} \quad , \quad [n_{d-1} \rightarrow d-(n_{d-1}-1)]^{\mathbf{d}}_{ish} \ , \tag{2.17}$$

where n_{d-1} represents the number of $(d-1)$-simplices (belonging to a single d-simplex) involved in an elementary shelling and in an inverse shelling, respectively. Then the full set of operations is found when n_{d-1} runs over $(1, 2, \ldots, d)$ in both cases.

Example: Bistellar moves in $d = 3$

Let $T \rightarrow M$ represent a triangulation of a closed 3-dimensional PL manifold. Let $A \in T$ be a subsimplex of the triangulation with $dimA = r$ (from Definition 2 we can restrict our attention to subsimplices), and let B be a simplex not belonging to T with $dimB = k$. Then we can classify the bistellar moves according to the dimensionality of A, namely

1. **TYPE I** ($r = 3$). The subsimplex A is a tetrahedron $\sigma^3_{(I)}$ while, from the relation $k+3 = 3$, B is a point $\hat{\sigma}^0_{(I)} \notin T$. The joint $A \star \partial B$ is equivalent to $\sigma^3_{(I)}$; the join $B \star \partial A$ is represented by four tetrahedra, glued among them, sharing the vertex $\hat{\sigma}^0_{(I)}$; its free faces coincide with $\partial\sigma^3_{(I)}$. The bistellar of type I is represented explicitly by the map

$$[1 \to 4]^3_{bst} := K^I : T \to (T \backslash \hat{\sigma}^0_{(I)} \star \sigma^3_{(I)}) \cup (\sigma^0_{(I)} \star \partial\hat{\sigma}^0_{(I)}) \tag{2.18}$$

2. **TYPE II** ($r = 2$). The subsimplex A is the triangle $\sigma^2_{(II)}$, hence B is an edge $\hat{\sigma}^1_{(II)} \notin T$. The joint $A \star \partial B$ is equivalent to two tetrahedra sharing the face $\sigma^2_{(II)}$ and whose opposite vertices are the boundary of $\hat{\sigma}^1_{(II)}$; the join $B \star \partial A$ represents three tetrahedra, sharing the edge $\hat{\sigma}^1_{(II)}$; each one of them has two free faces, one for each initial tetrahedra, sharing an edge of $\partial\sigma^2_{(II)}$. The bistellar of type II is represented by the map:

$$[2 \to 3]^3_{bst} := K^{II} : T \to (T \backslash \sigma^2_{(II)} \star \partial\hat{\sigma}^1_{(II)}) \cup (\hat{\sigma}^1_{(II)} \star \partial\sigma^2_{(II)}) \tag{2.19}$$

3. **TYPE III** ($r = 1$). The subsimplex A is an edge $\sigma^1_{(III)}$ while B is a triangle $\hat{\sigma}^2_{(III)} \notin T$. The joint $A \star \partial B$ is equivalent to three tetrahedra glued along the line $\sigma^1_{(III)}$, and with the free faces of each one glued along an element of $\partial\hat{\sigma}^2_{(III)}$; $B \star \partial A$ are two tetrahedra, glued along the triangle $\hat{\sigma}^2_{(III)}$, and with opposite vertices on the boundary of $\sigma^1_{(III)}$. The bistellar of type III is represented by the map:

$$[3 \to 2]^3_{bst} := K^{III} : T \to (T \backslash \sigma^1_{(III)} \star \partial\hat{\sigma}^2_{(III)}) \cup (\hat{\sigma}^2_{(III)} \star \partial\sigma^1_{(III)}). \tag{2.20}$$

   Notice that it is the inverse map of $[2 \to 3]^3_{bst}$.

4. **TYPE IV** ($r = 0$). The subsimplex A is a point $\sigma^0_{(IV)}$ and B is a tetrahedron $\hat{\sigma}^3_{(IV)} \notin T$. The joint $A \star \partial B$ is equivalent to four tetrahedra sharing the vertex $\sigma^0_{(IV)}$ and whose free faces realize $\partial\hat{\sigma}^3_{(IV)}$; the join $B \star \partial A$ is the tetrahedron $\sigma^3_{(IV)}$. The bistellar of type IV is represented explicitly by the map:

$$[4 \to 1]^3_{bst} := K^{IV} : T \to (T \backslash \sigma^0_{(IV)} \star \partial\hat{\sigma}^3_{(IV)}) \cup (\hat{\sigma}^3_{(IV)} \star \partial\sigma^0_{(IV)}). \tag{2.21}$$

   Which is is the inverse map of $[1 \to 4]^3_{bst}$.

The pictures showing the actions of these moves are given in Fig. 2.1.□

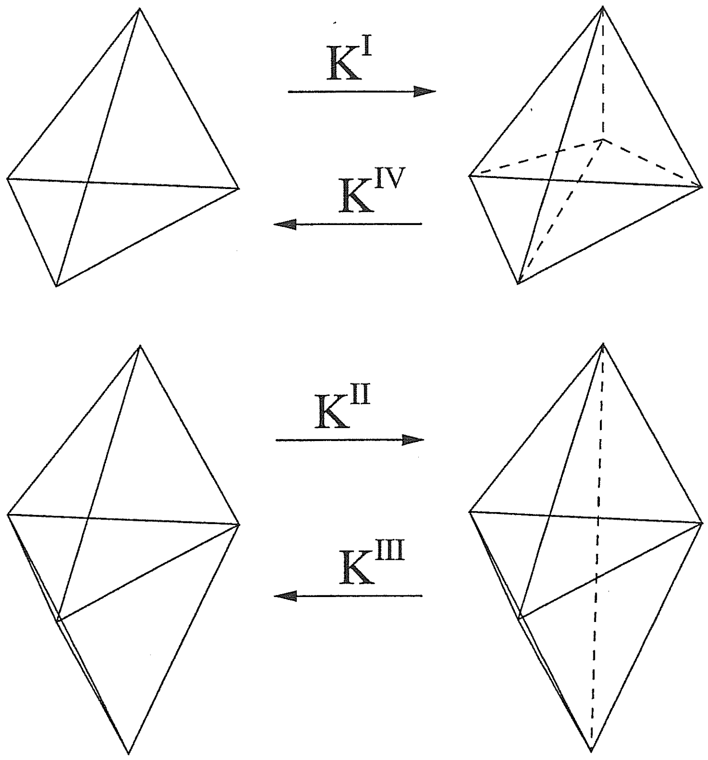

Fig. 2.1: Bistellar moves in $d = 3$.

Example: elementary shellings in $d = 3$

Let $(T, \partial T) \to (M, \partial M)$ represent a triangulation of a 3-dimensional PL-pair and let σ^3 be a facet with some component in ∂T. According to Definition 10 we can write:

$$\sigma^3 = \tau \star \sigma^r \ (r = 0, 1, 2) \tag{2.22}$$

where $\tau \in int(T)$ and $\sigma^r \in \partial T$. As we noticed in *Remark 1*, for every $\sigma^r \in \partial T$ there exists at most one $\tau \in int(T)$ which satisfies (2.22). Then we can classify the possible facets and the corresponding elementary shellings according to the dimensionality of σ^r and using (2.11) (these different configurations are depicted in the Figures (5.2), (5.3), (5.1) of chapter 5).

1. **TYPE I** ($r = 0$). The facet $\sigma^{3(I)}$ admits the decomposition $\sigma^{3(I)} = \tau^{(I)} \star \sigma^0$, where $\tau^{(I)}$ is a 2-simplex and belongs to $int(T)$. The vertex σ^0 and the three 2-dimensional faces of $\sigma^{3(I)}$

which have σ^0 as a common subsimplex are in ∂T. The shelling of $\sigma^{3(I)}$ is represented by the map:

$$[1 \to 3]^3_{sh} := \varrho^{-(I)} : (T, \partial T) \longrightarrow (T, \partial T) \setminus \{\mathcal{F}(\tau^{(I)}) \star \sigma^0\} \tag{2.23}$$

2. **TYPE II** ($r = 1$). The facet $\sigma^{3(II)}$ admits the decomposition $\sigma^{3(II)} = \tau^{(II)} \star \sigma^1$, where $\tau^{(II)}$ is a 1-simplex and belongs to $int(T)$. The 1-simplex σ^1 and the two 2-dimensional faces of $\sigma^{3(II)}$ which have σ^1 as a common subsimplex are in ∂T. The shelling of $\sigma^{3(II)}$ is represented by the map:

$$[2 \to 2]^3_{sh} := \varrho^{-(II)} : (T, \partial T) \longrightarrow (T, \partial T) \setminus \{\mathcal{F}(\tau^{(II)}) \star \sigma^1\} \tag{2.24}$$

3. **TYPE III** ($r = 2$). The facet $\sigma^{3(III)}$ admits the decomposition $\sigma^{3(III)} = \tau^{(III)} \star \sigma^2$, where $\tau^{(III)}$ is a vertex and belongs to $int(T)$. The 2-simplex σ^2 is in ∂T. The shelling of $\sigma^{3(III)}$ is represented by the map:

$$[3 \to 1]^3_{sh} := \varrho^{-(III)} : (T, \partial T) \longrightarrow (T, \partial T) \setminus \{\mathcal{F}(\tau^{(III)}) \star \sigma^2\} \tag{2.25}$$

The inverse elementary shellings $\varrho^{+(I)}$, $\varrho^{+(II)}$ and $\varrho^{+(III)}$ are nothing but maps which are the inverse operations with respect to the former ones, and represent attachments of 3-simplices of types I, II, III respectively.□

Associated with simplicial d-dimensional PL space we can consider also the so called dual complex, which is the natural generalization of the Voronoi construction of the dual lattice for a random lattice in Euclidean space. An intuitive (but not fully rigorous) definition is as follows: to any given p-dimensional subsimplex σ we associate the flat $(d-p)$-dimensional dual polytope σ^* that consists of all the points which are at equal distances from all the vertices of σ, but closer to this vertices than to the others of the complex. The dual polytopes of a simplicial complex $\mathbb{C}$ form a polytopal (but non simplicial) complex, $\mathbb{C}^*$. Simple example in two and three dimensional cases are given in Fig. 2.2. We may consider the n-skeleton of such dual d-dimensional complex

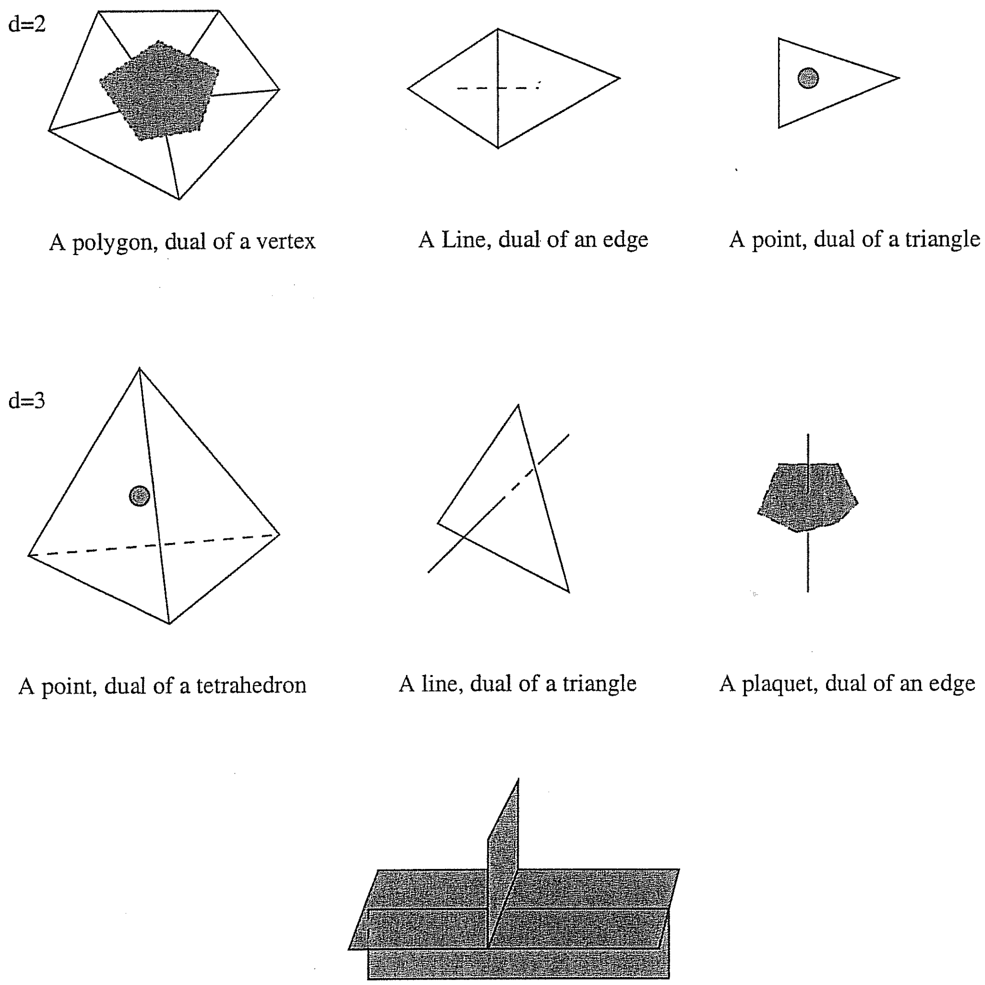

A polygon, dual of a vertex — A Line, dual of an edge — A point, dual of a triangle

A point, dual of a tetrahedron — A line, dual of a triangle — A plaquet, dual of an edge

Dual block associated to a tetrahedron

Fig. 2.2: Elements of the dual lattices in $d = 2, 3$.

(namely the collection of its subsets of dimension $\leq n$). For n=1 we found a graph with $(d+1)$ valent vertices and for n=2 a particular type of surface; for example, in $d = 3$, denoting by X this 2-polyhedron (with boundary), it is characterized by the condition: each point of X has a neighborhood homeomorphic either to

1) the plane R^2, or

2) the union of 3 half-planes meeting each other in their common boundary line, or

3) the cone over the 1-skeleton of a tetrahedron, or

4) the half-plane R^2_+, or

5) the union of 3 copies of the quadrant $\{(x,y) \in R^2 : x \geq 0, y \geq 0\}$ meeting each other in the copies of the half-line $x = 0$.

Such 2-polyhedron is called *simple.* The set of points of the polyhedron X which have no neighborhoods of type 1, 2, 3 is called the boundary of X and denoted by ∂X. It is a graph.

The 2-dimensional polyhedron X is naturally stratified. In this stratification each stratum of dimension 2 is a connected component of the set of points having neighborhoods homeomorphic to R^2. This class of 2-polyhedra is interesting from many viewpoints. Just to mention one, they are generic in the following sense: a) they are obtained by glueing surfaces in their boundary to other surfaces or simple 2-polyhedra by generic mappings of boundary components; b) they constitute a dense subset in the space of all metric 2-polyhedra; c) by local operations, preserving simple homotopy type, one can transform any compact 2-polyhedron into a simple one.

Chapter 3

An outlook of Racah-Wigner algebra.

In this chapter we give a brief review on some basic definitions and relations from the standard theory of quantum angular momenta. From now on, we agree that the spin variable $j = 0, 1/2, 1, 3/2, \dots$ labels the irreducible representations of the group $SU(2)$, while the Dirac notation is employed when matrix elements are considered. In particular the set $\{|jm\rangle\}$, for a fixed j, spans the $(2j+1)$-dimensional complex eigenspace associated with the two Casimir operators of $SU(2)$, while we shall use suitable shorthand notations to deal with tensor product involving the couplings of two or more eigenvectors. We refer the reader mainly to [47] for more details on the content of all Sections except 3.4, about which more information can be found in [48]. From what concerns the extension of the definition of (re)coupling coefficients to the quantum deformation of $SU(2)$, we collect the basic notations in Appendix 8.1.

3.1 Wigner D-functions.

The first quantity that we consider is the Wigner D-function $D^j_{m,m'}(\alpha, \beta, \gamma)$, representing the matrix elements of the rotation operator $\hat{D}(\alpha, \beta, \gamma)$ in the jm-representation. The arguments α, β, γ are the Euler angles which specify the rotation, and we have:

$$\left\langle jm|\hat{D}(\alpha, \beta, \gamma)|j'm'\right\rangle = \delta_{jj'} D^j_{m,m'}(\alpha, \beta, \gamma).$$

The D-functions realize transformations of covariant components of any irreducible tensor of rank j under coordinate rotations.The inverse transformation is performed by the inverse matrix, whose elements are $D^{j*}_{m,m'}(\alpha,\beta,\gamma)$. The unitary condition of the Wigner D-functions may be written as:

$$\sum_{m=-j}^{j} D^{j}_{mm'}(\alpha,\beta,\gamma)D^{j\star}_{m\bar{m}'}(\alpha,\beta,\gamma) = \delta_{m'\bar{m}'}, \quad \sum_{m'=-j}^{j} D^{j\star}_{mm'}(\alpha,\beta,\gamma)D^{j}_{\bar{m}m'}(\alpha,\beta,\gamma) = \delta_{m\bar{m}}.$$

The matrix $D^{j}_{mm'}(\alpha,\beta,\gamma)$ is unimodular. The Wigner D-functions are complex and depend on three real arguments (α,β,γ) defined in the domain

$$0 \le \alpha < 2\pi, 0 \le \beta \le \pi, 0 \le \gamma < 2\pi.$$

As is well known, $D^{j}_{mm'}(\alpha,\beta,\gamma)$ may be expressed as a product of three functions, each one of which depends only on one arguments, namely:

$$D^{j}_{mm'}(\alpha,\beta,\gamma) = \exp^{-im\alpha} d^{j}_{mm'}(\beta) \exp^{-im'\gamma}$$

where $d^{j}_{mm'}(\beta)$ is a real function. The symmetries of the $d^{j}_{mm'}(\beta)$ are

$$\begin{aligned} d^{j}_{mm'}(\beta) &= d^{j}_{-m'-m}(\beta) \\ d^{j}_{mm'}(-\beta) &= d^{j}_{m'm}(\beta) \\ d^{j}_{mm'}(\pi-\beta) &= (-1)^{j-m'} d^{j}_{-mm'}(\beta) = (-1)^{j+m} d^{j}_{m-m'}(\beta) \end{aligned}$$

We list now some expressions involving sums of product of D-functions. The product of two D-functions with the same arguments may be expanded according to

$$D^{j_1}_{m_1m_2}(\alpha,\beta,\gamma)D^{j_2}_{m_2m_2}(\alpha,\beta,\gamma) = \sum_{j=|j_1-j_2|}^{j_1+j_2} C^{jm}_{j_1m_1j_2m_2} D^{j}_{mn}(\alpha,\beta,\gamma) C^{jm}_{j_1m_1j_2m_2}$$

where $C^{jm}_{j_1m_1j_2m_2}$ is a Clebsch-Gordan coefficient (cfr. the next section). The Clebsch-Gordon series enables one to calculate sums of products of D-function with identical arguments:

$$\sum\nolimits_{m_1m_2n_1n_2} C^{jm}_{j_1m_1j_2m_2} D^{j_1}_{n_1n_1}(\alpha,\beta,\gamma) D^{j_2}_{m_2n_2}(\alpha,\beta,\gamma) C^{j'n}_{j_1n_1j_2n_2} = \delta_{jj'}\{j_1j_2j\} D^{j}_{mn}(\alpha,\beta,\gamma)$$

$$\sum\nolimits_{j=|j_1-j_2|}^{j_1+j_2} \sum\nolimits_{m_1m_2} C^{jm}_{j_1m_1j_2m_2} D^{j\star}_{m_1n_1}(\alpha,\beta,\gamma) D^{j}_{mn}(\alpha,\beta,\gamma) C^{jn}_{j_1n_1'j_2n_2} = \delta_{n_1n_1'} D^{j_2}_{m_2n_2}(\alpha,\beta,\gamma)$$

$$\sum\nolimits_{n_1n_2} D^{j_1}_{m_1n_1}(\alpha,\beta,\gamma) D^{j_2}_{m_2n_2}(\alpha,\beta,\gamma) C^{jn}_{j_1n_1j_2n_2} = C^{jm}_{j_1m_1j_2m_2} D^{j}_{mn}(\alpha,\beta,\gamma)$$

$$\sum\nolimits_{nn_1n_2} D^{j\star}_{mn}(\alpha,\beta,\gamma) D^{j_1}_{m_1n_1}(\alpha,\beta,\gamma) D^{j_2}_{m_2n_2}(\alpha,\beta,\gamma) C^{jn}_{j_1n_1j_2n_2} = C^{jm}_{j_1m_1j_2m_2}$$

$$\sum\nolimits_{m_1m_2mn_1n_2} C^{jm}_{j_1m_1j_2m_2} D^{j\star}_{mn}(\alpha,\beta,\gamma) D^{j_1}_{m_1n_1}(\alpha,\beta,\gamma) D^{j_2}_{m_2n_2}(\alpha,\beta,\gamma) C^{j'n'}_{j_1n_1J_2n_2} = \delta_{jj'}\delta_{nn'}\{j_1j_2j\}.$$

From now on we shall denote by $\{a,b,c\}$, $a,b,c = 0, 1/2, 1, \ldots$ a triangular delta, namely a quantity which is equal to 1 if a, b, c satisfy the triangular inequalities, and zero otherwise. The Clebsch-Gordan series can be generalized to the case of an arbitrary number of D-functions of identical arguments, thus obtaining

$$\sum_{\substack{m_1,\cdots m_k\\ n_1,\cdots n_k}} \prod_{i=1}^k C^{j_i m_i}_{J_{i-1}M_{i-1}j_i m_i} D^{j_i}_{m_i n_i}(\alpha,\beta,\gamma) C^{j_i' n_i}_{j_{i-1}' n_{i-1} j_i n_i} =$$

$$D^{j_k}_{m_k n_k}(\alpha,\beta,\gamma) \prod_{i=1}^k \delta_{j_i j_i'} \{j_i j_{i-1} j_i\}$$

with $J_i = j_1 + j_2 + \cdots + j_i$, $M_i = m_1 + m_2 + \cdots + m_i$ and $N_i = n_1 + n_2 + \cdots n_i$. Finally, integral expressions involving D-functions which will be used in the following are:

$$\int_0^{2\pi} d\alpha \int_0^{\pi} d\beta \sin\beta \int_0^{2\pi} d\gamma D^j_{mm'}(\alpha,\beta,\gamma) = \delta_{j0}\delta_{m0}\delta_{m'0} 8\pi^2;$$

$$\int_0^{2\pi} d\alpha \int_0^{\pi} d\beta \sin\beta \int_0^{2\pi} d\gamma D^{j_1}_{m_1 m_1'}(\alpha,\beta,\gamma) D^{j_2}_{m_2 m_2'}(\alpha,\beta,\gamma) =$$

$$= (-1)^{m_2 - m_2'} \frac{8\pi^2}{2j_2+1} \delta_{j_1 j_2} \delta_{-m_1 m_2} \delta_{-m_1' m_2'} \quad (j_1 + j_2 \, integer);$$

$$\int_0^{2\pi} d\alpha \int_0^{\pi} d\beta \sin\beta \int_0^{2\pi} d\gamma D^{j_1 \star}_{m_1 m_1'}(\alpha,\beta,\gamma) D^{j_2}_{m_2 m_2'}(\alpha,\beta,\gamma) =$$

$$= (-1)^{m_2 - m_2'} \frac{8\pi^2}{2j_2+1} \delta_{j_1 j_2} \delta_{m_1 m_2} \delta_{m_1' m_2'} \quad (j_1 + j_2 \, integer);$$

$$\int_0^{2\pi} d\alpha \int_0^{\pi} d\beta \sin\beta \int_0^{2\pi} d\gamma D^{j_1}_{m_1 m_1'}(\alpha,\beta,\gamma) D^{j_2}_{m_2 m_2'}(\alpha,\beta,\gamma) D^{j_3}_{m_3 m_3'}(\alpha,\beta,\gamma) =$$

$$= (-1)^{m_3 - m_3'} \frac{8\pi^2}{2J_3+1} C^{j_3 - m_3}_{j_1 m_1 j_2 m_2} C^{j_3 - m_3'}_{j_1 m_1' j_2 m_2'}, \quad (j_1 + j_2 + j_3 \, integer);$$

$$\int_0^{2\pi} d\alpha \int_0^{\pi} d\beta \sin\beta \int_0^{2\pi} d\gamma D^{j_1}_{m_1 m_1'}(\alpha,\beta,\gamma) D^{j_2}_{m_2 m_2'}(\alpha,\beta,\gamma) D^{j_3 \star}_{m_3 m_3'}(\alpha,\beta,\gamma) =$$

$$= \frac{8\pi^2}{2j_3+1} C^{j_3 m_3}_{j_1 m_1 j_2 m_2} C^{j_3 m_3'}_{j_1 m_1' j_2 m_2'}, \quad (j_1 + j_2 + j_3 \, integer).$$

3.2 Clebsh-Gordan coefficients and 3jm-symbols.

Let j_1 and j_2 be two angular momenta of $SU(2)$ with projections m_1 and m_2 on the quantization axis respectively. A Clebsh-Gordan coefficient represents the probability amplitude that j_1 and j_2 are coupled into a resultant angular momentum j with projection m. The Clebsh-Gordan coefficient vanishes unless the triangular inequalities are fulfilled for the triad (j_1, j_2, j_3) and the request $m_1 + m_2 = m$ is satisfied. The arguments of Clebsh-Gordan coefficients satisfy the following conditions:

a) j_1, j_2 and j are integer or half-integer non negative numbers;

b) m_1, m_2 and m are integer or half-integer (positive or negative) numbers;

c) $|m_1| \leq j_1, |m_2| \leq j_2, |m| \leq j$;

d)$j_1 + m_1, j_2 + m_2, j + m, j_1 + j_2 + j$ are integer non negative numbers.

The absolute value of the Clebsch-Gordan coefficient is given by

$$|C^{jm}_{j_1 m_1 j_2 m_2}| =$$

$$\frac{2j+1}{8\pi} \int_0^{2\pi} d\alpha \int_0^{\pi} d\beta \sin\beta \int_0^{2\pi} d\gamma D^{j_1}_{m_1 m_1}(\alpha,\beta,\gamma) D^{j_2}_{m_2 m_2}(\alpha,\beta,\gamma) D^{j\star}_{mm}(\alpha,\beta,\gamma)$$

The Clebsch-Gordan coefficients are elements of the unitary matrix which transforms the state vectors $|j_1 m_1 j_2 m_2\rangle \doteq |j_1 m_1\rangle \otimes |j_2 m_2\rangle$ and $|j_1 j_2 j m\rangle$ one into the other, namely

$$\begin{aligned} C^{jm}_{j_1 m_1 j_2 m_2} &= \langle j_1 m_1 j_2 m_2 | j_1 j_2 j m\rangle \\ &= \langle j_1 j_2 j m | j_1 m_1 j_2 m_2\rangle \end{aligned}$$

The unitary relations reads:

$$\begin{aligned} \sum_{m_1 m_2} C^{jm}_{j_1 m_1 j_2 m_2} C^{j'm'}_{j_1 m_1 j_2 m_2} &= \delta_{jj'}\delta_{mm'} \\ \sum_{jm} C^{jm}_{j_1 m_1 j_2 m_2} C^{jm}_{j_1 m_1' j_2 m_2'} &= \delta_{m_1 m_1'}\delta_{m_2 m_2'} \end{aligned}$$

Notice also that all recoupling coefficients which will be introduced in the following sections can be expressed as sums of products of Clebsch-Gordan coefficients as well as in terms of the next symbols which we are going to define.

The Wigner 3jm-symbols are strictly related to the Clebsch-Gordan coefficients, and possess simpler symmetry properties. A 3jm symbols and the associated Clebsch-Gordan coefficients may be obtained one from the other through the relations:

$$\begin{pmatrix} j_1 & j_2 & j_3 \\ m_1 & m_2 & m_3 \end{pmatrix} = (-1)^{j_3+m_3+2j_1} \frac{1}{\sqrt{2j_3+1}} C^{j_3 m_3}_{j_1 -m_1 j_2 -m_2};$$

$$C^{j_3 m_3}_{j_1 m_1 j_2 m_2} = (-1)^{j_1+m_3-j_2}\sqrt{2j_3+1}\begin{pmatrix} j_1 & j_2 & j_3 \\ m_1 & m_2 & -m_3 \end{pmatrix}$$

Notice that the factor is chosen in such a way that any cyclic permutation of columns leaves the

3jm symbols unchanged. The symmetry properties of 3jm symbols can be written explicitly as

$$\begin{pmatrix} j_1 & j_2 & j_3 \\ m_1 & m_2 & m_3 \end{pmatrix} = \begin{pmatrix} j_2 & j_3 & j_1 \\ m_2 & m_3 & m_1 \end{pmatrix} =$$

$$= \begin{pmatrix} j_3 & j_1 & j_2 \\ m_3 & m_1 & m_2 \end{pmatrix} =$$

$$= (-1)^{j_1+j_2+j_3} \begin{pmatrix} j_1 & j_3 & j_2 \\ m_1 & m_3 & m_2 \end{pmatrix} =$$

$$(-1)^{j_1+j_2+j_3} \begin{pmatrix} j_2 & j_1 & j_3 \\ m_2 & m_1 & m_3 \end{pmatrix} = (-1)^{j_1+j_2+j_3} \begin{pmatrix} j_3 & j_2 & j_1 \\ m_3 & m_2 & m_1 \end{pmatrix}$$

and the change of sign of all the momentum projection gives:

$$\begin{pmatrix} j_2 & j_1 & j_3 \\ m_2 & m_1 & m_3 \end{pmatrix} = (-1)^{j_1+j_2+j_3} \begin{pmatrix} j_2 & j_1 & j_3 \\ -m_2 & -m_1 & -m_3 \end{pmatrix}.$$

Finally we write down some other relations involving products of Clebsch-Gordan coefficients, namely

$$\sum_{m_1 m_2 m_3} C^{J_4 M_4}_{J_1 M_1 J_2 M_2} C^{J_6 M_6}_{J_3 M_3 J_2 M_2} C^{j_3 m_3}_{j_1 m_1 j_5 m_5} = (-1)^{j_2+j_3+j_4+j_5} \prod_{j_4 j_3} C^{j_3 m_3}_{j_1 m_1 j_2 m_2} \begin{Bmatrix} j_1 & j_2 & j_4 \\ j_6 & j_5 & j_3 \end{Bmatrix}$$

$$\sum_{j_6 m_6} (-1)^{2j_6} \prod_{J_4 J_3} C^{J_6 M_6}_{J_2 M_2 J_3 M_3} C^{J_6 M_6}_{J_5 M_5 J_4 M_4} \begin{Bmatrix} j_1 & j_2 & j_4 \\ j_6 & j_5 & j_3 \end{Bmatrix} = C^{J_4 M_4}_{J_1 M_1 J_2 M_2} C^{J_3 M_3}_{J_1 M_1 J_5 M_5}$$

Here $\prod_{j_1 \cdots j_n} \doteq (2j_1+1) \cdots (2j_n+1)$ and $\begin{Bmatrix} j_1 & j_2 & j_4 \\ j_6 & j_5 & j_3 \end{Bmatrix}$ is a 6j symbols the definition of which will be given in the next section.

The definition of the Clebesch-Gordan coefficients can be generalized to consider the addition of an arbitrary number of angular momenta to give a total J with projection M. The generalized Clebsch-Gordan coefficient (GCG) represents the elements of the matrix that reduces the direct product of an arbitrary number of irreducible representations of $SU(2)$ and is formally expressed as

$$\langle (j_1 \cdots j_n)^A a J M | j_1 m_1 \cdots j_n m_n \rangle$$

where $(j_1 \cdots j_n)^A$ is a scheme of reduction of the set $(j_1 \cdots j_n)$ and a is the set $\{a_1, \cdots a_{n-2}\}$ of intermediate angular momenta.

The GCGs are non zero when the following requirements are fullfilled

$$\sum_{i=1}^n j_i + J = integer\,, \quad \sum_{i=1}^n m_i = M\,,$$

$$\sum_{i=1}^n j_i \geq J \geq 2j_k - \sum_{i=1}^n j_i \quad with \quad k = 1, 2, \cdots n$$

They satisfy the orthogonality relations

$$\sum_{m_1\cdots m_n}\langle (j_1\cdots j_n)^A aJM|j_1m_1\cdots j_nm_n\rangle\langle j_1m_1\cdots j_nm_n|(j_1\cdots j_n)^A a'J'M'\rangle = \\ = \delta_{aa'}\delta_{JJ'}\delta_{MM'},$$

$$\sum_{aJM}\langle (j_1\cdots j_n)^A aJM|j_1m_1'\cdots j_nm_n'\rangle\langle j_1m_1\cdots j_nm_n|(j_1\cdots j_n)^A aJM\rangle = \\ = \delta_{m_1m_1'}\cdots\delta_{m_nm_n'},$$

where $\delta_{aa'} \equiv \delta_{a_1a_1'}\cdots\delta_{a_{n-2}a_{n-2}'}$. The above expressions admit expansions in terms of usual Clebsch-Gordan coefficients, (see [48]).

3.3 6j symbols.

The Wigner 6j symbols are related to the coefficients (or better, they are matrix elements) of unitary transformations between different coupling schemes of three angular momenta to give a total momentum j. Denote by $|j_1j_2(j_{12})j_3jm\rangle$ the state vector corresponding to the coupling scheme $j_1+j_2=j_{12}, j_{12}+j_3=j$. Then we have

$$|j_1j_2(j_{12})j_3jm\rangle = \sum_{m_1m_2m_3} C^{jm}_{j_{12}m_{12}j_3m_3}C^{j_{12}m_{12}}_{j_1m_1j_2m_2}|j_1m_1j_2m_2j_3m_3\rangle,$$

Let now $|j_2j_3(j_{23})j_1jm\rangle$ be the state vector corresponding to the coupling scheme $j_2+j_3=j_{23}, j_{23}+j_1=j$; in this case we get

$$|j_2j_3(j_{23})j_1jm\rangle = \sum_{m_1m_2m_3} C^{jm}_{j_1m_1j_{23}m_{23}}C^{j_{23}m_{23}}_{j_2m_2j_3m_3}|j_1m_1j_2m_2j_3m_3\rangle.$$

Finally, if $|j_1j_3(j_{13})j_2jm\rangle$ is the state vector corresponding to the coupling scheme $j_1+j_3=j_{13}, j_{13}+j_2=j$, we obtain

$$|j_1j_3(j_{13})j_2jm\rangle = \sum_{m_1m_2m_3} C^{jm}_{j_{13}m_{13}j_2m_2}C^{j_{13}m_{13}}_{j_1m_1j_3m_3}|j_1m_1j_2m_2j_3m_3\rangle.$$

States belonging to each of the above coupling schemes form a complete set of states by their own. A transition from one coupling scheme to another is achieved by some unitary transformation which relates couples of different set of the states (with the same total angular momentum j and projection m). If we denote by U this transformation, the Wigner 6j symbols $\left\{\begin{matrix} j_1 & j_2 & j_{12} \\ j_3 & j & j_{23}\end{matrix}\right\}$ is defined by means of one of the following relations:

$$\langle j_1 j_2 (j_{12}) j_3 j m | j_2 j_3 (j_{23}) j_1 j' m' \rangle = \delta_{jj'} \delta_{mm'} U(j_1 j_2 j_3; j_{12} j_{23}) =$$

$$\delta_{jj'} \delta_{mm'} (-1)^{j_1+j_2+j_3+j} \sqrt{(2j_{12}+1)(2j_{23}+1)} \left\{ \begin{array}{ccc} j_1 & j_2 & j_{12} \\ j_3 & j & j_{23} \end{array} \right\};$$

$$\langle j_1 j_2 (j_{12}) j_3 j m | j_1 j_3 (j_{13}) j_1 j' m' \rangle = \delta_{jj'} \delta_{mm'} (-1)^{j+j_1-j_{12}-j_{13}} U(j_1 j_2 j_3; j_{12} j_{13}) =$$

$$\delta_{jj'} \delta_{mm'} (-1)^{j_{12}+j_2+j_3+j_{13}} \sqrt{(2j_{12}+1)(2j_{13}+1)} \left\{ \begin{array}{ccc} j_2 & j_1 & j_{12} \\ j_3 & j & j_{13} \end{array} \right\};$$

$$\langle j_2 j_3 (j_{23}) j_3 j m | j_1 j_3 (j_{13}) j_1 j' m' \rangle = \delta_{jj'} \delta_{mm'} (-1)^{j_2+j_3-j_{23}} U(j_1 j_2 j_3; j_{13} j_{23}) =$$

$$\delta_{jj'} \delta_{mm'} (-1)^{j_1+j+j_{23}} \sqrt{(2j_{23}+1)(2j_{13}+1)} \left\{ \begin{array}{ccc} j_1 & j_3 & j_{13} \\ j_2 & j & j_{23} \end{array} \right\}$$

According to its definition, the 6j symbol may be also written in terms of Clebsch-Gordan coefficients, namely

$$\sum C^{jm}_{j_{12}m_{12}j_3m_3} C^{j_{12}m_{12}}_{j_1m_1j_2m_2} C^{j'm'}_{j_1m_1j_{23}m_{23}} C^{j_{23}m_{23}}_{j_2m_2j_3m_3} =$$

$$\delta_{jj'} \delta_{mm'} (-1)^{j_1+j_2+j_3+j} \sqrt{(2j_{12}+1)(2j_{23}+1)} \left\{ \begin{array}{ccc} j_1 & j_2 & j_{12} \\ j_3 & j & j_{23} \end{array} \right\}$$

Here the sum is over $m_1, m_2, m_3, m_{12}, m_{23}$ while m and m' are keeped fixed. According to the convention on the Clebsh-Gordan coefficients the 6j symbols turns out to be real. All momenta are integer or half integer nonnegative numbers and each triad $(j_1j_2j_{12})$, $(j_{12}j_3j)$, $(j_2j_3j_{23})$, and $(j_{23}j_1j)$ must satisfy the triangular conditions. The unitarity of the recoupling transformations implies the orthogonality and normalization conditions of the 6j symbols, which read

$$\sum_{j_{12}} (2j_{12}+1)(2j_{23}+1) \left\{ \begin{array}{ccc} j_1 & j_2 & j_{12} \\ j_3 & j & j_{23} \end{array} \right\} \left\{ \begin{array}{ccc} j_1 & j_2 & j_{12} \\ j_3 & j & j'_{23} \end{array} \right\} = \delta_{j_{23}j'_{23}}$$

$$\sum_{j_{23}} (2j_{12}+1)(2j_{23}+1) \left\{ \begin{array}{ccc} j_1 & j_2 & j_{12} \\ j_3 & j & j_{23} \end{array} \right\} \left\{ \begin{array}{ccc} j_1 & j_2 & j'_{12} \\ j_3 & j & j_{23} \end{array} \right\} = \delta_{j_{12}j'_{12}}$$

The 6j symbols is invariant under any permutation of its columns or under interchange of the upper and lower arguments in each of any two columns. We collect now in an uniform notation some of the most important identities and conditions involving products of 6j symbols. Notice first that we have trivially:

$$\sum_x (2x+1) \left\{ \begin{array}{ccc} a & b & x \\ a & b & c \end{array} \right\} = (-1)^{2c} \{abc\} \tag{3.1}$$

where $\{a,b,c\}$ is the triangular delta. Orthogonality condition:

$$\sum_x (2x+1) \left\{ \begin{array}{ccc} a & b & x \\ c & d & p \end{array} \right\} \left\{ \begin{array}{ccc} a & b & x \\ c & d & q \end{array} \right\} = \delta_{pq} \frac{\{adp\}\{bcp\}}{2p+1}; \tag{3.2}$$

Racah identity:

$$\sum_x (-1)^{p+q+x} (2x+1) \left\{ \begin{array}{ccc} a & b & x \\ c & d & p \end{array} \right\} \left\{ \begin{array}{ccc} a & b & x \\ d & c & q \end{array} \right\} = \left\{ \begin{array}{ccc} a & c & q \\ b & d & p \end{array} \right\}; \tag{3.3}$$

Biedenhar-Elliot identity:

$$\sum_x (-1)^{a+b+c+d+e+f+p+q+r+x} (2x+1) \left\{ \begin{array}{ccc} a & b & x \\ c & d & p \end{array} \right\} \left\{ \begin{array}{ccc} a & b & x \\ e & f & q \end{array} \right\} \left\{ \begin{array}{ccc} e & f & x \\ b & a & r \end{array} \right\} = \left\{ \begin{array}{ccc} p & q & r \\ e & a & d \end{array} \right\} \left\{ \begin{array}{ccc} p & q & r \\ f & b & c \end{array} \right\}. \tag{3.4}$$

3.4 3nj-symbols.

When dealing with coupling schemes of $(n+1)$ angular momenta of $SU(2)$ to give a fixed total angular momentum, we should consider several possibilities which can be worked out by generalizing the procedure outlined in the previous section. For a fixed n, the unitary transformations between two of the coupling schemes can be uniquely associated with recoupling coefficients, the so called 3nj-symbols. As n grows, more and more different 3nj symbol can be defined, owing to the plenty of parings among the couplings. For instance, while we have just one 9j symbol (type II), we find two types of 12j symbols (I and II), five types of 15j symbols, and so on. As a matter of fact, we can write down in a simple closed form the expressions defining the 3nj symbols of type II in terms of a single sum over a j variable of the product of n 6j symbols. On adopting the convention of [47] (although a more complete account on the subject can be found in [48]), the 3nj symbols of type II turns out to be defined trough the relation:

$$\left[\begin{array}{cccccccc} a_1 & & a_2 & & \cdots & & a_n & \\ & b_1 & & b_2 & & \cdots & & b_n \\ c_1 & & c_2 & & \cdots & & c_n & \end{array} \right] = \sum_z (-1)^{S+nz} (2z+1) \left\{ \begin{array}{ccc} a_1 & c_1 & z \\ c_2 & a_2 & b_1 \end{array} \right\} \times \times \left\{ \begin{array}{ccc} a_2 & c_2 & z \\ c_3 & a_3 & b_2 \end{array} \right\} \cdots \left\{ \begin{array}{ccc} a_n & c_n & z \\ c_1 & a_1 & b_n \end{array} \right\}, \tag{3.5}$$

where S denotes the sum of all the 3n arguments.

Notice that such kind of notation put all j variables, namely the $(n+1)$ original ones and the intermediate ones, on the same foot. On the other hand, as will be clear when we shall deal with state sums from the recoupling of angular momenta, we need an expression of the 3nj in terms of a sum over all magnetic quantum numbers of 2n Wigner symbols. Such an expression reads:

$$[a_1, a_2, \cdots a_{2n}] = \sum_{All\, m} (-1)^{\sum m_i} \begin{pmatrix} b_1 & a_1 & b_2 \\ m_{b_1} & m_{a_1} & m_{b_2} \end{pmatrix} \begin{pmatrix} b_2 & a_2 & b_3 \\ -m_{b_2} & m_{a_2} & m_{b_3} \end{pmatrix} \cdots$$
$$\begin{pmatrix} b_{2n-1} & a_{2n-1} & b_{2n} \\ m_{b_{2n-1}} & m_{a_{2n-1}} & m_{b_{2n}} \end{pmatrix} \begin{pmatrix} b_{2n} & a_{2n} & b_1 \\ -m_{b_{2n}} & m_{a_{2n}} & -m_{b_1} \end{pmatrix} \qquad (3.6)$$

with the identification $a_{\frac{1+\sqrt{9+3n}}{2}-m} = a_{m\frac{1+\sqrt{9+3n}}{2}-(m+2)}$ and the constraint $n = (b-1)(b+2)/2$ for generic b. We are non able to specify in general which type of symbol the above relation corresponds to, at least for $n > 5$ (indeed, in the case $n = 5$ it is the 15j symbol of type II).

3.5 The graphical method.

The analitycal relations that will appear in this thesis involve several summations of products of many elements (basically, recoupling coefficients and/or more complicated combinations of symbols), so that the representation of such expressions in a diagrammatic form greatly facilitates their general analysis. Generally speaking, a graphical representation is more compact and clear and reduces drastically the calculations. The starting point of any graphical method consists in establishing a one to one correspondence between the elements of a diagram and the constituents of the analytic expression, namely any expression inherent in the theory must be represented by a definite diagram, and viceversa. Moreover, a transformation of the expression under some analytical operations must correspond to a definite sequence of operations on the associated diagram. As a first illustration of the graphical method we adopt (which is borrowed from [47]), we show a list of diagrams corresponding to some of the quantities introduced above in Figures (3.1),(3.2), (3.3).

As general remark, note that expressions which occur in calculations based on the quantum theory of angular momentum may essentially contain spin variables of two kinds, namely external and internal ones. In particular:

i)External variables are actual arguments of the expression under consideration. The evaluation of the given expression does not involve any integration or summation over these variables: they

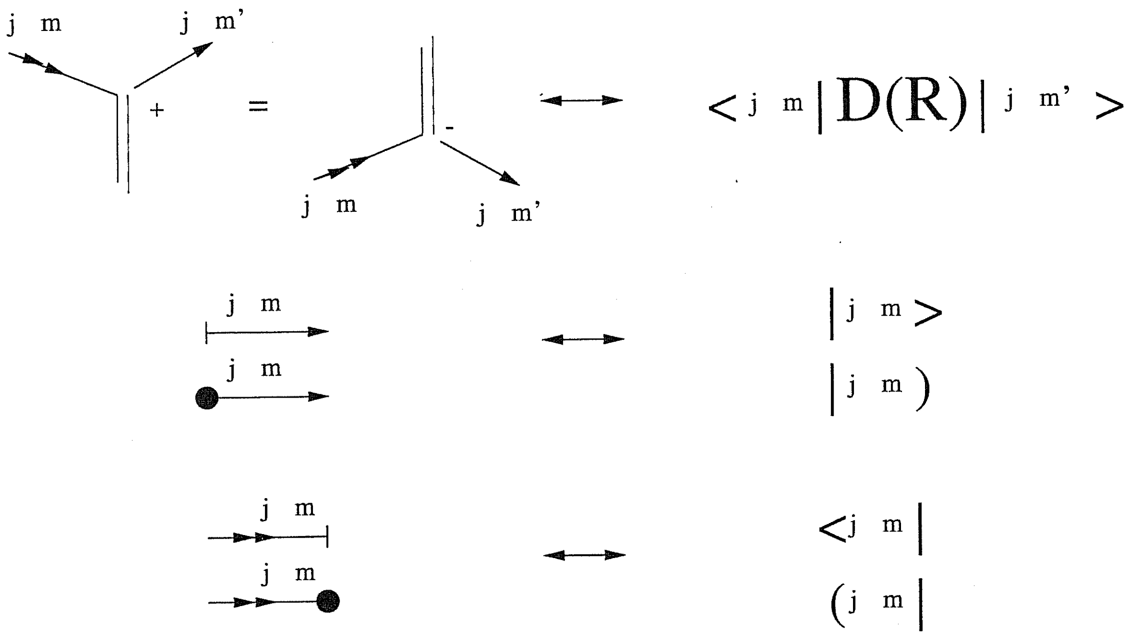

Fig. 3.1: Graphical representation of vector states and rotation operators.

are fixed parameters.

ii)Internal variables are those with respect to which either integration or summation has to be performed (in a given expression). Thus each internal variable which enters an expression corresponds in fact to some scalar product $|\psi\rangle\langle\psi|$ between suitable ψ. This is why one does not need to take into account any transformation of internal variable under rotation of the coordinate system.

The product (direct product) of factors M and N is represented graphically by two unlinked subdiagrams (blocks) which correspond to the factors. The mutual disposition and orientation of these subdiagrams are inessential.

The scalar product of two irreducible tensor of rank j, M_{jm} and N_{jm}, i.e. the following sum of bilinear combinations over all possible values of the projection m

$$\sum_{m=-j}^{j} \langle\cdot|M|jm\rangle\langle jm|N|\cdot\rangle \tag{3.7}$$

is represented by the conjunction (closure) of the lines $|jm\rangle$ and $\langle jm|$ or of other subdiagrams corresponding to $\langle\cdot|M|jm\rangle$ and $\langle jm|M|\cdot\rangle$ as shown in Fig. 3.4.

A thick j-line linking two subdiagrams as shown in Fig. 3.5 represents the sum both over j and

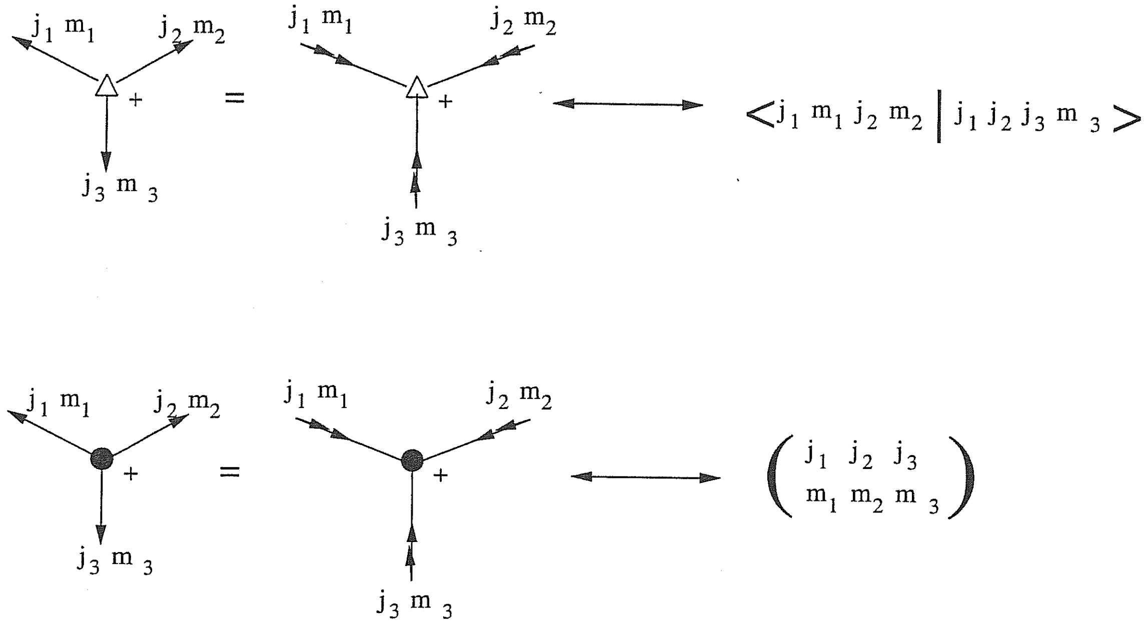

Fig. 3.2: Graphical representations of Clebsh-Gordan and 3jm symbols.

m of scalar products of irreducible tensor of rank j, namely:

$$\sum_{j=0}^{\infty}(2j+1)\sum_{m=-j}^{j}\langle\cdot|M|jm\rangle\langle jm|N|\cdot\rangle. \tag{3.8}$$

If we are not interested in the structure of the inner part of a given diagram, it may be replaced by a block with the same external lines, simply because the external lines determine the transformation properties of the diagram (or subdiagram) under rotations of the coordinate system. For instance, any closed diagram without external lines is invariant under such rotations, and turns out be reduced to some of the 3nj symbols or their combinations.

The length of the lines, their curvature and orientation are not important. Consequently, any diagram may be arbitrarily rotated and deformed. Two diagrams will be called topologically similar if it is possible to make them coincident by means of rotations, deformations and reflections. Topologically similar diagrams have the same number of nodes and lines (solid and dashed), but they may differ by directions of lines and by node signs. The expressions corresponding to two topological similar diagrams are equal in absolute value, but may differ by a phase factor. So if we are interested only of the absolute value or if we have sum over all variable, we may discard orientations and node signs.

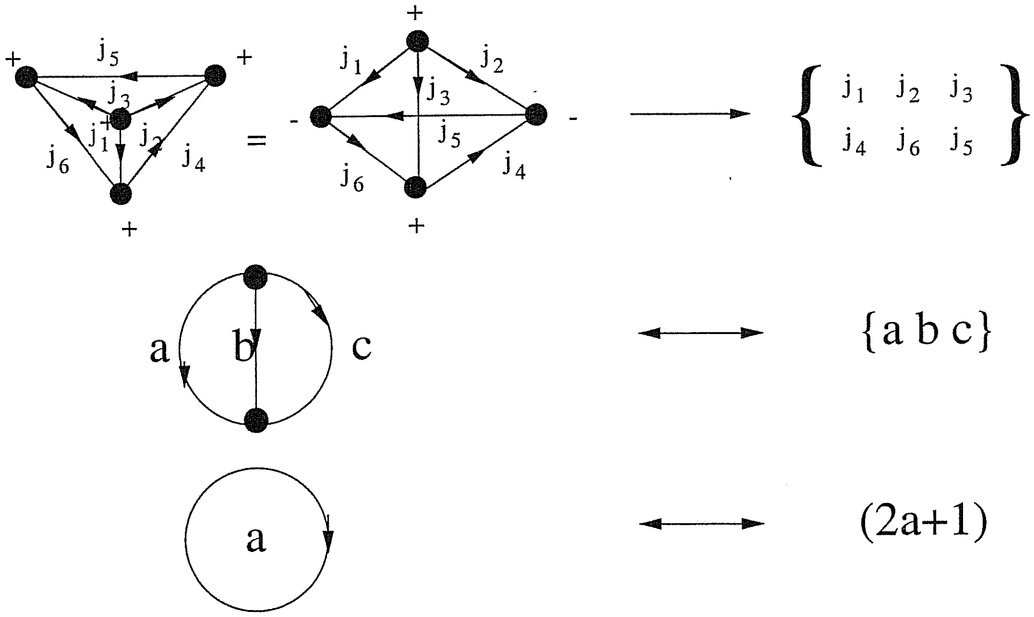

Fig. 3.3: Graphical representations of some invariant functions.

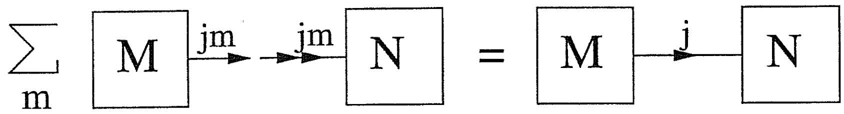

Fig. 3.4: Graphical representation of the relation (3.7).

Now we give the graphical rules for the multiplication of subdiagrams, namely for linking the subdiagrams (blocks) into a connected diagram.

a) Two subdiagrams representing factors M and N, both with at least one identical j-line, may be linked together into the combined diagram which displays the product of this factors as shown in Fig. 3.6. The necessary condition for such a linking is that at least one of this subdiagrams must have no external line. The above graphical rule is equivalent to the relation

$$\left(\sum_m \langle jm|M|jm\rangle\right) \times \left(\sum_{m'} \langle jm'|N|jm'\rangle\right) = (2j+1) \sum_{mm'} \langle jm|M|jm'\rangle\langle jm'|N|jm\rangle. \qquad (3.9)$$

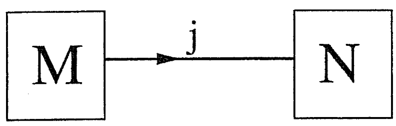

Fig. 3.5: Graphical representation of the relation (3.8)

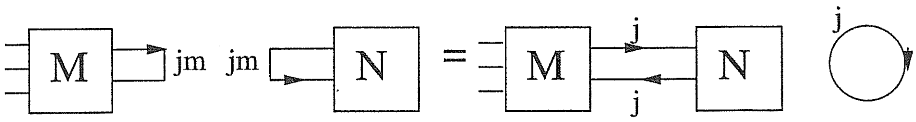

Fig. 3.6: Graphical representation of relation (3.9).

b) Two subdiagrams representing the factors M and N, both with at least one identical node, three coupled j-line, say (j_1, j_2, j_3), may be linked into the combined diagram which corresponds to the product of these factors as shown in Fig. 3.7. The corresponding analytical relation is:

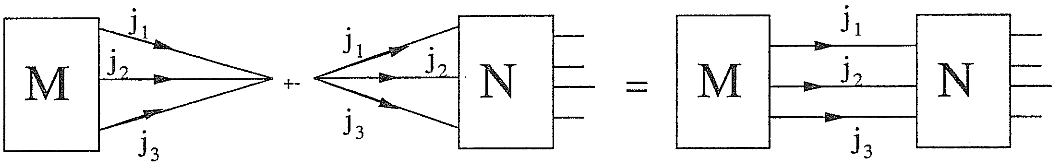

Fig. 3.7: Graphical representation of the relation (3.10).

$$\left[\sum_{m_1 m_2 m_3} \langle 00|M|j_1 m_1 j_2 m_2 j_3 m_3\rangle \begin{pmatrix} j_1 & j_2 & j_3 \\ m_1 & m_2 & m_3 \end{pmatrix}\right] \times$$

$$\times \left[\sum_{m_1' m_2' m_3'} \begin{pmatrix} j_1 & j_2 & j_3 \\ m_1' & m_2' & m_3' \end{pmatrix} \langle j_1 m_1' j_2 m_2' j_3 m_3'|M|\cdot\rangle\right] \tag{3.10}$$

$$= \{j_1 j_2 j_3\} \sum_{m_1 m_2 m_3} \langle 00|M|j_1 m_1 j_2 m_2 j_3 m_3\rangle \langle j_1 m_1 j_2 m_2 j_3 m_3|M|\cdot\rangle$$

A summation over an angular momentum variable j and its projection m may be easily performed by the diagrammatic technique, if this thick j-line connects two identical nodes.

Any thick j-line which connects identical pair of j line, may be removed provided the ends of the thin lines with equal momenta are linked together. An example is displayed in Fig. 3.8. Such a

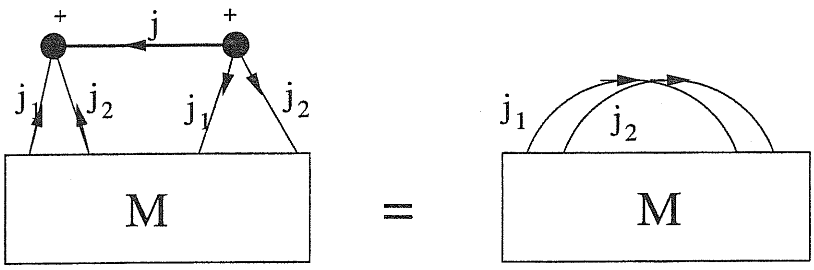

Fig. 3.8: Graphical representation of the relation (3.11).

graphical operation does not change the content of the diagram and corresponds to the identity

$$\sum_{jm}(2j+1)\langle j_1j_2jm|M|j_1j_2jm\rangle = \sum_{m_1m_2}\langle j_1m_1j_2m_2|M|j_1m_1j_2m_2\rangle, \tag{3.11}$$

where

$$\langle j_1m_1j_2m_2|M|j_1'm_1'j_2'm_2'\rangle =$$

$$= \sum_{jm}(2j+1)\begin{pmatrix} j_1 & j_2 & j \\ m_1 & m_2 & m \end{pmatrix}\langle j_1j_2jm|M|j_1'j_2'jm\rangle\begin{pmatrix} j_1' & j_2' & j \\ m_1' & m_2' & m \end{pmatrix}.$$

When a common thick j-line is included into two or more unlinked subdiagrams, one should preliminary link together these subdiagrams with the aid of the rules of subdiagrams multiplication in order to get just one thick j-line. Only after this operation one can go on with graphical summation over j and m according to the rule said before. An example of this combined graphical operation is displayed in Fig. 3.9, which represents the relation

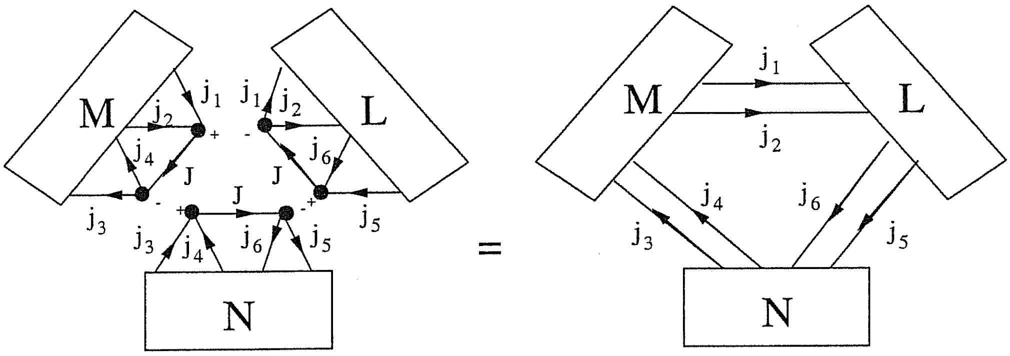

Fig. 3.9: Graphical representation of the relation (3.12).

$$\sum_{JMM'M''}(2J+1)\langle j_1j_2;JM|\mathcal{M}|j_3j_4;JM\rangle\langle j_3j_4;JM'|\mathcal{N}|j_5j_6;JM'\rangle\cdot$$

$$\cdot\langle j_5j_6;JM''|\mathcal{L}|j_1j_2;JM''\rangle =$$

$$= \sum_{\substack{m_1m_2m_3 \\ m_4m_5m_6}}\langle j_1m_1j_2m_2|\mathcal{M}|j_3m_3j_4m_4\rangle\cdot \tag{3.12}$$

$$\cdot\langle j_3m_3j_4m_4|\mathcal{N}|j_5m_5j_6m_6\rangle\langle j_5m_5j_6m_6|\mathcal{L}|j_1m_1j_2m_2\rangle.$$

Chapter 4

Invariants of closed M^d from colorings of $(d-1)$-simplices.

In this Chapter we deal with state sums built up from $SU(2)$ colorings of the (d-1) dimensional skeleton of a triangulation $T^d \to M^d$ of a closed PL-manifold M^d. A direct inspection of the properties of such class of state sums under bistellar moves (recall their definitions given in Chapter 2) provide us with both a classical $SU(2)$ invariant $Z_\chi[M^d]$ and a quantum $Z_\chi[M^d]$(q). These invariant are related to the Euler character of M^d, and moreover they correspond in the continuum approach to a well known class of topological quantum field theories (TQFTs), as discussed in Section 4.3. Although the meaning of these invariants is obvious, the procedure given here turns out to give the basis starting point in view of the definition of the new invariants presented in the next two chapters.

4.1 Definition of the invariant $Z_\chi[M^d]$.

According to the remarks at the end of the Chapter 2, associated with each $(d-1)$-simplex σ^{d-1} of a closed triangulation T^d we have an edge of the dual lattice; in other words, there exists a one to one correspondence between the structure of the $(d-1)$-skeleton of the triangulation and the structure of the 1-skeleton of the dual complex. Thus we get a graph Γ, the vertices of which are 3-valent in $d = 2$, 4-valent in $d = 3$ and $d+1$ valent in d dimension. We can define a map $\phi : \sigma^{d-1} \to SU(2)$, called a coloring, in such a way that each $\sigma^{d-1} \in T^d$, or each edge of the 1-skeleton, turns out to be associated with a representation labelled by j. As we shall see in a moment, we can assign in a consistent way a $D^j_{m\mu}(R)$, $R \in SU(2)$, to each edge incident on the vertices of such a graph. In this framework the role of the magnetic quantum numbers m, μ is made manifest by introducing the fat graph associated with each one of the former graphs: any edge actually acquires two sets of $SU(2)$-colorings, namely $\{j, m\}$ and $\{j, \mu\}$.

Thus consistent $SU(2)$-colorings on Γ generated by the fat graph are achieved if we consider the assignments

$$(\{j\}; m, \mu) \longrightarrow \Gamma \subset \tilde{T}^d, \tag{4.1}$$

where $\tilde{T}^d$ is the dual complex associated with T^d.

The next step consists in performing an integral over the R-variables of the product of the D-functions associated with the legs of the graph incident on each vertex. According to this prescription, we can now define the following limit of admissible sums of configurations

$$\begin{aligned} Z_{\chi}[M^d] = \lim_{L\to\infty} \sum_{\left\{ \begin{array}{c} T^d(\{j\}; m, \mu) \\ \{j\}, m, \mu \leq L \end{array} \right\}} & w_L^{(-1)^{(d-1)}\Psi} \\ \prod_{all\, \sigma^{d-1}} (-1)^{2j_{\sigma^{d-1}}} (2j_{\sigma^{d-1}} + 1) & \left(\int \prod_{\sigma^{d-1}\subset\sigma^d} D^{j_{\sigma^{d-1}}}_{m\mu}(R)dR \right)_{\sigma^d}, \end{aligned} \tag{4.2}$$

where $\Psi = 2(N_0 - N_1 + \ldots + (-1)^{d-2}N_{d-2})$, $(N_0, N_1, N_2, \ldots)$ are the numbers of $(0, 1, 2, \ldots)$-simplices in T^d respectively, the range of variation of each m, μ with respect to its $\{j\}$ is the usual one and the identifications over the magnetic numbers acts as glueing operations among d-simplices.

The factor $w_L = \frac{1}{2j_1+1} \sum_{\substack{j_2 j_3 \\ with\, \{j_1, j_2, j_3\}}} (2j_2 + 1)(2j_3 + 1)$ is included to regularize the expression of the state sum. The presence of a pair of magnetic numbers for each j variable which appears tell us that we will get a double 3jm symbol after integration, namely a product of two 3jm's with the same $\{j\}$ but different m and μ, for each elementary configuration of the dual graph (cfr. the integral expression given at the end of Section 2.1 in [47]). The formal calculations can be easily translated in the diagrammatic language as shown in Fig. 4.1 for the cases $d = 2, 3$.

By collecting the terms generated by all vertices, we would get a products of double $3jm$ symbols. This is achieved by exploiting the relationships between integrals of products of several

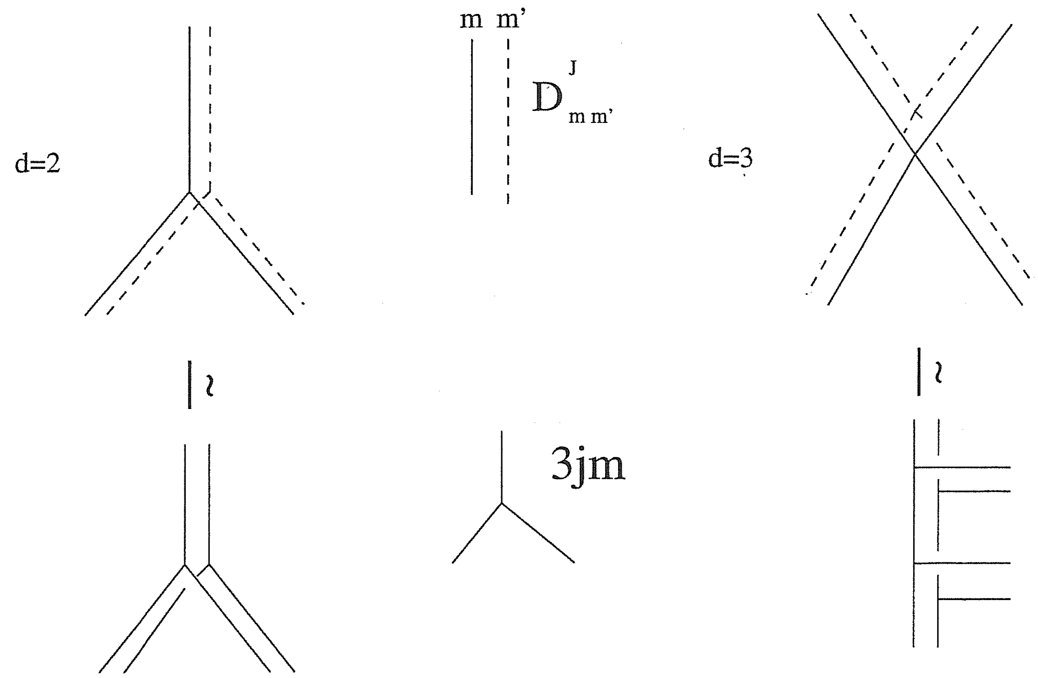

Fig. 4.1: The graph representing the 1-skeleton of the dual lattice of each 2 and 3 dimensional simplex, with a D function associated with each edge, and the derived elementary diagrams occurring in Z^2_χ and Z^3_χ in terms of 3jm symbols.

D-functions and suitable combinations of Wigner symbols: this amounts to recognize that the product under integration in (4.2) can be transformed into

$$\sum_{\{J\}}\prod_{k=1}^{d-3}(-1)^{2J_k}(2J_k+1)\sum_{\mathcal{M},\nu}(-1)^{\mathcal{M}+\nu}\begin{pmatrix} j_1 & j_2 & J_1 \\ m_1 & m_2 & \mathcal{M}_1 \end{pmatrix}\cdot\begin{pmatrix} J_1 & j_3 & J_2 \\ -\mathcal{M}_1 & m_3 & \mathcal{M}_2 \end{pmatrix}\cdot$$
$$\begin{pmatrix} j_1 & j_2 & J_1 \\ \mu_1 & \mu_2 & \nu_1 \end{pmatrix}\begin{pmatrix} J_1 & j_3 & J_2 \\ -\nu_1 & \mu_3 & \nu_2 \end{pmatrix}\cdots\begin{pmatrix} J_{d-4} & j_{d-2} & J_{d-3} \\ -\mathcal{M}_{d-4} & m_{d-2} & \mathcal{M}_{d-3} \end{pmatrix}\cdot$$
$$\begin{pmatrix} J_{d-3} & j_{d-1} & j_d \\ -\mathcal{M}_{d-3} & m_{d-1} & m_d \end{pmatrix}\begin{pmatrix} J_{d-4} & j_{d-2} & J_{d-3} \\ -\nu_{d-4} & \mu_{d-2} & \nu_{d-3} \end{pmatrix}\begin{pmatrix} J_{d-3} & j_{d-1} & j_d \\ -\nu_{d-3} & \mu_{d-1} & \mu_d \end{pmatrix} \tag{4.3}$$

Here, besides the colorings $\{j\}$, there appears the set $\{J\}$, where a J variables is assumed to be associated with an internal glueing between the two portions of a double symbol; moreover, we denoted by $\mathcal{M},\nu$ the pair of magnetic numbers associated with each J and by m,μ those associated with each j, respectively.

The diagrammatic counterpart of the procedure described above is shown in Fig. 4.2, where for

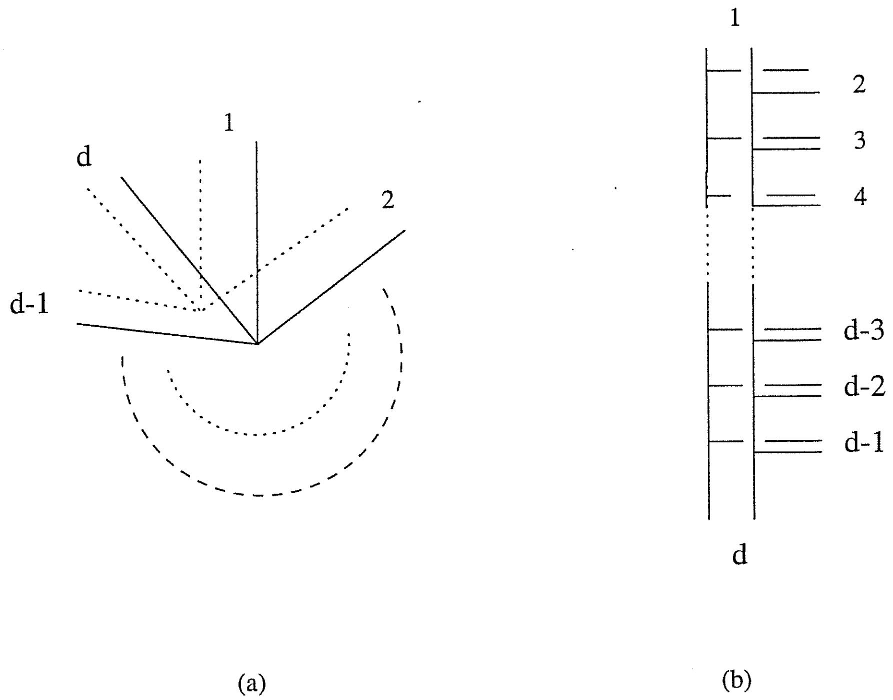

Fig. 4.2: The graph representing the 1-skeleton of the dual lattice of each d dimensional simplex, with a D function associated to each edge, and the derived elementary diagrams occurring in Z_χ^d in terms of 3jm symbols.

simplicity just one of the possible coupling schemes is considered (the other ones giving equivalent analytical expressions). The invariant can be rewritten as

$$Z_\chi[M^d] \equiv \lim_{L\to\infty} \sum_{\left\{ \begin{array}{c} T^d(\{j\},\{J\};m,\mu) \\ all\; j,m \leq L \end{array} \right\}} w_L^{(-1)^{(d-1)}\Psi} \cdot$$

$$\sum_{\{J\}} \prod_{k=1}^{d-3} (-1)^{2J_k}(2J_k+1)(-1)^{\sum \mathcal{M}+\sum \nu} \begin{pmatrix} j_1 & j_2 & J_1 \\ m_1 & m_2 & \mathcal{M}_1 \end{pmatrix} \begin{pmatrix} J_1 & j_3 & J_2 \\ -\mathcal{M}_1 & m_3 & \mathcal{M}_2 \end{pmatrix} \cdot$$

$$\begin{pmatrix} j_1 & j_2 & J_1 \\ \mu_1 & \mu_2 & \nu_1 \end{pmatrix} \begin{pmatrix} J_1 & j_3 & J_2 \\ -\nu_1 & \mu_3 & \nu_2 \end{pmatrix} \cdots \begin{pmatrix} J_{d-4} & j_{d-2} & J_{d-3} \\ -\mathcal{M}_{d-4} & m_{d-2} & \mathcal{M}_{d-3} \end{pmatrix} \cdot$$

$$\begin{pmatrix} J_{d-3} & j_{d-1} & j_d \\ -\mathcal{M}_{d-3} & m_{d-1} & m_d \end{pmatrix} \begin{pmatrix} J_{d-4} & j_{d-2} & J_{d-3} \\ -\nu_{d-4} & \mu_{d-2} & \nu_{d-3} \end{pmatrix} \begin{pmatrix} J_{d-3} & j_{d-1} & j_d \\ -\nu_{d-3} & \mu_{d-1} & \mu_d \end{pmatrix} . \tag{4.4}$$

Let us focus our attention on the topological content of (4.4). If we agree that each double 3jm symbol must be associated with an Euclidean triangle, than the collection of symbols given above for a given triangulation $T^d \to M^d$ turns out to be associated (through the sum over those magnetic number which represent the glueings along edges of contiguous triangles) with a closed surface S. This triangulated 2-manifold is generated by the integration of the quantities arising from the colorings of the graph Γ (cfr. (4.2)); namely S is spanned by the 1-skeleton of the dual complex of the original triangulation T^d by adding discs along the loops of the graph. Thus, by reminding that the 1-skeleton of the dual complex give us information on the combinatorial structure of the $(d-1)$-skeleton of T^d, we easily see that the surface S must share the same combinatorial properties of the collection of d simplices in T^d with respect the glueings along their common $(d-1)$-simplices. From this remark it should be clear that the case $d=2$ is quite peculiar, since the surface S associated with a given $T^2 \to M^2$ is nothing but T^2 itself (and indeed in the next section we shall recover the same expression given in (4.4) in a more straightforward way). Then if we are able to prove the invariance of (4.4) under the set of bistellar moves in the 2-dimensional case, all we have to do is just to generalize the result to any surface S generated by a T^d through the procedure explained above.

4.2 $Z_\chi[M^2]$ and its invariance.

Following [13] the state sum for a 2-dimensional triangulation of a closed PL-manifold M^2

$$T^2(j; m, m') \longrightarrow M^2 \tag{4.5}$$

can be consistently defined if we require that

- each 2-simplex $\sigma^2 \in T^2$ is associated with the following product of two Wigner symbols (a *double* $3jm$ symbol for short)

$$\sigma^2 \longleftrightarrow (-1)^{\sum_{s=1}^{3}(m_s+m'_s)/2} \begin{pmatrix} j_1 & j_2 & j_3 \\ m_1 & m_2 & -m_3 \end{pmatrix} \begin{pmatrix} j_1 & j_2 & j_3 \\ m'_1 & m'_2 & -m'_3 \end{pmatrix}, \tag{4.6}$$

where $\{m_s\}$ and $\{m'_s\}$ are two different sets of momentum projections associated with the same angular momentum variables $\{j_s\}$, $-j \leq m_s, m'_s \leq j \;\forall s = 1,2,3$. The expression of the state sum proposed in [13] reads

$$Z_\chi[T^2(j; m, m') \to M^2; L] =$$

$$= w_L^{-N_0} \prod_{A=1}^{N_1} (2j_A+1)(-1)^{2j_A}(-1)^{-m_A-m'_A}$$

$$\prod_{B=1}^{N_2} \begin{pmatrix} j_1 & j_2 & j_3 \\ m_1 & m_2 & -m_3 \end{pmatrix}_B \begin{pmatrix} j_1 & j_2 & j_3 \\ m'_1 & m'_2 & -m'_3 \end{pmatrix}_B , \tag{4.7}$$

where N_0, N_1, N_2 are the numbers of vertices, edges and triangles in T^2, respectively. Summing over all of the admissible assignments of $\{j; m, m'\}$ we get

$$Z_\chi[M^2] = \lim_{L\to\infty} \sum_{\{T^2(j;m,m'),j\leq L\}} Z[T^2(j; m.m') \to M^2; L], \tag{4.8}$$

where the regularization is carried out according to the usual prescription.

The invariance of (4.8) is ensured as far as the bistellar moves in $d = 2$ can be implemented. One of these move is expressed according to

$$\sum_q \sum_{\kappa,\kappa'} (2q+1)(-1)^{2q}(-1)^{-\kappa-\kappa'} \begin{pmatrix} p & a & q \\ \psi & \alpha & -\kappa \end{pmatrix} \begin{pmatrix} q & b & r \\ \kappa & \beta & \rho \end{pmatrix} \cdot$$
$$\cdot \begin{pmatrix} p & a & q \\ \psi' & \alpha' & -\kappa' \end{pmatrix} \begin{pmatrix} q & b & r \\ \kappa' & \beta' & \rho' \end{pmatrix} = \sum_c \sum_{\gamma,\gamma'} (2c+1)(-1)^{2c}(-1)^{-\gamma-\gamma'} \cdot$$
$$\cdot \begin{pmatrix} a & b & c \\ \alpha & \beta & \gamma \end{pmatrix} \begin{pmatrix} r & p & c \\ \rho & \psi & -\gamma \end{pmatrix} \begin{pmatrix} a & b & c \\ \alpha' & \beta' & \gamma' \end{pmatrix} \begin{pmatrix} r & p & c \\ \rho' & \psi' & -\gamma' \end{pmatrix} \tag{4.9}$$

and represents the so called *flip*, namely the bistellar move $[2 \to 2]^2_{bst}$, having taken into account the notation introduced in (2.16) (refer to the bottom of Fig. 5.1 for the corresponding picture). The identity corresponding to the remaining moves, namely $[1 \leftrightarrow 3]^2_{bst}$, reads

$$\sum_{q,r,p} (2q+1)(2r+1)(2p+1)(-1)^{2q+2r+2p} \sum_{\kappa,\kappa'} \sum_{\rho,\rho'} \sum_{\psi,\psi'} (-1)^{-\kappa-\kappa'}(-1)^{-\rho-\rho'} \cdot$$
$$\cdot (-1)^{-\psi-\psi'} \begin{pmatrix} p & a & q \\ \psi & \alpha & -\kappa \end{pmatrix} \begin{pmatrix} q & b & r \\ \kappa & \beta & -\rho \end{pmatrix} \begin{pmatrix} r & c & p \\ \rho & \gamma & -\psi \end{pmatrix} \cdot$$
$$\cdot \begin{pmatrix} p & a & q \\ \psi' & \alpha' & -\kappa' \end{pmatrix} \begin{pmatrix} q & b & r \\ \kappa' & \beta' & -\rho' \end{pmatrix} \begin{pmatrix} r & c & p \\ \rho' & \gamma' & -\psi' \end{pmatrix} =$$
$$= w_L^{-1} \begin{pmatrix} a & b & c \\ \alpha & \beta & \gamma \end{pmatrix} \begin{pmatrix} a & b & c \\ \alpha' & \beta' & \gamma' \end{pmatrix} \tag{4.10}$$

and these moves are depicted on the bottoms of Fig. 5.2 and Fig 5.3.

As a matter of fact, the state sum given in (4.7) and (4.8) is formally invariant under (a finite number of) topological operations represented by (4.9) and (4.10). Thus, from Pachner's theorem proved in [14], we conclude that it is a (PL) topological invariant. Its expression the can be easily evaluated also in the q-case (see Appendix 8.1 for the notation), providing us with a finite quantum invariant given by

$$Z^2_\chi(q) \equiv Z_\chi[M^2](q) \;=\; w_q^2 \, w_q^{-2\chi(M^2)}, \tag{4.11}$$

where $\chi(M^2)$ is the Euler characteristic of the manifold M^2 and $w_q^2 = -2k/(q-q^{-1})^2$.

The detail of the above calculation are explained in Appendix 8.2.

Coming now to the invariance of $Z_\chi[M^d]$ in (4.4), we could implement explicitly the bistellar moves in dimension d by means of suitable identities containing sums of products of 3jm double symbols, and such identities could be written down simply generalizing the fundamental relations given above in the 2-dimensional case. For what concerns the explicit calculation of $Z_\chi[M^d]$ we notice first that the auxiliary surface S associated with each T^d is built up by assembling $(d-2)$ triangles for each $\sigma^d \in T^d$, joined together through $(d-2)$ edges. Denoting by N_1^S and N_2^S the numbers of edges and triangles in S, respectively, the contribution from the factors in in (4.3) (after summation over j variables) amounts to $w_L^2 w_L^{2(N_1^S - N_2^S)}$. Since $N_1^S = (N_{d-1} + (d-2)N_d)(T^d)$ and $N_2^S = (d-1)N_d(T^d)$, for each finite value of L we obtain $Z^d[M^d] \;=\; w_L^{2[1+(-1)^{(d-1)}\chi(M^d)}$ (the quantum version given by substituting w_L with w_q). $\chi[M^d]$ is the Euler characteristic of the PL-manifold M^d and in the odd dimensional case we have $\chi = 0$, so that the invariant is trivially equal to w^2.

4.3 The TQFT associated with $Z_\chi[M^d]$.

A particular type of Topological Quantum Field Theory, connected to the Euler character (see [28]), turns out to be associated with the PL invariant model introduced in the previous sections. In this section we give a brief review on this subject.

We recall that the Euler character for a d dimensional compact manifold M without boundary can be defined also as $\chi(M) = \sum_{i=0}^{d}(-1)^i b_i(M)$, where b_i is the ith Betti number of the manifold, namely the dimension of the ith cohomology group. By Poincare-Hodge duality $b_i = b_{d-i}$, and the Hodge theorem equates the dimension of $H^i(M, R)$ to the number of independent forms of degree i on the Riemannian manifold (M, g). Witten noticed that one may profitably generalize the construction of the de Rham cohomology. Let d_s be defined as $d_s = \exp^{-sV} d(\exp^{sV})$, where d is the usual exterior derivative and where $V : M \to R$ is a Morse function on the manifold, namely V has only isolated critical points and these must be non-degenerate ($\det(V'') \neq 0$ at these points). The adjoint is defined similarly as $d_s^\star = \exp^{sV} d^\star(\exp^{-sV})$. Both d_s and $d_s^\star$ are nilpotent. The cohomology groups defined by d_s are isomorphic to the de Rham groups and we denote them by $H^i(s)$. The Laplacian in this case is $\Delta_s = (d_s + d_s^\star)^2$. To express it in a compact explicit form, we introduce creation and annihilation operators $a^{\star i}$, a^i at each point p of M. These operators satisfy the algebra $\{a^i, a^{\star j}\} = g^{ij}$ where g^{ij} is the metric, and they have the following geometric interpretation. The $a^i(p)$ may be thought of as forming an orthonormal basis of tangent vectors at the point p. Being operators, they act on the exterior algebra at p by interior multiplication. The $a^{\star i}(p)$ are the adjoint counterparts, acting by exterior multiplication by the one-form dual to $a^i(p)$. In this basis we have

$$d\alpha = a^{\star i}\partial\alpha/\partial\phi^i, \; d^\star\alpha = -a^i\partial\alpha/\partial\phi^i + \Gamma_{ijk}a^i a^{\star i} a^k \alpha$$

where Γ_{ijk} are the connection coefficients associated with g^{ij} and ϕ^i the local chart about p. With this notation we obtain

$$\Delta_s = \Delta + s^2 g^{ij}\frac{\partial V}{\partial\phi^i}\frac{\partial V}{\partial\phi^j} + s\frac{D^2V}{D\phi^i D\phi^j}[a^{\star i}, a^j],$$

were D represents the covariant derivative with respect the metric g^{ij} and Δ is the standard Laplacian. The Euler character may now be expressed as

$$\chi(M) = \sum_{i=0}^{d}(-1)^i b_i(s)$$

where $b_i(s)$ are the Betti numbers of the chomology groups $H_i(s)$. Thus, it makes sense to rewrite the above quantity once more as

$$\chi(M) = Tr_h[(-1)^F]$$

where the trace is restricted over the harmonic modes of Δ_s; $(-1)^F$ gives $+1$ on even forms and -1 on odd forms, and commutes with the Laplacian.

To put the trace in a more useful form, one would like to relax the restriction that it is taken only over harmonic modes; on the other hand, we would like to extend the trace to be over all eigenvalues of the Laplacian. This is possible as far as the non zero modes are paired with opposite eigenvalues of $(-1)^F$. But this is exactly what happens. The trace may now be extended over the complete spectrum of the Laplacian as the eigenvectors of positive and negative eigenvalue of $(-1)^F$ cancel between each other. A term that allows the cutting out of large modes is offered by the exponential damping factor $\exp^{-\beta\Delta_s}$, for $\beta > 0$. The final form for the Euler character as a trace over differential forms is

$$\chi(M) = Tr[(-1)^F \exp^{-\beta\Delta_s}]. \tag{4.12}$$

Now, thinking of Δ_s as a Hamiltonian, say H_s, we may give a path integral representation for this trace by setting

$$\chi(M) = Tr[(-1)^F \exp^{-\beta\Delta_s}] = \int_\phi \exp^{-S}. \tag{4.13}$$

where, owing to the presence of $(-1)^F$ in the trace, the boundary condition are periodic for all fields and the action is the action of supersymmetric quantum mechanics which reads

$$\begin{aligned} S = \int d\tau[i(\tfrac{d\phi^i}{d\tau} + sg^{ij}(\phi)\tfrac{\partial V}{\partial\phi^j}B_i + \tfrac{1}{2}g^{ij}(\phi)B_iB_j \\ +\tfrac{1}{4}R_{ijkl}\hat{\psi}^i\psi^k\hat{\psi}^j\psi^l - i\hat{\psi}_i(\delta^i_j\tfrac{D}{D\tau} + sg^{ij}(\phi)\tfrac{D^2V}{D\phi^k\phi^j})\psi^j] \end{aligned} \tag{4.14}$$

Here ϕ^i are coordinates on the Riemannian manifold (M, g), R_{ijkl} is the curvature tensor, ψ^i and $\hat{\psi}^j$ are the Grassmann odd coordinates of the particle, V is a function on M and s a parameter. We choose the spinor to be real. β is incorporated on the right hand side as a circumference of the time circle. The trace does not depend on the parameter β: this can be seen from the path integral point of view using the argument that the variation with respect to β gives, on the right hand side of (4.14), the expectation value of Q-exact term, with Q the supersymmetry generator, and hence vanishes.

Chapter 5

Invariants of $(M^d, \partial M^d)$ induced by Z_{χ}^{d-1}.

In this chapter we construct new combinatorial invariants of the pairs $(M^d, \partial M^d)$ starting from the information carried by the boundary manifold, where we assume that the invariant Z_{χ}^{d-1} is given. We begin by analyzing the $d = 3, 4$ cases that represent generalizations in the presence of boundaries of the models by Ponzano and Regge and by Turaev and Viro [2] [3] in $d = 3$ and by Crane-Yetter-Ooguri [15] [6] in $d = 4$, respectively. These two cases are interesting by themselves since all the calculation can be done analytically, although in $d = 4$ we employ also the graphical method (which in turns is extensively used in dimension d). The key point in our discussion is that, starting from the expression of Z_{χ}^{d-1} and considering the state sum for a simplicial sphere $S^{d-1} \cong \partial\sigma^d$, we get in fact a sort of square of the symbol to be associated with $\sigma^d \in T^d$, where $(T^d, \partial T^d)$ is a triangulation of for the pair $(M^d, \partial M^d)$. In other words the contribution to the invariant due to σ^d, $Z[\sigma^d, S^{d-1}]$, is equal to $Z_{\chi}[S^{d-1}]$. This means, equivalently, that a "square root" of the symbol associate with $\sigma^{d-1} \in T^{d-1} = \partial T^d$ in the definition of Z_{χ}, is the fundamental block to built up the symbol associated with σ^d in the definition of $Z[(M^d, \partial M^d)]$.

5.1 The invariant $Z[(M^3, \partial M^3)]$.

The Ponzano–Regge partition function [2] for a closed manifold M^3 can be written simply as

$$Z_{PR}[M^3] = \lim_{L\to\infty} \sum_{\{T^3(j), j \leq L\}} Z[T^3(j) \to M^3; L], \tag{5.1}$$

where the sum is extended to all assignments of $SU(2)$ spin variables such that each of them is not greater than the cut–off L, and each term under the sum is given by

$$Z[T^3(j) \to M^3; L] = \Lambda(L)^{-N_0} \prod_{A=1}^{N_1} (-1)^{2j_A}(2j_A+1) \prod_{B=1}^{N_3} (-1)^{\sum_{p=1}^{6} j_p} \left\{ \begin{array}{ccc} j_1 & j_2 & j_3 \\ j_4 & j_5 & j_6 \end{array} \right\}_B . \quad (5.2)$$

N_0 is the number on vertices in the triangulation. Notice that there appears a factor $\Lambda(L)^{-1}$ for each vertex in $\partial T^3(j', m)$, with $\Lambda(L) \equiv 4L^3/3C$, C an arbitrary constant.

As is well known, the above state sum gives the semiclassical partition function of Euclidean 3-gravity with an action discretized according to Regge's prescription [1]. Moreover, it is formally invariant under any finite set of *bistellar moves* performed on 3-simplices in $T^3(j)$ (cfr. [14] and Chapter 2). It is a classical result (see *e.g.* [2] and [7]) that such moves can be expressed algebraically in terms of the Biedenharn–Elliott identity given in (3.4) (representing the moves (2 tetrahedra) $\leftrightarrow$ (3 tetrahedra)) and of both the B-E identity and the orthogonality conditions for $6j$ symbols given in (3.2), which represent the barycentic move together with its inverse, namely (1 tetrahedron) $\leftrightarrow$ (4 tetrahedra).

Thus, owing to the theorem by Pacner given in [14], the state sum (5.1) is formally an invariant of the PL-structure of M^3 (the regularized counterpart being the Turaev–Viro invariant found in [3]).

Following [12] and [13], the connection between a recoupling scheme of $SU(2)$ angular momenta and the combinatorial structure of a compact, 3-dimensional simplicial pair $(M^3, \partial M^3)$ can be established by considering *colored* triangulations which allow us to specialize the map (2.8) according to

$$(T^3(j), \partial T^3(j', m)) \longrightarrow (M^3, \partial M^3). \quad (5.3)$$

This map represents a triangulation associated with an admissible assignment of both spin variables to the collection of the edges ($(d-2)$-simplices) in $(T^3, \partial T^3)$) and of momentum projections to the subset of edges lying in ∂T^3. The collective variable $j \equiv \{j_A\}$, $A = 1, 2, \ldots, N_1$, denotes all the spin variables, n_1' of which are associated with the edges in the boundary (for each A:

$j_A = 0, 1/2, 1, 3/2, \ldots$ in $\hbar$ units). Notice that the last subset is labelled both by $j' \equiv \{j'_C\}$, $C = 1, 2, \ldots, n'_1$, and by $m \equiv \{m_C\}$, where m_C is the projection of j'_C along the fixed reference axis (of course, for each m, $-j \leq m \leq j$ in integer steps). The consistency in the assignment of the j, j', m variables is ensured if we require that

- each 3-simplex σ^3_B, $(B = 1, 2, \ldots, N_3)$, in $(T^3, \partial T^3)$ must be associated, apart from a phase factor, with a $6j$ symbol of $SU(2)$, namely

$$\sigma^3_B \longleftrightarrow (-1)^{\sum_{p=1}^{6} j_p} \left\{ \begin{array}{ccc} j_1 & j_2 & j_3 \\ j_4 & j_5 & j_6 \end{array} \right\}_B ; \tag{5.4}$$

- each 2-simplex σ^2_D, $D = 1, 2, \ldots, n'_2$ in ∂T^3 must be associated with a Wigner $3jm$ symbol of $SU(2)$ according to

$$\sigma^2_D \longleftrightarrow (-1)^{(\sum_{s=1}^{3} m_s)/2} \left(\begin{array}{ccc} j'_1 & j'_2 & j'_3 \\ m_1 & m_2 & -m_3 \end{array} \right)_D . \tag{5.5}$$

Then the following state sum can be defined

$$\begin{aligned} Z^3_{PR} \equiv Z_{PR}[(M^3, \partial M^3)] = \\ = \lim_{L \to \infty} \sum_{\left\{ \begin{array}{c} (T^3, \partial T^3) \\ j, j', m \leq L \end{array} \right\}} Z[(T^3(j), \partial T^3(j', m)) \to (M^3, \partial M^3); L], \end{aligned} \tag{5.6}$$

where

$$\begin{aligned} & Z[(T^3(j), \partial T^3(j', m)) \to (M^3, \partial M^3); L] = \\ & = \Lambda(L)^{-N_0} \prod_{A=1}^{N_1} (-1)^{2j_A} (2j_A + 1) \prod_{B=1}^{N_3} (-1)^{\sum_{p=1}^{6} j_p} \left\{ \begin{array}{ccc} j_1 & j_2 & j_3 \\ j_4 & j_5 & j_6 \end{array} \right\}_B \cdot \\ & \cdot \prod_{D=1}^{n'_2} (-1)^{(\sum_{s=1}^{3} m_s)/2} \left(\begin{array}{ccc} j'_1 & j'_2 & j'_3 \\ m_1 & m_2 & -m_3 \end{array} \right)_D . \end{aligned} \tag{5.7}$$

N_0, N_1, N_3 denote respectively the total number of vertices, edges and tetrahedra in $(T^3(j), \partial T^3(j', m))$, while n'_2 is the number of 2-simplices lying in $\partial T^3(j', m)$.

We may notice that if we consider a PL ball represented the pair $(\sigma^3, \partial\sigma^3)$ we would obtain exactly the square of one 6j symbol in the previous state sum. This would be the same value associated with a simplicial 2-sphere in the invariant Z^2_χ.

Having to do with simplicial pair, we must now implement algebraically the elementary boundary operations in $d = 3$ (see [11] and the example in chapter 2). In [12] identities representing the three types of elementary shellings (and their inverse moves) for the 3-dimensional triangulations given in (5.3) were established.

The first identity represents, according to (2.17), the move $[2 \to 2]^3_{sh}$. The topological content of this identity is drawn on the top of Fig. 5.1, while its formal expression reads

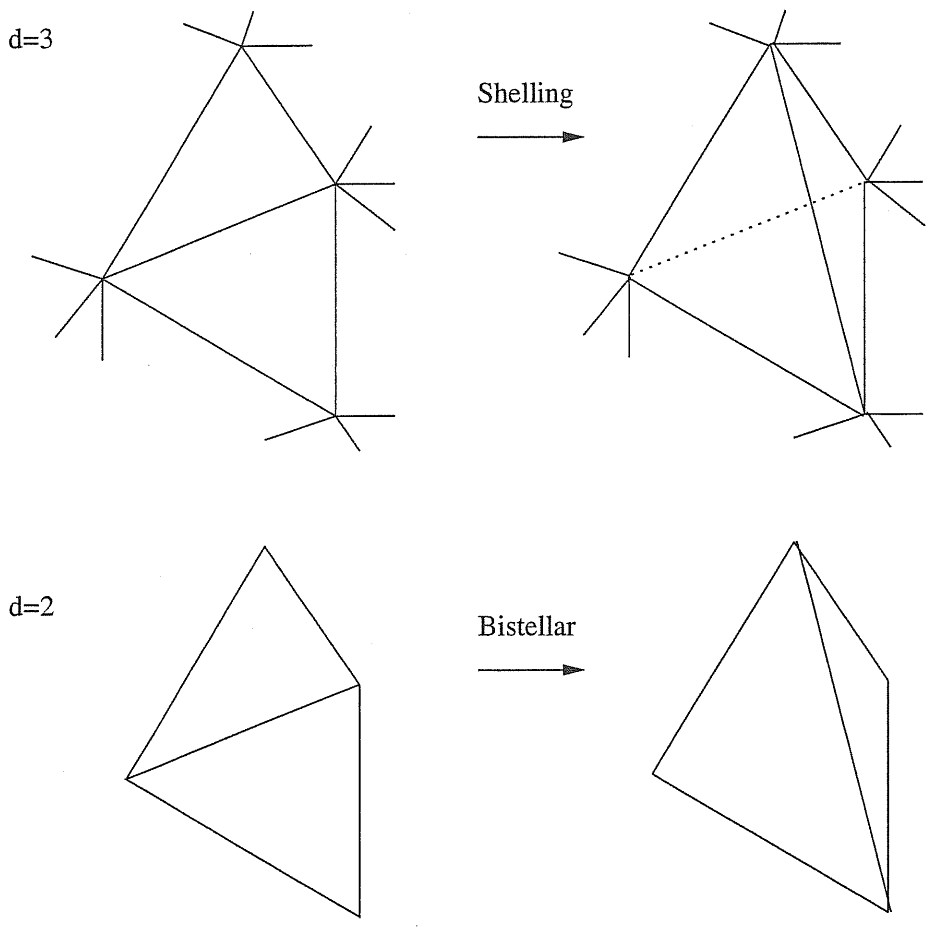

Fig. 5.1: Shelling $[2 \to 2]^3_{sh}$ and the corresponding bistellar $[2 \to 2]^2_{bst}$.

$$\sum_{c\gamma}(2c+1)(-1)^{2c-\gamma}\begin{pmatrix} a & b & c \\ \alpha & \beta & \gamma \end{pmatrix}\begin{pmatrix} c & r & p \\ -\gamma & \rho' & \psi \end{pmatrix}(-1)^{\Phi}\begin{Bmatrix} a & b & c \\ r & p & q \end{Bmatrix} =$$

$$= (-1)^{-2\rho}\sum_{\kappa}(-1)^{-\kappa}\begin{pmatrix} p & a & q \\ \psi & \alpha & -\kappa \end{pmatrix}\begin{pmatrix} q & b & r \\ \kappa & \beta & -\rho' \end{pmatrix}, \qquad (5.8)$$

where Latin letters a, b, c, r, p, q denote angular momentum variables, Greek letters $\alpha, \beta, \gamma, \rho, \psi, \kappa$ are the corresponding momentum projections and $\Phi \equiv a + b + c + r + p + q$.

Notice that here we agree that all j variables appearing in $3jm$ symbols are associated with edges lying in ∂T^3 in a given configuration, while j arguments of the $6j$ may belong either to ∂T^3 (if they have a counterpart in the nearby $3jm$) or to $int(T^3)$.

The other identities can be actually derived (up to suitable regularization factors) from (5.8) and from both the orthogonality conditions for the $6j$ symbols and the completeness conditions for the $3jm$ symbols (cfr. Chapter 3). In particular, the shelling $[1 \to 3]^3_{sh}$ is sketched on the top of Fig. 5.2 and the corresponding identity is given by

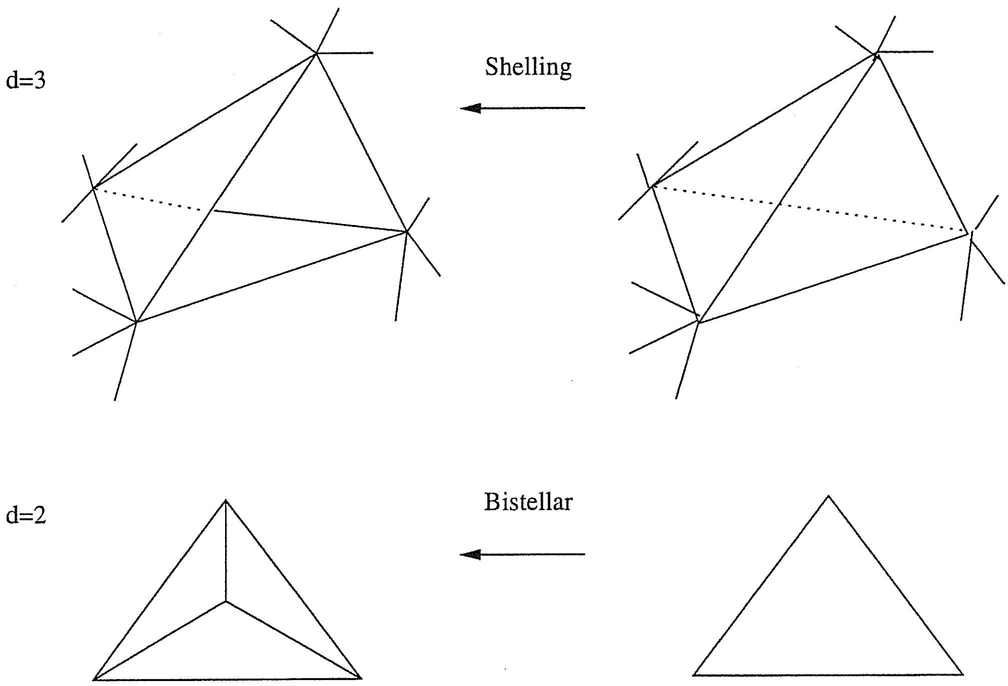

Fig. 5.2: Shelling $[1 \to 3]^3_{sh}$ and the corresponding bistellar $[1 \to 3]^2_{bst}$.

$$\begin{pmatrix} a & b & c \\ \alpha & \beta & \gamma \end{pmatrix} (-1)^{\Phi} \begin{Bmatrix} a & b & c \\ r & p & q \end{Bmatrix} =$$

$$= \sum_{\kappa\psi\rho} (-1)^{-\psi-\kappa-\rho} \begin{pmatrix} p & a & q \\ \psi & \alpha & -\kappa \end{pmatrix} \begin{pmatrix} q & b & r \\ \kappa & \beta & -\rho \end{pmatrix} \begin{pmatrix} r & c & p \\ \rho & \gamma & -\psi \end{pmatrix}. \quad (5.9)$$

Finally, the shelling $[3 \to 1]^3_{sh}$ is depicted on the top of Fig. 5.3 and the associated identity reads

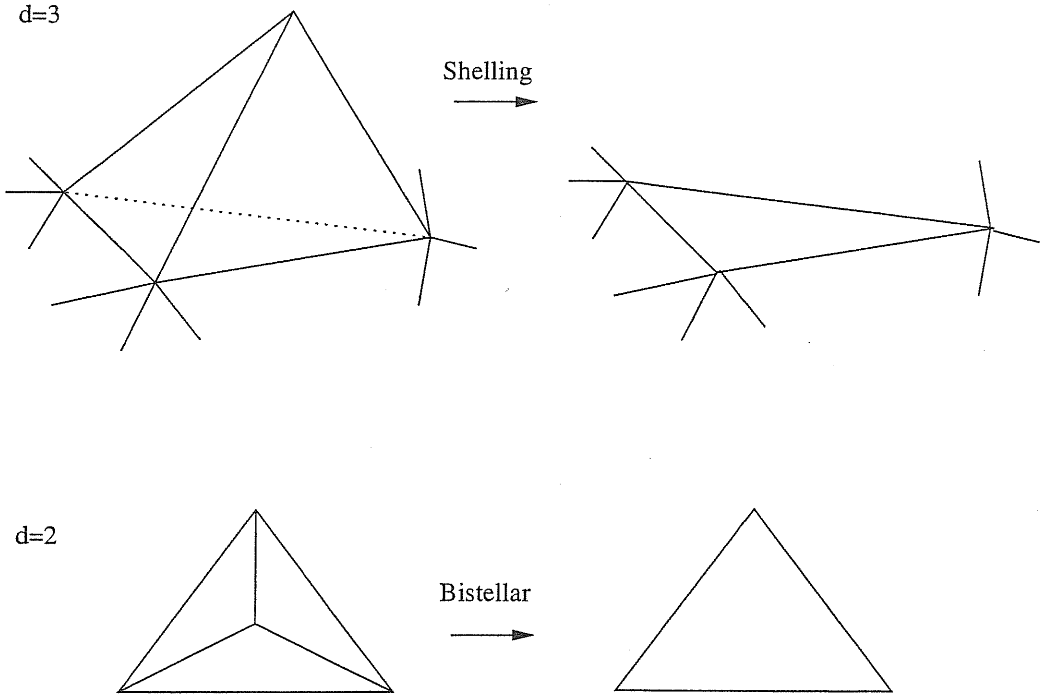

Fig. 5.3: Shelling $[3 \to 1]^3_{sh}$ and the corresponding bistellar $[3 \to 1]^2_{bst}$.

$$\Lambda(L)^{-1} \textstyle\sum_{q\kappa',p\psi',r\rho'} (-1)^{-\psi'-\kappa'-\rho'} (-1)^{2(p+q+r)} (2p+1)(2r+1)(2q+1) \begin{pmatrix} a & p & q \\ \alpha & -\psi' & \kappa' \end{pmatrix} \cdot$$

$$\begin{pmatrix} b & q & r \\ \beta & -\kappa' & \rho' \end{pmatrix} \begin{pmatrix} c & r & p \\ \gamma & -\rho' & \psi' \end{pmatrix} (-1)^{\Phi} \begin{Bmatrix} a & b & c \\ r & p & q \end{Bmatrix} n = \begin{pmatrix} b & a & c \\ \beta & \alpha & \gamma \end{pmatrix}, \quad (5.10)$$

where $\Lambda(L)$ is defined as in (5.7).

Notice that in each of the above identities we can read also the corresponding inverse shelling, namely the operation consisting in the attachment of a 3-simplex to suitable component(s) in ∂T^3, simply by exchanging the role of internal and external labellings.

Comparing the above identities representing the elementary shellings and their inverse moves with the expression given in (5.7), we see that the state sum $Z_{PR}\ [(M^3, \partial M^3)]$ in (5.6) is formally invariant both under (a finite number of) bistellar moves in the interior of M^3, and under (a finite number of) elementary boundary operations. Following now [11] we are able to conclude that (5.6) is indeed an invariant of the PL-structure (as well as a topological invariant, since we are dealing with 3-dimensional PL-manifolds).

5.2 The invariant $Z[(M^4, \partial M^4)]$.

In this section we revise first the results found in [15] (see also [6] and [49]) concerning the q-invariant $Z_{CY}[M^4](q)$ for a closed PL-manifold M^4. However, for the sake of simplicity, we limit ourselves to a detailed analysis of the ($q = 1$) case, and moreover we write down the expression of the resulting $Z_{CY}[M^4] \doteq Z_{CY}[M^4](q)|_{q=1}$ in terms of the $3jm$ symbols appearing in the definition of the $SU(2)$ $15j$ symbol of the second type (cfr Section 3.4). This last step turns out to be crucial in order to define the new invariant $Z_{CY}[(M^4, \partial M^4)]$ for a PL-pair $(M^4, \partial M^4)$.

Thus, consider a *multi-colored* triangulation of a given closed PL-manifold M^4 denoting it by the map

$$T^4(j_{\sigma^2},\ J_{\sigma^3})\ \longrightarrow\ M^4, \tag{5.11}$$

where j_{σ^2} is an $SU(2)$-coloring on the 2-dimensional simplices σ^2 in T^4 and J_{σ^3} is an $SU(2)$-coloring on tetrahedra $\sigma^3 \subset \sigma^4 \in T^4$ (recall that an ordering on the vertices of each 4-simplex σ^4 has to be chosen; however, the final expression of the state sum turns out to be independent of this choice). The consistency in the assignment of the $\{j, J\}$ spin variables is ensured for a fixed ordering if we require that

- each 3-simplex ${\sigma^3}_a \subset \sigma^4$ ($a = 1, 2, \ldots, N_3$, N_3 being the number of 3-simplices in T^4) must be associated, apart from a phase factor, with a product of two $3jm$ symbols, namely

$${\sigma^3}_a \longleftrightarrow \begin{pmatrix} j_1 & j_2 & J_a \\ m_1 & m_2 & m_a \end{pmatrix} \begin{pmatrix} j_3 & j_4 & J_a \\ m_3 & m_4 & -m_a \end{pmatrix}; \tag{5.12}$$

- each 4-simplex $\sigma^4 \in T^4$ must be associated, apart from a phase factor, with a summation of the product of ten suitable $3jm$ symbols (cfr. (3.6) and also below for its explicit expression), giving rise to a $15j$ symbol of the second type which we represent for short as

$$\sigma^4 \longleftrightarrow [J_a, J_b, J_c, J_d, J_e]_{\sigma^4}, \tag{5.13}$$

where $J_a, \ldots, J_e$ are labellings assigned to the five tetrahedra $\sigma_a, \ldots, \sigma_e \subset \sigma^4$.

Then we can define the following state sum

$$\begin{aligned} & Z[T^4(j_{\sigma^2}, J_{\sigma^3}) \to M^4; L] = \\ & = \Lambda(L)^{N_0 - N_1} \prod_{\sigma^2 \in T^4} (-1)^{2j_{\sigma^2}} (2j_{\sigma^2} + 1) \prod_{\sigma^3 \in T^4} (-1)^{2J_{\sigma^3}} (2J_{\sigma^3} + 1) \cdot \\ & \cdot \prod_{\sigma^4 \in T^4} [J_a, J_b, J_c, J_d, J_e]_{\sigma^4}, \end{aligned} \tag{5.14}$$

where N_0, N_1 are the number of vertices and edges in T^4, respectively. The $15j$ symbol associated with each 4-simplex is given explicitly by

$$\begin{aligned} & [J_a, J_b, J_c, J_d, J_e]_{\sigma^4} \doteq \{15j\}_{\sigma^4}(J) = \\ & = \sum_m (-1)^{\sum m} \begin{pmatrix} j_1 & j_2 & J_a \\ m_1 & m_2 & m_a \end{pmatrix} \begin{pmatrix} j_3 & j_4 & J_a \\ m_3 & m_4 & -m_a \end{pmatrix} \begin{pmatrix} j_5 & j_6 & J_b \\ m_5 & m_6 & m_b \end{pmatrix} \cdot \\ & \cdot \begin{pmatrix} j_3 & j_7 & J_b \\ -m_3 & m_7 & -m_b \end{pmatrix} \begin{pmatrix} j_5 & j_8 & J_c \\ -m_5 & m_8 & m_c \end{pmatrix} \begin{pmatrix} j_1 & j_9 & J_c \\ -m_1 & m_9 & -m_c \end{pmatrix} \cdot \\ & \cdot \begin{pmatrix} j_6 & j_{10} & J_d \\ -m_6 & m_{10} & -m_d \end{pmatrix} \begin{pmatrix} j_2 & j_8 & J_d \\ -m_2 & -m_8 & -m_d \end{pmatrix} \begin{pmatrix} j_7 & j_{10} & J_e \\ -m_7 & -m_{10} & -m_e \end{pmatrix} \cdot \\ & \cdot \begin{pmatrix} j_4 & j_9 & J_e \\ -m_4 & -m_9 & -m_e \end{pmatrix}, \end{aligned} \tag{5.15}$$

where the summation is extended to all admissible values of the m variables, and the planar diagram corresponding to the symbol is sketched in Fig. 5.4.

It can be shown (see [15], [19]) that the expression

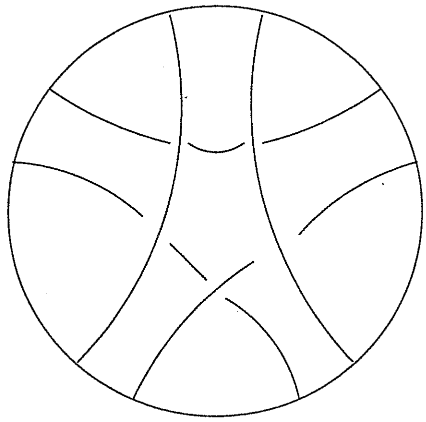

Fig. 5.4: Diagrammatic representation of the 15j symbol.

$$Z_{CY}[M^4] = \lim_{L\to\infty} \sum_{\left\{ \begin{array}{c} T^4(j,J) \\ j,J\leq L \end{array} \right\}} Z[T^4(j_{\sigma^2},J_{\sigma^3}) \to M^4; L] \tag{5.16}$$

is formally a PL-invariant, and that its value is given by $\Lambda(L)^{\chi(M^4)/2}\ K^{\sigma(M^4)}$, where $\chi(M^4)$, $\sigma(M^4)$ are the Euler characteristic and the signature of M^4 respectively, and K is a constant.

Following [39] the former state sum can be generalized to the case of a compact 4-dimensional PL-pair by considering the map

$$(T^4(j_{\sigma^2},J_{\sigma^3}), \partial T^4(j'_{\sigma^2},J'_{\sigma^3};m_{\sigma^2},m_{\sigma^3})) \longrightarrow (M^4,\partial M^4), \tag{5.17}$$

where $\{j_{\sigma^2},J_{\sigma^3}\}$ denotes the entire set of spin variables, ranging from 1 to N_2 and from 1 to N_3, respectively. The subset $\{j'_{\sigma^2},J'_{\sigma^3}\}\subset\{j_{\sigma^2},J_{\sigma^3}\}$ contains the colorings of the subsimplices in ∂T^4, the corresponding magnetic numbers of which can be collectively denoted by $m\equiv\{m_{\sigma^2},m_{\sigma^3}\}$ since no confusion can arise. The assignment of the above variables turns out to be consistent if we agree with the statements in (5.13)(for all $\sigma^4\in(T^4,\partial T^4)$, taking into account the fact that some of the J labels may become J' for those 4-simplices which have component(s) in ∂T^4)and with (5.12)(for 3-simplices in the interior of the triangulation). Moreover, we require that

- each 3-simplex ${\sigma^3}_a\subset\sigma^4$ lying in the boundary ∂T^4 must be associated, apart from a phase factor, with the following product of $3jm$ symbols

$$\sigma^3{}_a \longleftrightarrow \begin{pmatrix} j'_1 & j'_2 & J'_a \\ m_1 & m_2 & m_a \end{pmatrix} \begin{pmatrix} j'_3 & j'_4 & J'_a \\ m_3 & m_4 & -m_a \end{pmatrix}. \tag{5.18}$$

With these premises, we consider now the following expression.

$$Z[(M^4, \partial M^4)] = \lim_{L\to\infty} \sum_{\left\{\begin{array}{c} T^4, \partial T^4 \\ j, J, m \le L \end{array}\right\}} Z(T^4(j,J), \partial T^4(j', J'; m) \to (M^4, \partial M^4); L), \tag{5.19}$$

where we have used a shorthand notation instead of (5.17), and where

$$\begin{aligned} &Z[(T^4(j,J), \partial T^4(j', J', ; m)] \to (M^4, \partial M^4); L] = \\ &= \Lambda(L)^{N_0 - N_1} \prod_{all\, \sigma^2} (-1)^{2j_{\sigma^2}} (2j_{\sigma^2} + 1) \prod_{all\, \sigma^3} (-1)^{2J_{\sigma^3}} (2J_{\sigma^3} + 1) \cdot \\ &\cdot \prod_{all\, \sigma^4} \{15j\}_{\sigma^4}(J, J') \prod_{\sigma^3 \in \partial T^4} (-1)^{\sum m_{j'}/2 + \sum m_{J'}} \begin{pmatrix} j'_1 & j'_2 & J'_a \\ m_1 & m_2 & m_a \end{pmatrix} \cdot \\ &\cdot \begin{pmatrix} j'_3 & j'_4 & J'_a \\ m_3 & m_4 & -m_a \end{pmatrix}. \end{aligned} \tag{5.20}$$

We note that, if we consider the pair $(\sigma^4, \partial\sigma^4 \cong S^3)$, the state sum given above amounts to the square of one 15j symbol and the invariants $Z_\chi[S^3]$ and $Z_4[(\sigma^d, S^3)]$ coincide.

As discussed in *Chapter 2*, for a PL-pair in dimension d there exist d different types of elementary shellings (and d inverse shellings), parametrized by the number n_{d-1} of faces in a boundary d-simplex according to (2.17). Thus in the present case we are dealing with four different shellings, $n_3 = 1, 2, 3, 4$ being the number of tetrahedra in ∂T^4 which are going to disappear (together with the underlying 4-simplex), respectively. The diagrammatic representations of the moves $[1 \to 4]^4_{sh}$, $[2 \to 3]^4_{sh}$, $[3 \to 2]^4_{sh}$, $[4 \to 1]^4_{sh}$ are displayed in Fig. 5.5, Fig. 5.6, Fig. 5.7, Fig. 5.8, respectively, where we have made use of diagrammatical relations to handle products of $3jm$ symbols (see Fig. 5.9 and Fig. 5.10). For the sake of completeness, the identities corresponding to the four types of *elementary shellings* in $d = 4$ are given explicitly in Appendix 8.3.

According to these remarks, $Z[(M^4, \partial M^4)]$ in (5.19) turns out to be formally equivalent under the action of a finite set of the above operations and their inverse moves and thus, owing to the

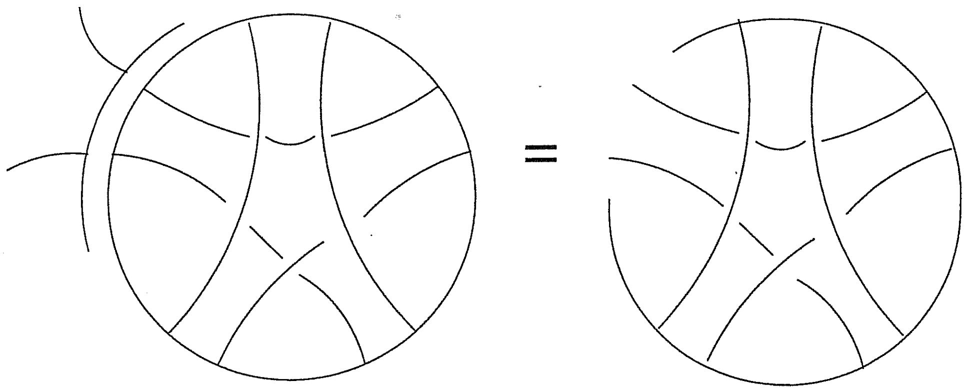

Fig. 5.5: Diagrammatic representation of the move $[1 \to 4]^4_{sh}$.

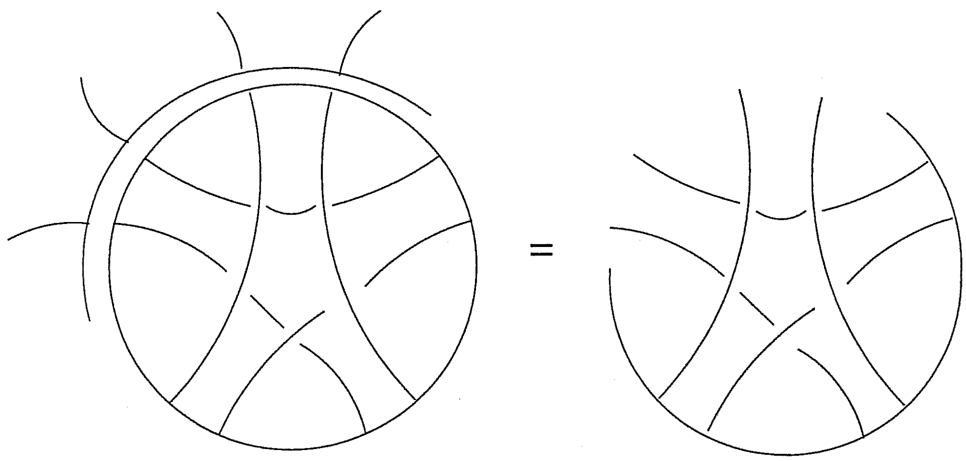

Fig. 5.6: Diagrammatic representation of the move $[2 \to 3]^4_{sh}$.

theorem proved in [11], it defines an invariant of the PL-structure. Its q-deformed counterpart, $Z[(M^4, \partial M^4)](q)$, can be worked out according to the prescription given in Appendix 8.1 and represents a well–defined quantum invariant.

We may notice also that, since (5.19) reduces to (5.16) when $\partial M^4 = \emptyset$, $Z[(M^4, \partial M^4)]$ must be invariant under bistellar moves performed in $int(T^4)$ too. However, we will show in *Chapter 6* that the equivalence of our d-dimensional $Z[(M^d, \partial M^d)]$ under elementary shellings implies (in a non trivial way) the invariance under bistellar moves of the state sum induced by setting $\partial M^d = \emptyset$.

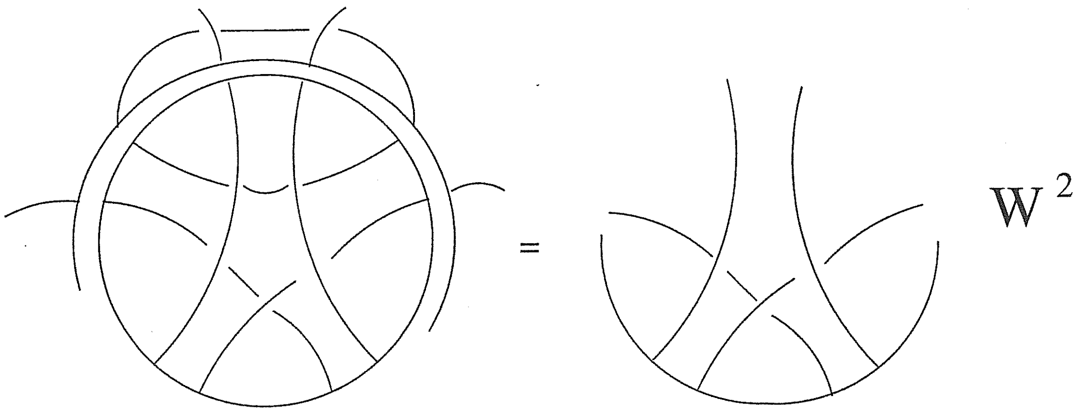

Fig. 5.7: Diagrammatic representation of the move $[3 \rightarrow 2]^4_{sh}$.

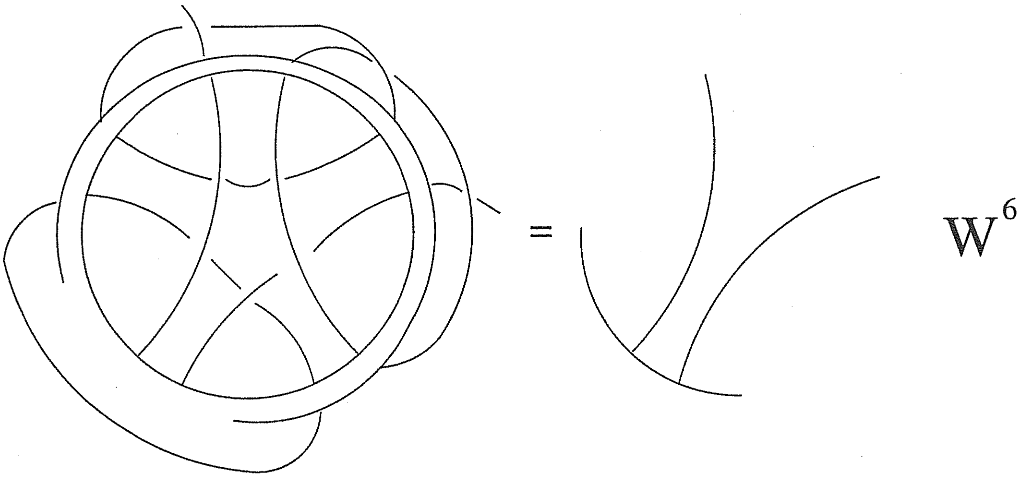

Fig. 5.8: Diagrammatic representation of the move $[4 \rightarrow 1]^4_{sh}$.

5.3 $Z^d[(M^d, \partial M^d)]$ and its equivalence under elementary boundary operations.

According to the program outlined in *steps 1),2)* of the Introduction of the Thesis, we build up in the following a state sum for a pair $(T^d, \partial T^d)$ induced by examining the expression of $Z_\chi[\partial M^d \equiv M^{d-1}]$, with $Z_\chi[M^{d-1}]$ given in (4.3) of *Chapter 4*. The second part of the present section will be devoted to the proof that such a state sum is actually independent of the triangulation chosen, and thus the invariant $Z[(M^d, \partial M^d)]$ is well defined in any dimension d.

We learnt from the procedure followed in the previous Sections that once we give the *double* symbol associated with the $(d-1)$-simplex in a given closed T^{d-1}, we can recover the contribution from

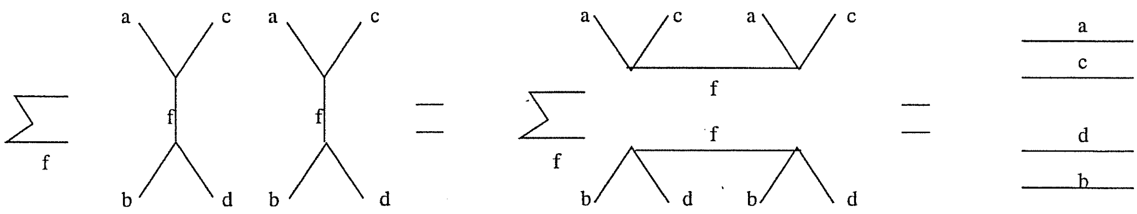

Fig. 5.9: Relation involving the product of two couple of 3jm symbols.

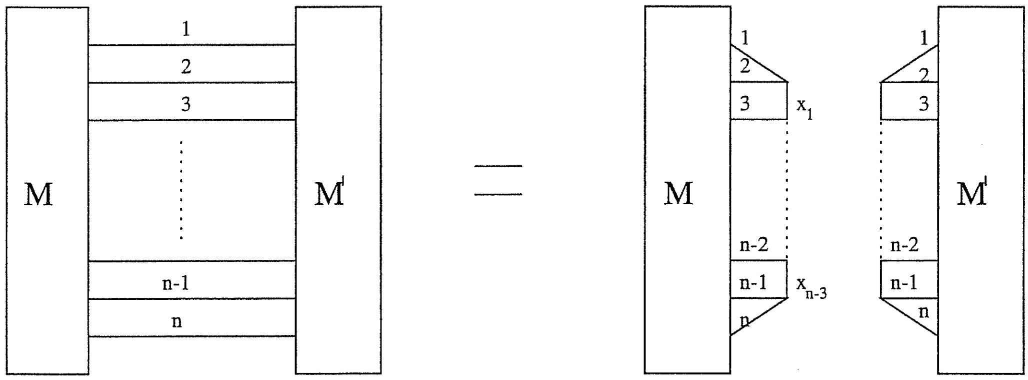

Fig. 5.10: Diagrammatical representation of the general relation involving the product of two quantity containing products of many 3jm symbols, where M and M' represent the rest of the diagram leaved unchanged by the relation.

a single d-simplex in $(T^d, \partial T^d \equiv T^{d-1})$ by taking first the *squared root* of the symbol itself. Then the recoupling symbol to be associated with the d-dimensional fundamental block is obtained by summing over the free m entries the product of $(d+1)$-contributions from its faces, with suitable j labels. In Z^2_χ and Z^3_χ the double symbol, used like fundamental blocks to define the invariants, looks like a square of some sub–symbol. Taking the squared root means that we pick up just one of the sub–symbols (*e.g.* either the Wigner symbol with m entries in (4.6) or the product of two Wigner symbols with m entries in the $d = 3$ case). By summing over all m entries the product of four sub–symbols with suitable j labellings and phase factors in $d = 3$ we get the expression of the $6j$ symbol which enters $Z_{PR}[M^3]$. In turn, a summation over m variables of the product of five sub–symbols with suitable j labellings and phase factors in $d = 4$ reproduces the $15j$ symbol which represents the fundamental block in $Z_{CY}[M^4]$ (see (5.15)). Notice also that the procedure works with PL-pairs as well: we simply associate one of the former sub–symbol (with an m' coloring, say) with each $(d-1)$-simplex in ∂T^d.

The above remarks suggest how an algorithmic procedure for generating $Z[(M^d,\ \partial M^d)]$ from $Z_\chi[M^{d-1}]$ could be actually established. To this end, we consider first the structure of the double symbol associated with the fundamental block in (4.3), written for a closed triangulation T^{d-1}. The corresponding planar graph is shown in Fig. 5.11 (compare also Fig. 4.2): the diagram

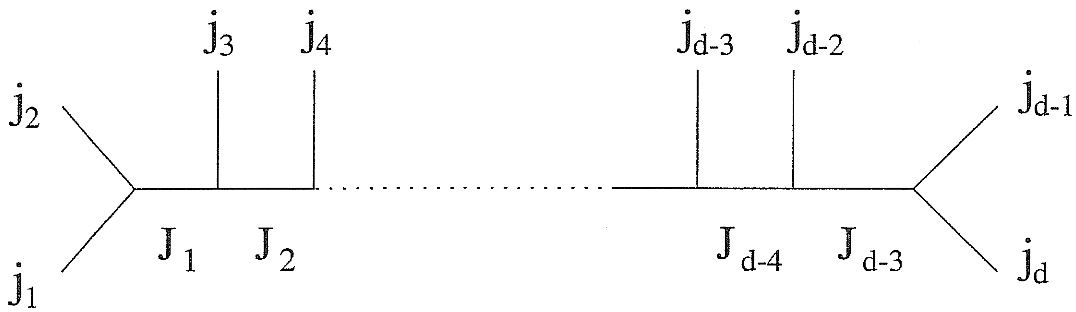

Fig. 5.11: Diagram corresponding to the fundamental block occurring in the recoupling symbol associated with the d-dimensional simplex.

includes d external legs, representing the faces of the $(d-1)$-simplex, and $(d-3)$ internal edges, the colorings of which are associated with the $(d-1)$-simplex itself, as explained below. The fundamental d-dimensional block which will enter the state sum is obtained by assembling $(d+1)$ simplices of dimension $(d-1)$ along their $(d-2)$-dimensional faces. Such a procedure can be described in some detail as follows. We first assign an overall ordering to the set of $(d-1)$-simplices of σ^d, namely we introduce $a = 1, 2, \ldots, d+1$. Then we denote by $j_1^a, j_2^a, \ldots, j_d^a$ the j labels of the external legs of the graph associated with the a-th $(d-1)$-simplex σ_a^{d-1} (the dimensionality of such colored faces is $(d-2)$). From a topological point of view, we are going to join a suitable number of other colored $(d-1)$-simplices along the faces of the chosen σ_a^{d-1} according to the rule: $\sigma_{a+1}^{d-1} \cap \sigma_a^{d-1} = j_d^a$, $\sigma_{a-1}^{d-1} \cap \sigma_a^{d-1} = j_1^a$, …, $\sigma_{a-i}^{d-1} \cap \sigma_a^{d-1} = j_{d-(i-1)}^a$, where $i = 1, 2, \ldots, d-3$. Thus the above prescription implies the identifications $j_d^a = j_d^{a+1}$, $j_1^a = j_d^{a-1}$, $j_{d-(i-1)}^a = j_i^{a+i}$ among j variables, while the glueing has to be accomplished by summing over all free m entries. The cyclic property of the joining implies that the procedure is actually independent of the label a chosen at the beginning. Moreover, by requiring that the unique $\tilde{\sigma}^d$, which shares σ_a^{d-1} with σ^d, has indeed the same graph associated with its own σ_a^{d-1}, but different magnetic numbers with respect to the other one, we obtain the diagram shown in Fig. 5.12 (which, by the above remarks, turns

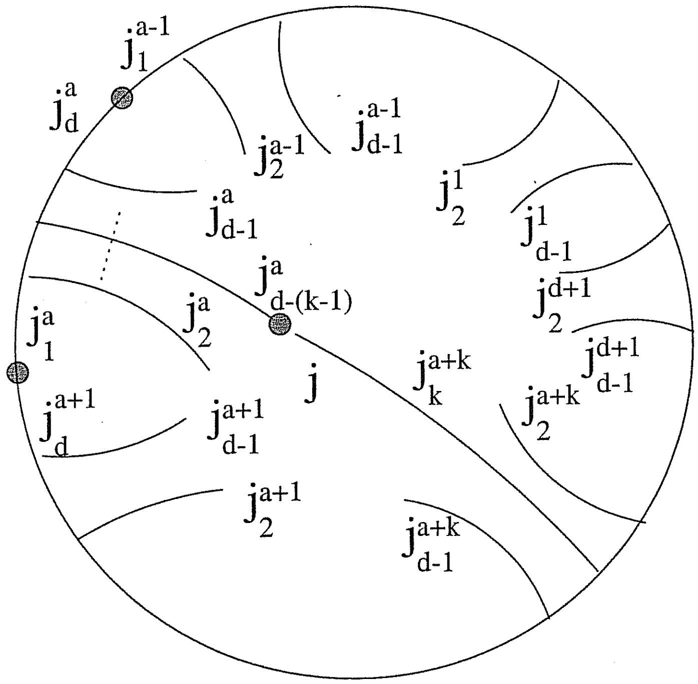

Fig. 5.12: Diagram representing the 3nj symbols with its internal structure.

out to be generic). A closer inspection of its combinatorial structure shows that we get in fact a $\{3(d-2)(d+1)/2\}j$ symbol written in terms of (sums of) $3jm$ symbols as in (3.6).

Collecting all the previous remarks we are now able to build up a state sum for $(T^d, \partial T^d)$ on the basis of the requirements listed below.

- For each $\sigma^d \in (T^d, \partial T^{d-1})$ we introduce:

  i) an admissible set of colorings on each of its $(d-2)$-faces, namely $j_1, j_2, \ldots, j_F$, where the value of the binomial coefficient

$$\binom{d+1}{2} \equiv F \tag{5.21}$$

  gives the number of $(d-2)$ subsimplices of a d-simplex;

  ii) other sets of $SU(2)$-colorings associated with each of its $(d-1)$-faces and denoted collectively by $\{J_{i_1}\}$, $\{J_{i_2}\}$, ..., $\{J_{i_{d+1}}\}$ (these sets are the counterparts of the five labels $J_a, \ldots, J_e$ used in (5.13)). Then we set

$$\sigma^d \longleftrightarrow \left\{\frac{3}{2}(d-2)(d+1)j\right\}_{\sigma^d} \doteq [\{J_{i_1}\}, \{J_{i_2}\}, \ldots, \{J_{i_{d+1}}\}]_{\sigma^d} \tag{5.22}$$

- For each $\sigma^{d-1} \subset \partial T^d$, denoting as usual by $\{j', J'\} \subset \{j, J\}$ the subsets of spin variables belonging to boundary components, and labelling as J_1', J_2', ..., J_C' ($C = d-3$) the variables associated with the internal legs of Fig. 5.11, we have the explicit correspondence

$$\sigma^{d-1} \longleftrightarrow \sum_{\mathcal{M}} (-1)^{\sum_{C=1}^{d-3} \mathcal{M}_C} \begin{pmatrix} j_1' & j_2' & J_1' \\ m_1 & m_2 & \mathcal{M}_1 \end{pmatrix} \cdot \\ \cdot \begin{pmatrix} J_1' & j_3' & J_2' \\ -\mathcal{M}_1 & m_3 & \mathcal{M}_2 \end{pmatrix} \cdots \begin{pmatrix} J_{d-4}' & j_{d-2}' & J_{d-3}' \\ -\mathcal{M}_{d-3} & m_{d-2} & \mathcal{M}_{d-3} \end{pmatrix} \cdot \\ \cdot \begin{pmatrix} J_{d-3}' & j_{d-1}' & j_d' \\ -\mathcal{M}_{d-3} & m_{d-1} & m_d \end{pmatrix}. \qquad (5.23)$$

Here we agree that each m variable is associated with the corresponding j' on the upper row, while an $\mathcal{M}$ entry is the magnetic number of the upper J', with the usual ranges of variations in both cases.

Then we can define the following state sum

$$Z[(T^d(j_{\sigma^{d-2}}, J_{\sigma^{d-1}}), \partial T^d(j'_{\sigma^{d-2}}, J'_{\sigma^{d-1}}; m, \mathcal{M}))] \rightarrow (M^d, \partial M^d); L] = \\ = w_L^{(-1)^d \Xi} \prod_{all\, \sigma^{d-2}} (-1)^{2j_{\sigma^{d-2}}} (2j_{\sigma^{d-2}} + 1) \prod_{all\, \sigma^{d-1}} \left(\prod_{C=1}^{d-3} (-1)^{2J_C} (2J_C + 1) \right)_{\sigma^{d-1}} \cdot \\ \cdot \prod_{all\, \sigma^d} \left\{ \frac{3}{2}(d-2)(d+1)j \right\}_{\sigma^d} (J, J') \prod_{\sigma^{d-1} \in \partial T^d} \sum_{\mathcal{M}} (-1)^{\sum m/2 + \sum \mathcal{M}} \cdot \\ \cdot \begin{pmatrix} j_1' & j_2' & J_1' \\ m_1 & m_2 & \mathcal{M}_1 \end{pmatrix} \cdots \begin{pmatrix} J_{d-3}' & j_{d-1}' & j_d' \\ -\mathcal{M}_{d-3} & m_{d-1} & m_d \end{pmatrix}, \qquad (5.24)$$

where $\Xi = 2(N_0 - N_1 + \ldots + (-1)^{d-3} N_{d-3})$, $(N_0, N_1, N_2, \ldots)$ being the total number of $(0, 1, 2, \ldots)$-dimensional simplices. Notice also that some of the recoupling coefficients associated with d-simplices may depend also on J' variables, if they have components in ∂T^d.

The limiting procedure for handling all state sums (5.24) for the given $(M^d, \partial M^d)$ can be defined as

$$Z[(M^d, \partial M^d)] = \\ = \lim_{L \to \infty} \sum_{\left\{ \begin{array}{c} T^d, \partial T^d \\ j, J \leq L \end{array} \right\}} Z[(T^d(j, J), \partial T^d(j', J'; m, \mathcal{M})) \rightarrow (M^d, \partial M^d); L], \qquad (5.25)$$

where the ranges of the magnetic quantum numbers are $|m| \leq j', |\mathcal{M}| \leq J'$ in integer steps, and where suitable shorthand notations have been employed.

As anticipated before, we turn now to the basic question of the equivalence of $Z[(M^d, \partial M^d)]$ in (5.25) under a suitable class of topological operations. In the present case we are going to implement the set of elementary inverse shellings $[n_{d-1} \rightarrow d - (n_{d-1})]^{\mathbf{d}}_{ish}$ in (2.17), involving the attachment of one d-simplex to ∂T^d along $n_{d-1} = 1, 2, \ldots, d$ simplices of dimension $(d-1)$ glued together in suitable configurations. The complementary set of the elementary shellings could be singled out simply by exchanging internal and external labellings in a consistent way. It should be clear from similar discussions on equivalence in Section 5.1, Section 5.2 and Appendix 8.3 that the explicit expressions of the identities associated with the moves become more and more complicated as dimension grows. Thus, we limit ourselves to the implementation of the moves through the diagrammatical method, which has been already used in Section 5.2. As a further remark, we note that glueing operations performed on triangulations underlying PL-pairs of manifolds (as happens in our context) involve joining of couples of p-dimensional simplices ($p = d, d-1$) along their *unique* common $(p-1)$-dimensional face. More precisely, also the joining of two $(d-1)$-dimensional simplices in ∂T^d has to fulfill this rule, since ∂T^d is a manifold (indeed, this would be true for pseudomanifols as well).

Before dealing with the full d-dimensional case, let us illustrate the case of elementary inverse shellings in $d = 5$ and $d = 6$.

Recall that a 5-simplex has six 4-dimensional simplices in its boundary and that in the present case n_{d-1} in (2.17) may run over $1, 2, 3, 4, 5$. Consider first the inverse shelling $[5 \rightarrow 1]^{\mathbf{5}}_{ish}$, the action of which is displayed in the diagram of Fig. 5.13 (where we have made use of the diagrams shown in Fig. 5.10. This operation amounts to glue a 5-simplex to ∂T^5 along five 4-simplices (joined among them along 3-dimensional faces). The resulting configuration in the modified $\partial T'^5$ gives rise to an unique new (open) 4-simplex, so that no new $(5-r)$-simplices ($r \geq 3$) appear. Thus the state sum (5.24) does not acquire any w_L^{-2} factor and is manifestly invariant under such a move.

The inverse shelling $[4 \rightarrow 2]^{\mathbf{5}}_{ish}$ consists in the attachment of a 5-simplex along four 4-simplices in

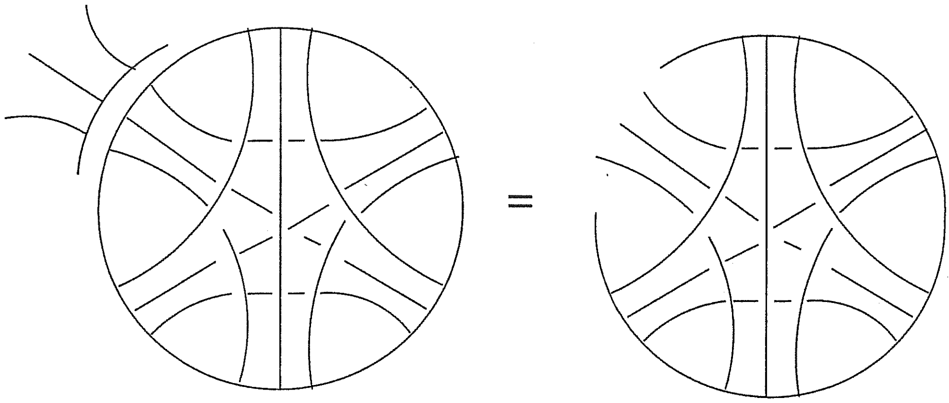

Fig. 5.13: Shelling of $[5 \to 1]^5_{ish}$ type.

∂T^5. In the new $\partial T'^5$ there appear two 4-simplices joined along a common 3-simplex (for what we said before), and thus also in this case we do not introduce new $(5-r)$-dimensional subsimplices $(r \geq 3)$ in the state sum and no additional w_L^{-2} factor arises. The diagrammatic proof is given in Fig. 5.14, where we have taken into account Fig. 5.10 again.

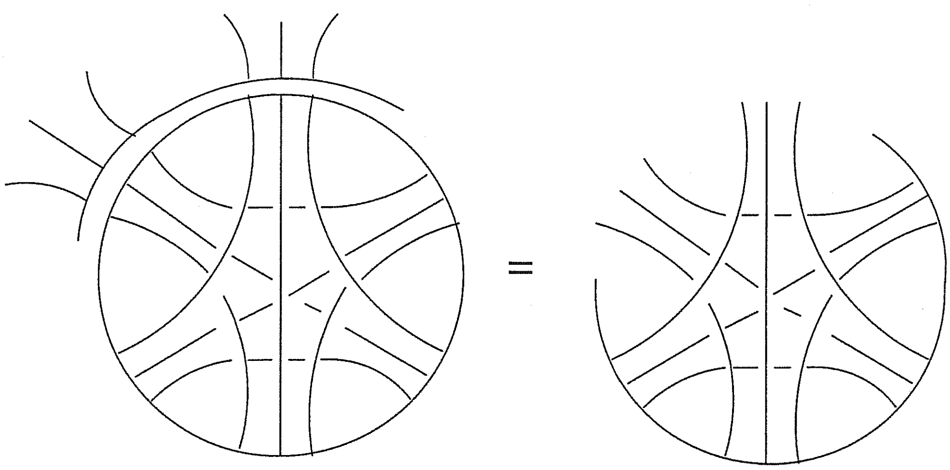

Fig. 5.14: Shelling of $[4 \to 2]^5_{ish}$ type.

The $[3 \to 3]^5_{ish}$ move amounts to the glueing of a 5-simplex along three 4-simplices lying in ∂T^5. Owing to the general remark that in a p-simplex $\subset \sigma^d$, exactly three $(p-2)$-dimensional subsimplices incide over a $(d-3)$-dimensional subsimplice, we see that such an inverse shelling generates just one new triangle in $\partial T'^5$ (and no additional $(5-r)$-simplices with $r \geq 4$), associated with a w_L^{-2} factor in the state sum. The action of this move is reproduced in Fig. 5.15, where

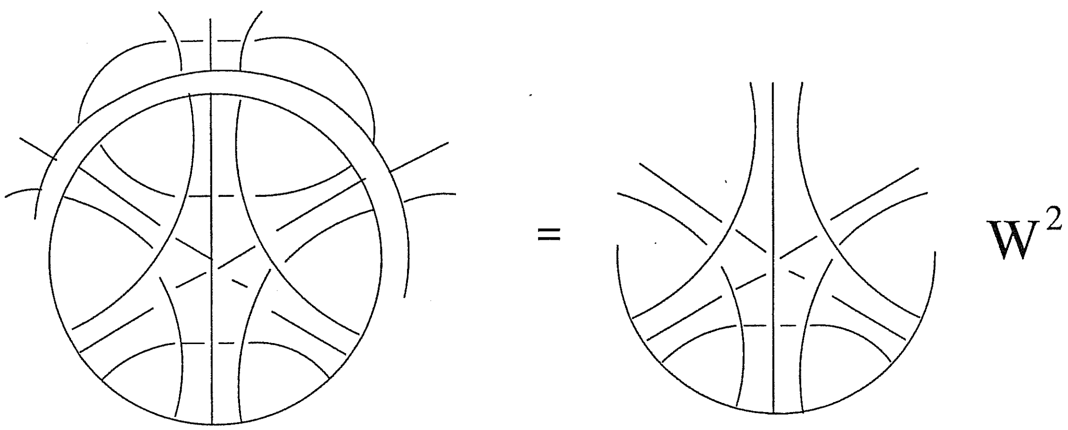

Fig. 5.15: Shelling of $[3 \rightarrow 3]^5_{ish}$ type.

we can see the loop bringing a w_L^2 factor which cancels the contribution coming from the new triangle.

The move $[2 \rightarrow 4]^5_{ish}$ represents the attachment of a 5-simplex to ∂T^5 along four 4-dimensional simplices. Recalling the expressions giving the number of subsimplices of a p-simplex (see below), we may see that the configuration of two 4-simplices, glued along their common 3-dimensional face, identifies six vertices, fourteen edges, sixteen triangles and nine tetrahedra; thus this type of inverse shelling generates in $\partial T'^5$ one new edge ($(d-4)$-simplex) and four triangles ($(d-3)$-simplices), giving rise to w_L^{-6} factor in the state sum. The above action in depicted in the diagram of Fig. 5.16, where we see three loops, the contributions of which cancel the above extra factor.

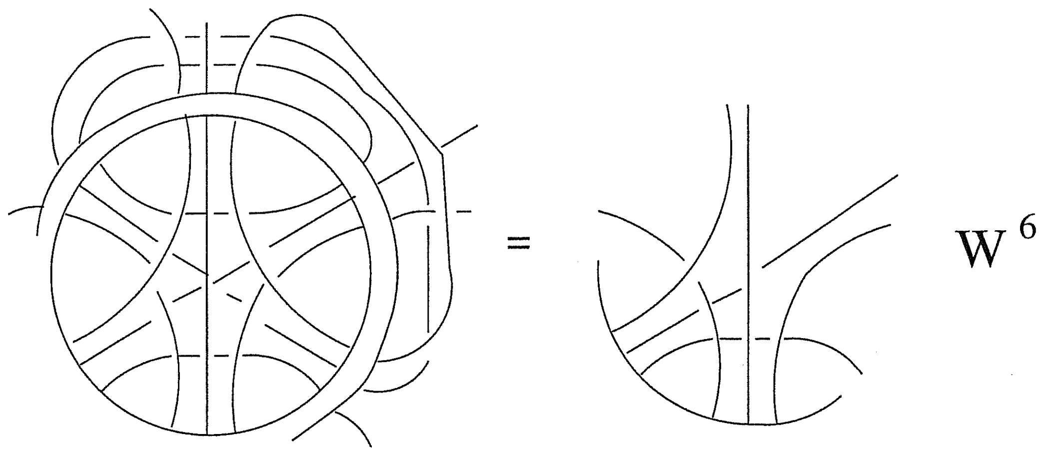

Fig. 5.16: Shelling of $[2 \rightarrow 4]^5_{ish}$ type.

The last type of inverse shelling that we deal with is $[1 \rightarrow 5]^5_{ish}$, representing the glueing of a 5-simplex along one 4-simplex. By counting in an appropriate way the subsimplices of the new configuration in $\partial T'^5$, we see that there appear ten triangles ($(d-3)$-simplices), five edges ($(d-4)$-simplices) and one vertex ($(d-5)$-simplex), which generate an overall w_L^{-12} factor. Looking now at Fig. 5.5, such extra factor turns out to be exactly cancelled by the contributions arising from the

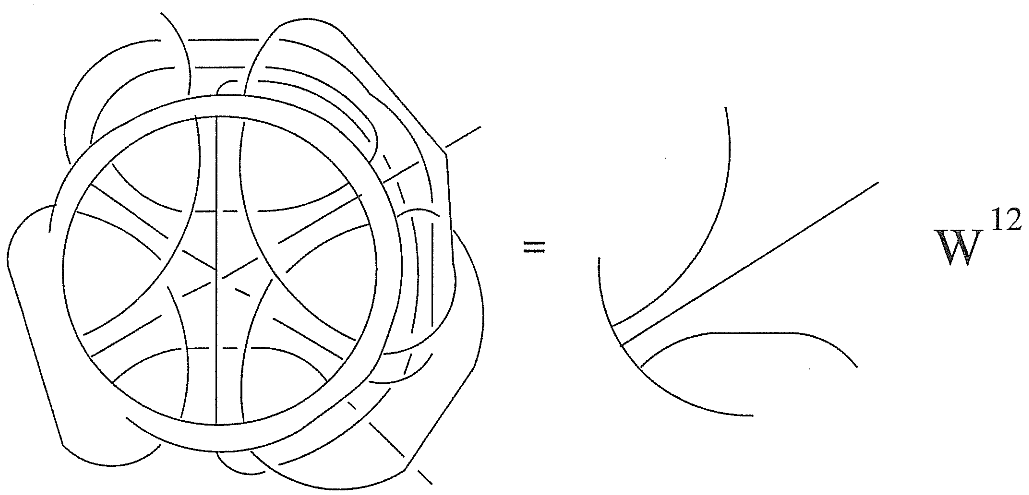

Fig. 5.17: Shelling of $[1 \rightarrow 5]^5_{ish}$ type.

loops. This completes the proof of the invariance of (5.25) under elementary boundary operations in the 5-dimensional case.

A 6-simplex has seven 5-dimensional simplices in its boundary and, in the present case, n_{d-l} in (2.17) may runs over 1,2,3,4,5,6. Consider first the inverse shelling $[6 \rightarrow 1]^6_{ish}$: this operation represents the glueing of a 6-simplex to ∂T^6 along six 5-simplices of boundary. The resulting configuration in the modified $\partial T'^6$ gives rise a unique new 5-simplex, so that no new $(6-r)$ simplices ($r \geq 3$) appear. We have no additional w_L^2 factors in the state sum (5.24). The relation that prove the invariance of the state sum is given in the Fig. 5.18. where we have taken in account the graphical relation showed in Fig. 5.10.

The inverse shelling $[5 \rightarrow 2]^6_{ish}$ identifies the glueing of a 6-simplex along five 5-simplices of ∂T^6. The two 5-simplices in $(\partial T')^6$ are joined along a 4-simplex and the other subsimplices are identified, with those on the boundary of the composition of the initial five 5-simplices respectively; thus, also in this case, we do not introduce new $(6-r)$-dimensional simplices with $r \geq 3$ an so no

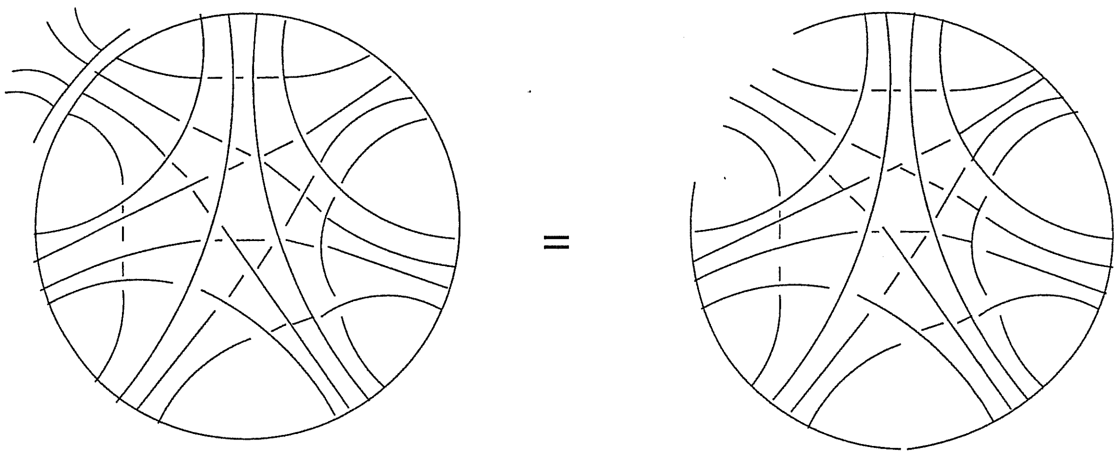

Fig. 5.18: Sheling of $[6 \rightarrow 1]^{\mathbf{6}}_{ish}$ type.

additional w_L^{-2} factors in the state sum. The relation that proves the invariance is represented by Fig. 5.19, using again the relations given in Fig. 5.10.

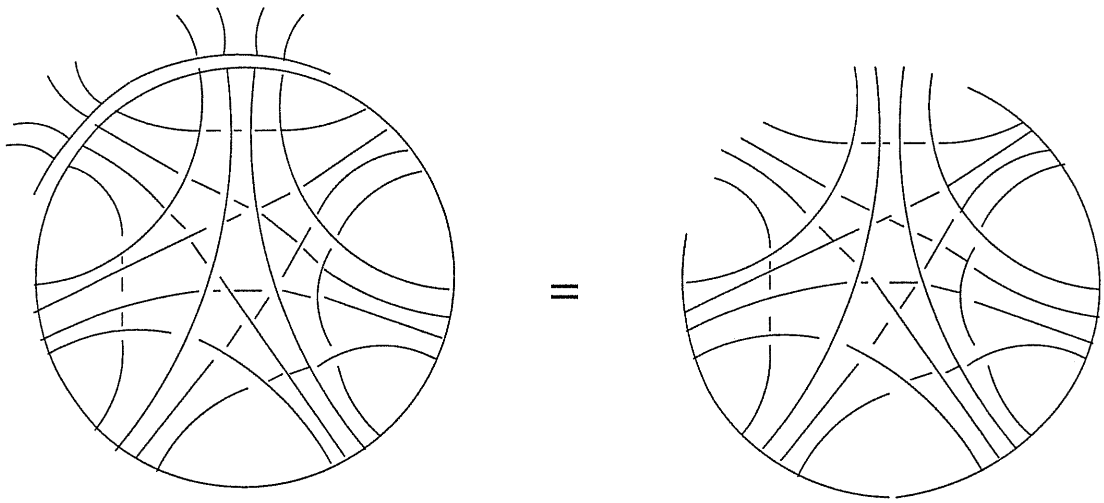

Fig. 5.19: Shelling of $[5 \rightarrow 2]^{\mathbf{6}}_{ish}$ type.

The $[4 \rightarrow 3]^{\mathbf{6}}_{ish}$ inverse shelling consists in the attachment of a 6-simplex along four 5-simplices of ∂T^6. Recalling what we said before about the structure of the d dimensional simplex, and by exploiting the same argument used for the move $[3 \rightarrow 3]^{\mathbf{5}}_{ish}$, we have the generation of a new tetrahedra ($(d-2)$-simplex) in the triangulation of $\partial T'^6$ and no additional $(6-r)$-dimensional simplices with $r \geq 4$; thus, a new factor w_L^{-2} appears in the state sum. The graph that reproduces this move in the definition of the invariant is given in Fig. 5.20 where we see the loop that brings

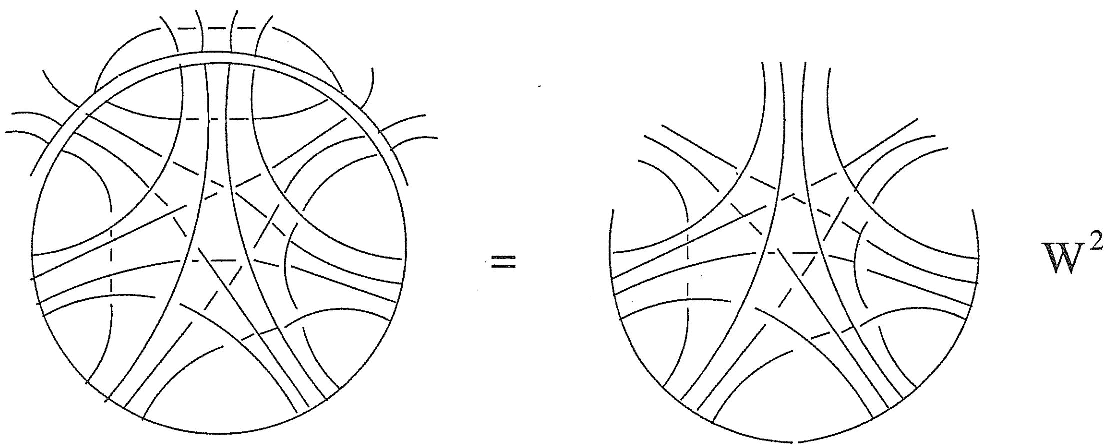

Fig. 5.20: Shelling of $[4 \to 3]^{\mathbf{6}}_{ish}$ type.

a w_L^2 factor which cancels the contribution coming from the new tetrahedron.

The move $[3 \to 4]^{\mathbf{6}}_{ish}$ represents the glueing of a 6-simplex along three 5-simplices. Examining the number of subsimplices of the 6-simplex, we obtain that the move introduces one new triangle (a $(d-4)$-simplex) and four tetrahedra ($(d-3)$-simplices), giving rise to an additional factor w_L^{-6}. The graph that reproduces this shelling in the state sum is given in Fig. 5.21 where we see three

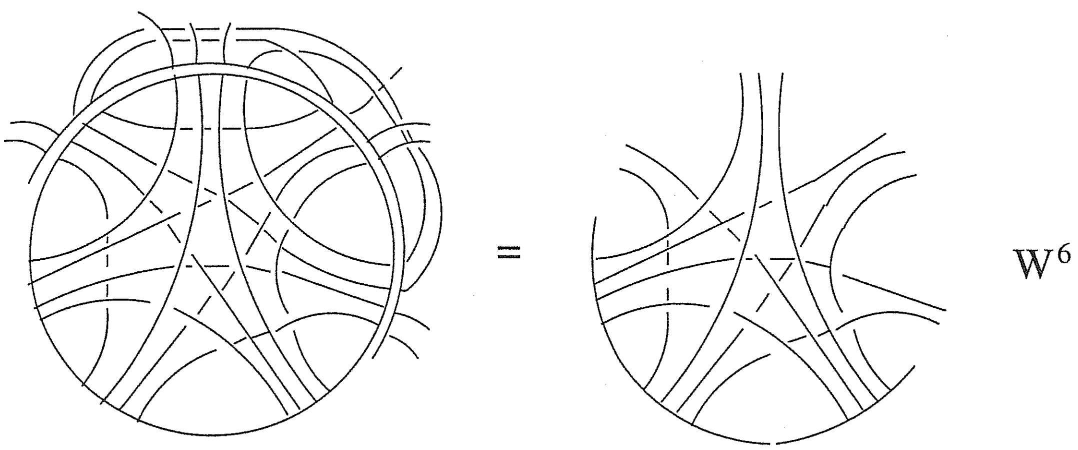

Fig. 5.21: Shelling of $[3 \to 4]^{\mathbf{6}}_{ish}$ type.

loops, the contribution of which cancels the above extra factor.

The $[2 \to 5]^{\mathbf{6}}_{ish}$ consists of the attachment of a 6-simplex along two 5-simplices of ∂T^6. The initial two 5-simplices identify seven vertices, twenty edges, thirty triangles and fifteen tetrahedra of the triangulation, so that the operation introduce ten new tetrahedra ($(d-3)$-simplices), five new triangles ($(d-4)$-simplices) and a new edge (a $(d-5)$-simplex); all that gives rise to a term w_L^{-12} coming from the prefactor in the state sum. The graph associated to this move is given in Fig. 5.22 The loop contributions reproduce the inverse of the new w factors and thus we obtain

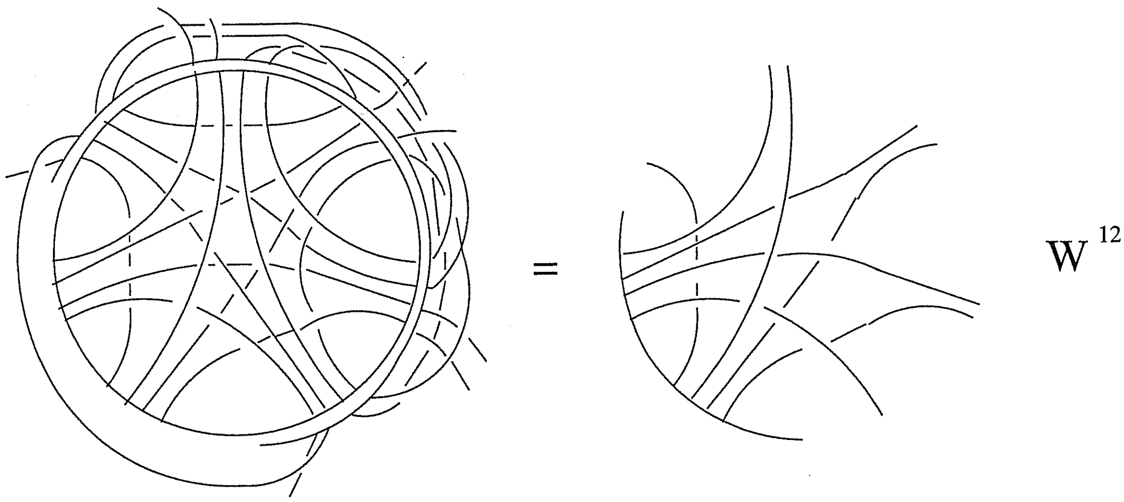

Fig. 5.22: Shelling of $[2 \to 5]^{6}_{ish}$ type.

in this way the invariance of the state sum.

The last type of inverse shelling is the move $[1 \to 6]^{6}_{ish}$ that represents the glueing of a 6-simplex along a 5-simplex. By counting the subsimplices of the configuration in $(\partial T')^6$, and by subtracting the number of subsimplices of a 6-simplex from those of a 5-simplex, there appear twenty new tetrahedra ($(d-3)$-simplices), fifteen new triangles ($(d-4)$-simplices), six new edges ($(d-5)$-simplices) and a new vertex (a $(d-6)$-simplex), summing to w_L^{-20}. The graph associated to this move is given in Fig. 5.23: the loop contributions cancel exactly the extra w_L factors.

This completes the proof of the invariance of $Z[(M^6, \partial M^6)]$.

Coming to the general d-dimensional case, we slightly change our previous notation, namely $[n_{d-1} \to d - (n_{d-1})]^{\mathbf{d}}_{ish}$ $(n_{d-1} = 1, 2, \ldots, d)$, by parametrizing the moves in terms of d according to

$$[(d-k) \to (k+1)]^{\mathbf{d}}_{ish} \ , k = 0, 1, 2, \ldots, (d-1), \tag{5.26}$$

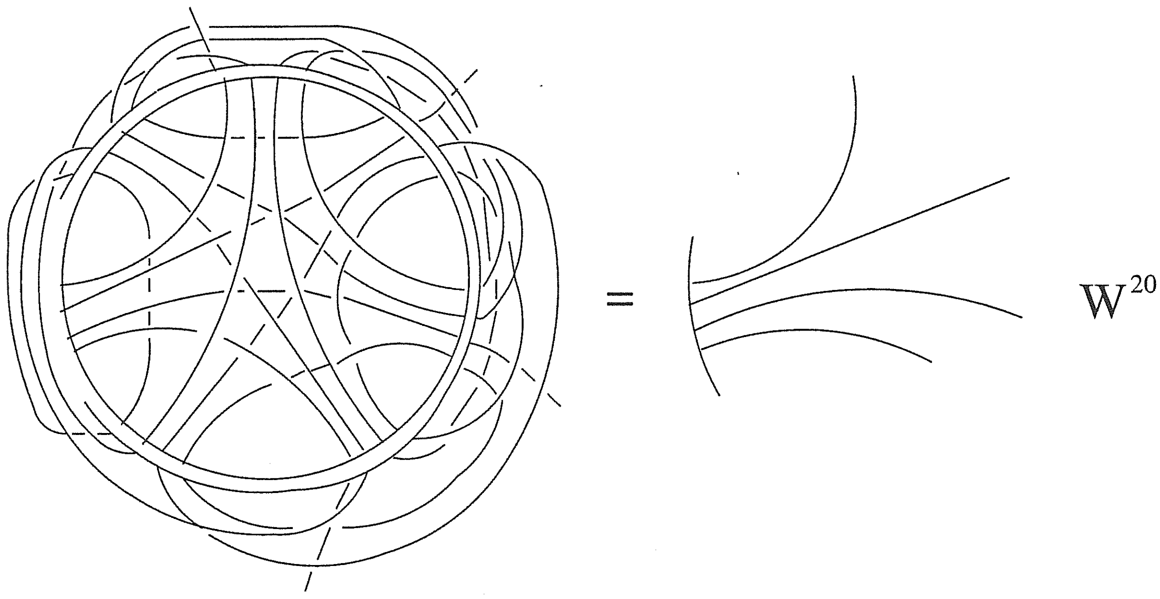

Fig. 5.23: Shelling of $[1 \to 6]^{\mathbf{6}}_{ish}$ type.

which of course turns out to be consistent with the previous one. Notice also that in what follows we shall make use of the diagrammatic relations shown in Fig. 5.9 and Fig. 5.10 whenever it is necessary.

Consider first $[d \to 1]^{\mathbf{d}}_{ish}$, representing the glueing of a d-simplex to ∂T^d along d $(d-1)$-dimensional simplices (the corresponding diagram is given in Fig. 5.24). Since we do not generate any $(d-r)$-

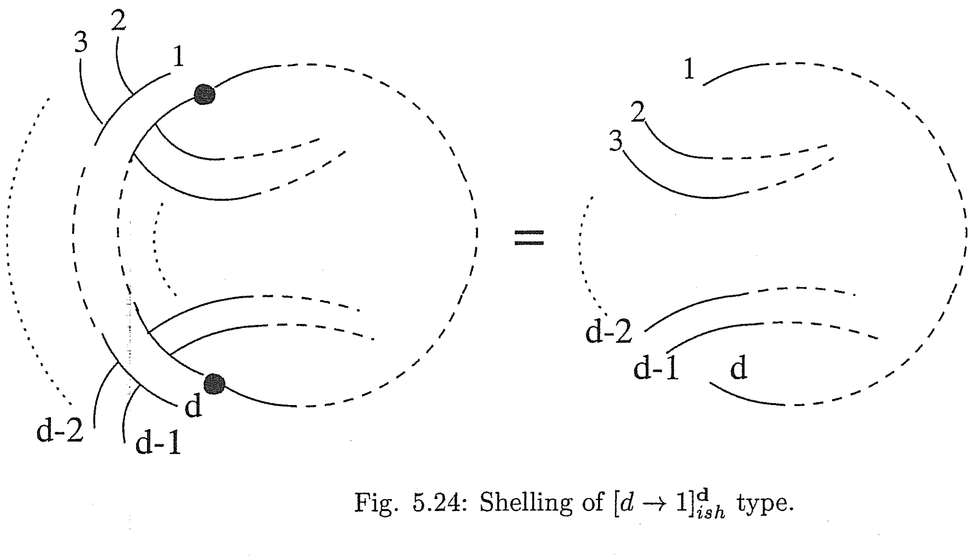

Fig. 5.24: Shelling of $[d \to 1]^{\mathbf{d}}_{ish}$ type.

simplex $(r \geq 3)$ in the new configuration $\partial T'^d$, no additional w_L^{-2} factors enter the state sum

(5.24) .

The $[(d-1) \to 2]^{\mathbf{d}}_{ish}$ move consists in the attachment of a d-simplex to ∂T^d along $(d-1)$ simplices of dimension $(d-1)$. Also the action of this inverse shellings does not give any $(d-r)$-simplex ($r \geq 3$) in the new $\partial T'^d$, and its graphical counterpart is shown in Fig. 5.25.

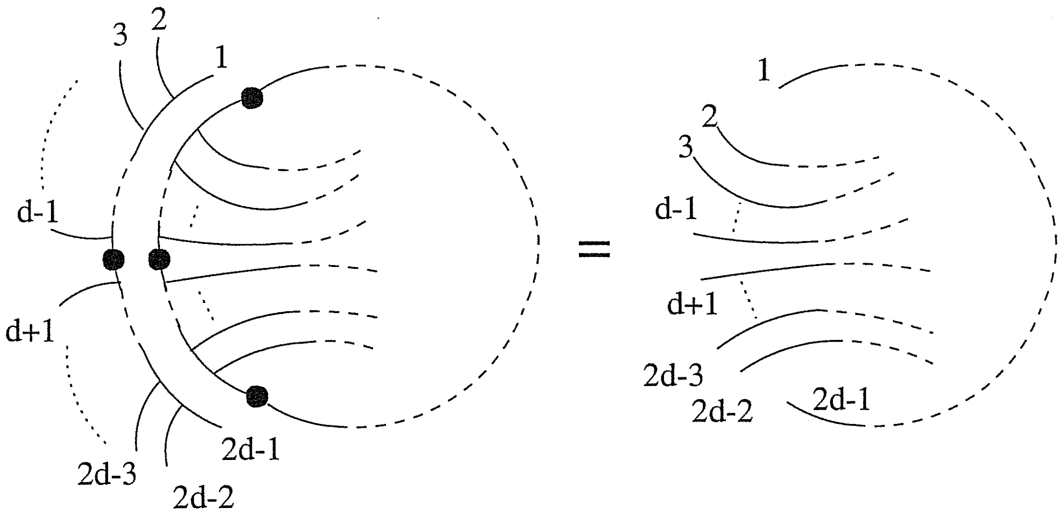

Fig. 5.25: Shelling of $[d-1 \to 2]^{\mathbf{d}}_{ish}$ type.

Coming to $[(d-2) \to 3]^{\mathbf{d}}_{ish}$, we see that it represents the glueing of a d-simplex along $(d-2)$ simplices of dimension $(d-1)$ lying in ∂T^d and its diagram is given in Fig. 5.26. In the new

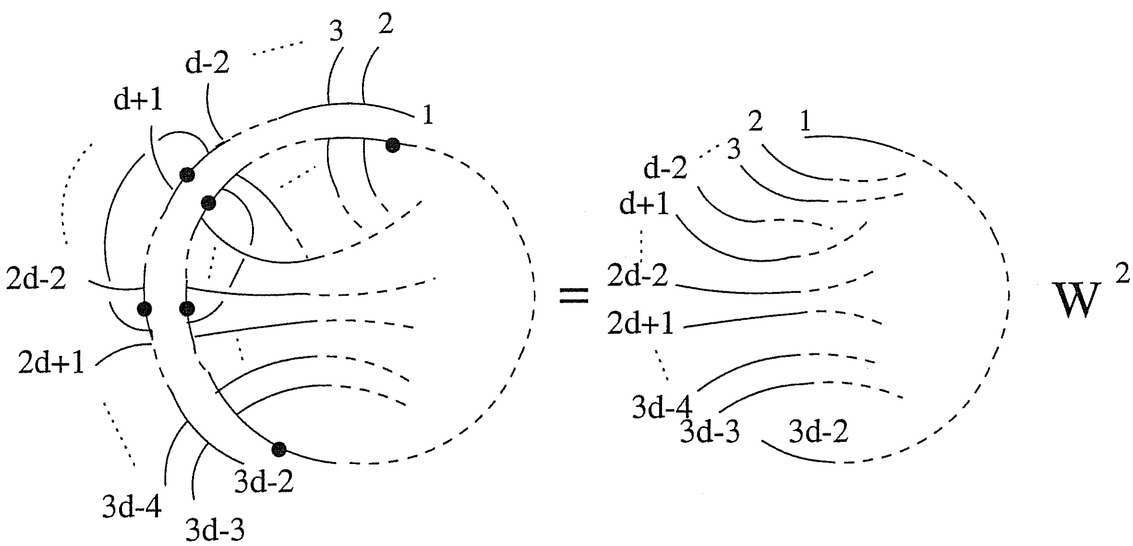

Fig. 5.26: Shelling of $[d-2 \to 3]^{\mathbf{d}}_{ish}$ type.

boundary triangulation one $(d-3)$-simplex (and no other simplices) appears. Thus the w_L^{-2} factor which comes out is exactly canceled by the contribution of the loop.

An algorithmic setting can now be easily established. For, the k-th inverse shelling, namely $[(d-k) \to (k+1)]^{\mathrm{d}}_{ish}$, represents the attachment of a new d-simplex along $(d-k)$ simplices of dimension $(d-1)$ in ∂T^d which generates in $\partial T'^d$ several kinds of new boundary components. The number of such new components is evaluated by using suitable binomial coefficients, according to the list given below

$$\binom{k+1}{3}\sigma^{d-3};\ \binom{k+1}{4}\sigma^{d-4};\ \ldots;\ \binom{k+1}{k+1}\sigma^{d-(k+1)}, \tag{5.27}$$

while for each k the following number of additional w_L^{-2} factors are generated

$$w_L^{2\sum_{i=3}^{k+1}\binom{k+1}{i}(-1)^{i+1}} = w_L^{-2\frac{k-1}{2}k}. \tag{5.28}$$

The action of the k-th inverse shelling is depicted in the diagram of Fig. 5.27, where the loops

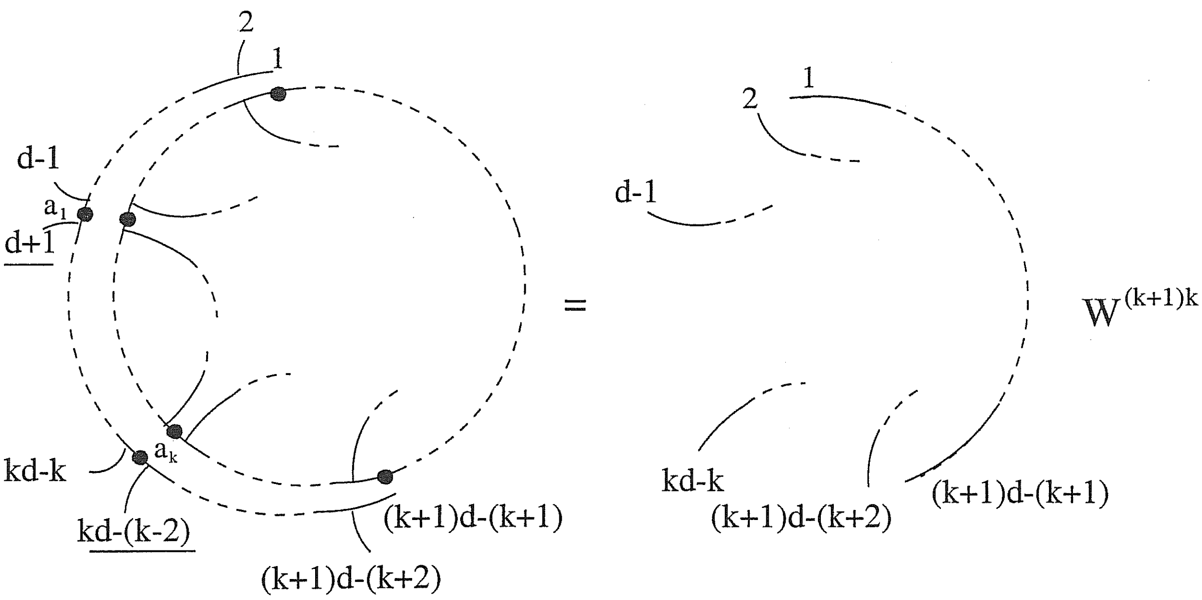

Fig. 5.27: Shelling of $[d-k \to k+1]^{\mathrm{d}}_{ish}$ type.

which cancel the weights given in (5.28) appear. More precisely, when we glue together $(k+1)$ $(d-1)$-simplices in the more symmetric way, we have to perform $(\sum_{l=1}^{k} l)$ identifications among their faces (and that is exactly the number of summations over j variables in the state sum). However, k of the above identifications do not bring loops (as can be inferred from the structure of the $\{3(d-2)(d+1)/2\}j$ symbol) and thus the remaining $(\sum_{l=1}^{k-1} l)$ glueing operations induce exactly the factors given in (5.28). This remark completes the proof of the equivalence of (5.24) under the entire set of boundary elementary operations. Thus, by Pachner's result found in [43], the expression given in (5.25) is formally an invariant of the PL-structure of $(M^d, \partial M^d)$. Its regularized counterpart, $Z[(M^d, \partial M^d)](q)$ can be written explicitly according to the prescription given in *Appendix 8.1*.

Chapter 6

Invariants of closed M^d from colorings of $(d-2)$-simplices.

In order to complete the program on PL invariants outlined in the Introduction to the thesis, in the present chapter we show how it is possible to generate from the extended invariant defined in *Chapter 5* a state sum model for a closed PL-manifold M^d. Obviously the form of the new state sum will be inferred from the extended one (see (5.24)) simply by ignoring the contribution from boundary (*cfr.* the 3 and 4-dimensional cases). Thus our first task here will consist in giving the proof that (5.25), and consequently $Z[M^d] \doteq Z[(M^d, \partial M^d)]|_{\partial M^d = \emptyset}$, are invariant under d-dimensional bistellar moves performed in the interior (bulk) of a triangulation $(T^d, \partial T^d)$ or in a closed T^d, respectively.

In the second part of this Chapter we shall discuss the connection between our closed spin models and the class of TQFT's defined by BF-type actions.

6.1 $Z[M^d]$ and its equivalence under bistellar moves.

The expression of the state sum for a closed triangulation T^d, colored according to the prescription of the previous section and with the same notations, reads

$$Z[T^d(j_{\sigma^{d-2}}, J_{\sigma^{d-1}}) \to M^d; L] =$$

$$= w_L^{(-1)^d \Xi} \prod_{all\,\sigma^{d-2}} (-1)^{2j_{\sigma^{d-2}}}(2j_{\sigma^{d-2}}+1) \prod_{all\,\sigma^{d-1}} \left(\prod_{C=1}^{d-3} (-1)^{2J_C}(2J_C+1) \right)_{\sigma^{d-1}} \cdot$$

$$\cdot \prod_{all\,\sigma^d} \left\{ \frac{3}{2}(d-2)(d+1)j \right\}_{\sigma^d} (J), \tag{6.1}$$

while the limit taken on all admissible colored triangulations of a PL-manifold M^d is formally written as follows

$$Z[M^d] = \lim_{L \to \infty} \sum_{\left\{ \begin{array}{c} T^d \\ j, J \leq L \end{array} \right\}} Z[T^d(j,J) \to M^d; L]. \tag{6.2}$$

The issue of the equivalence of (6.2) under the suitable set of topological operations can be addressed by exploiting some results from PL-topology (recall also the definitions given in Chapter 2) and on applying them to the extended state sum $Z^d[(T^d, \partial T^d) \to \ldots]$ given in (5.24).

Thus, let us start by considering the simplicial complex made up by a d-simplex σ^d together with all its subsimplices. From the topological point of view we get in fact what is called a (standard) simplicial PL-ball, and we denote it by $\mathcal{B}^d(\sigma)$ (we omit the dimensionality of simplices whenever it is clear from the context). The boundary of such a ball, $\partial\mathcal{B}^d(\sigma)$, is obviously homeomorphic to the $(d-1)$-dimensional sphere and in particular it is a simplicial PL-sphere containing the $(d+1)$ faces of dimension $(d-1)$ of the original $\mathcal{B}^d(\sigma)$. Notice however that a simplicial $(d-1)$-sphere can be defined by its own by joining in a suitable way some $(d-1)$-dimensional simplices $\subset \mathbb{R}^d$. The minimum number of $(d-1)$-simplices necessary to get a PL-sphere is just $(d+1)$: the resulting simplicial sphere will be denoted by $\mathcal{S}^{d-1}(\sigma_1 \cup \sigma_2 \cup \ldots \cup \sigma_{d+1})$. If we consider again the PL-ball $\mathcal{B}^d(\sigma)$, we would get $\partial\mathcal{B}^d(\sigma) \cong_{PL} \mathcal{S}^{d-1}(\sigma_1 \cup \sigma_2 \cup \ldots \sigma_{d+1})$, where $\cong_{PL}$ stands for a PL-homeomorphism.

Turning now to the structure of the extended state sum for a $(T^d, \partial T^d)$, we can reconsider its topological content as follows. Indeed, we see that the contribution of the configuration $\mathcal{S}^{d-1}(\sigma_1 \cup \sigma_2 \cup \ldots \cup \sigma_{d+1})$ to Z^d amounts exactly to one $\{3(d-2)(d+1)/2\}j$ symbol, namely it is the same that we would obtain by glueing a $\mathcal{B}^d(\sigma)$ to $\mathcal{S}^{d-1}(\sigma_1 \cup \sigma_2 \cup \ldots \cup \sigma_{d+1})$ along $\partial\mathcal{B}^d(\sigma)$ with a PL-homeomorphism. The reason why we stress this point relies on the fact that on this basis we are able to set up the following step–by–step procedure: *i)* we extract first some $\mathcal{B}^d(\sigma)$ from the bulk of $(T^d, \partial T^d)$, leaving an internal hole bounded by the PL-sphere $\mathcal{S}^{d-1}(\sigma_1 \cup \sigma_2 \cup \ldots \sigma_{d+1})$; *ii)* then we carry out elementary boundary operations on the PL-pair $(\mathcal{B}^d(\sigma)\ , \partial\mathcal{B}^d(\sigma))$ bringing $\partial\mathcal{B}^d(\sigma)$ into $\mathcal{S}^{d-1}(\tau_1 \cup \tau_2 \cup \ldots \cup \tau_{d+1})$ (notice that in doing that we do not alter the extended state sum, owing to its invariance under elementary shellings); *iii)* finally, we glue the ball back into the original triangulation through a PL-homeomorphism $\mathcal{S}^{d-1}$ $(\sigma_1 \cup \sigma_2 \cup \ldots \cup \sigma_{d+1}) \cong_{PL} \mathcal{S}^{d-1}$ $(\tau_1 \cup \tau_2 \cup \ldots \cup \tau_{d+1})$.

Such kinds of *cut and paste* represent nothing that the implementation of the set of d-dimensional bistellar moves in the bulk of each triangulation of $(M^d, \partial M^d)$ (and in the whole closed M^d). To be precise, some of the moves will be obtained by cutting away not just a standard PL-ball as before, but rather simplicial balls made up of a suitable collection of more than one d-simplex.

As an explicit example of how the above procedure works, consider the 3-dimensional case with the corresponding extended state sum given in (5.7). Recall from (2.16) that in this case we are dealing with four bistellar moves, $[1 \leftrightarrow 4]^3_{bst}$ and $[2 \leftrightarrow 3]^3_{bst}$, where the arguments refer to the number of 3-simplices involved in the corresponding transformation. The explicit implementation of some of these moves is given below.

- $[1 \rightarrow 4]^3_{bst}$. Since the initial configuration contains just one 3-simplex, we are just in the situation described above. Then we extract the ball $\mathcal{B}^3(\sigma^3)$ (the boundary of which is $\mathcal{S}^2$ $(\sigma^2_1 \cup \sigma^2_2 \cup \sigma^2_3 \cup \sigma^2_4)$) and perform on it the inverse shelling $[1 \rightarrow 3]^3_{ish}$, where the first triangle is chosen in an arbitrary way. Thus we get a configuration with two 3-simplices, the original σ^3 and a new τ^3_1, glued along the original triangle. The second operation is an inverse shelling $[2 \rightarrow 2]^3_{ish}$, where the two initial contiguous triangles belong to σ^3 and to τ^3_1, respectively. This generate a third tetrahedron, τ^3_2 joined to the previous ones through a 2-dimensional face. On this configuration we act now with $[3 \rightarrow 1]^3_{ish}$, where two of the three triangles of the initial arrangement were generated in the two previous steps, respectively, while the third one belongs to the original σ^3. Thus we get a fourth tetrahedron τ^3_3 which, together with the other ones, gives rise to the simplicial ball $\mathcal{B}^3(\sigma^3 \cup \tau^3_1 \cup\ \tau^3_2 \cup \tau^3_3)$, the boundary of which is $\mathcal{S}^2(\sigma^2 \cup \tau^2_{(2)} \cup \tau^2_{(3)} \cup \tau^2_{(4)})$, where the first entry is the initial triangle chosen in σ^3, and the other entries are the new faces generated in the three previous steps. Now we glue back the resulting ball into the triangulation through a PL-homeomorphism between the original $\mathcal{S}^2$ $(\sigma_1^2 \cup \sigma_2^2 \cup \sigma_3^2 \cup \sigma_4^2)$ and $\mathcal{S}^2(\sigma^2 \cup \tau_{(2)}^2 \cup \tau_{(3)}^2 \cup \tau_{(4)}^2$. The pictorial representation of the reconstruction of this particular move is shown in Fig. 6.1.

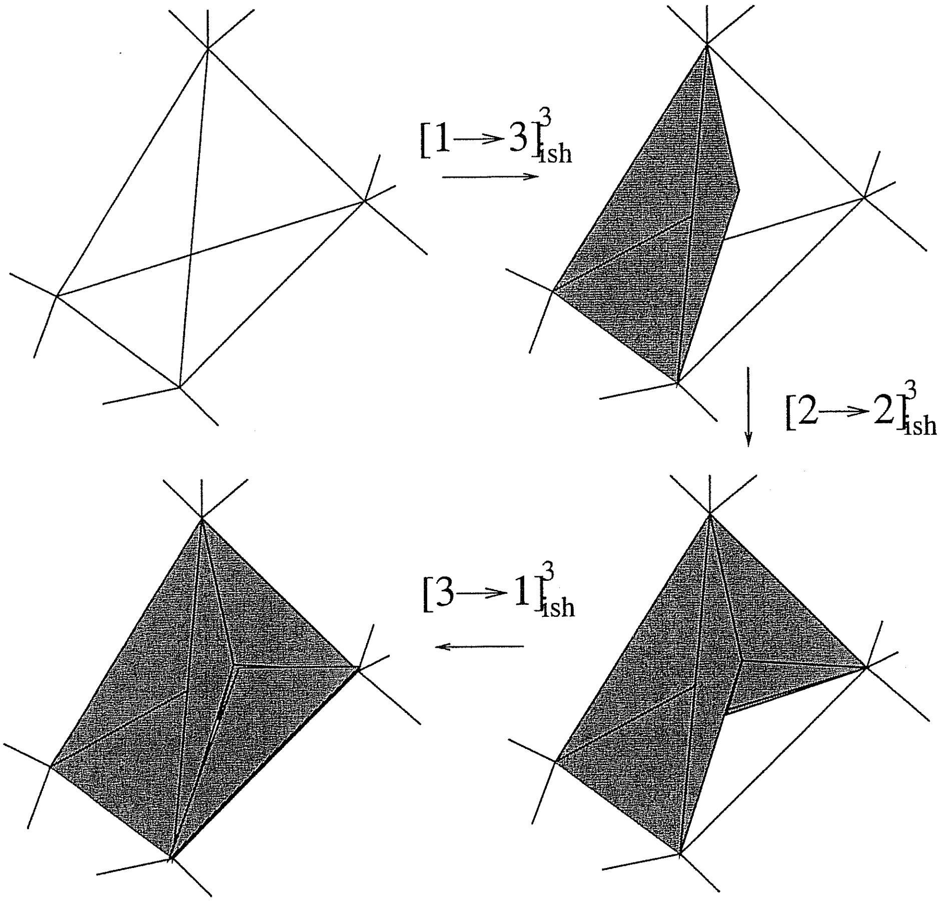

Fig. 6.1: The move $[1 \to 4]^3_{bst}$ in terms of inverse shellings performed on the removed PL-ball.

- $[2 \to 3]^3_{bst}$. The configuration we start with is a ball $\mathcal{B}^3(\sigma_1^3 \cup \sigma_2^3)$ having $\mathcal{S}^2$ $(\sigma_1^2 \cup \sigma_2^2 \cup \sigma_3^2 \cup \sigma_4^2 \cup \sigma_5^2 \cup \sigma_6^2)$ as its boundary. After the extraction, we perform first the inverse shelling $[2 \to 2]^3_{ish}$, where the two initial triangles are contiguous and belong to σ_1^3 and to σ_2^3, respectively. Finally, we apply $[3 \to 1]^3_{ish}$, where the three initial triangles belong to σ_1^3, σ_2^3 and to the component generated by the previous step, respectively. It is not difficult to realize that the resulting PL-ball has again six faces in its boundary PL-sphere, and thus we glue it back along the boundary of the original hole by means of a suitable PL-homeomorphism.

The sequence of operations we have performed is drawn in Fig. 6.2.

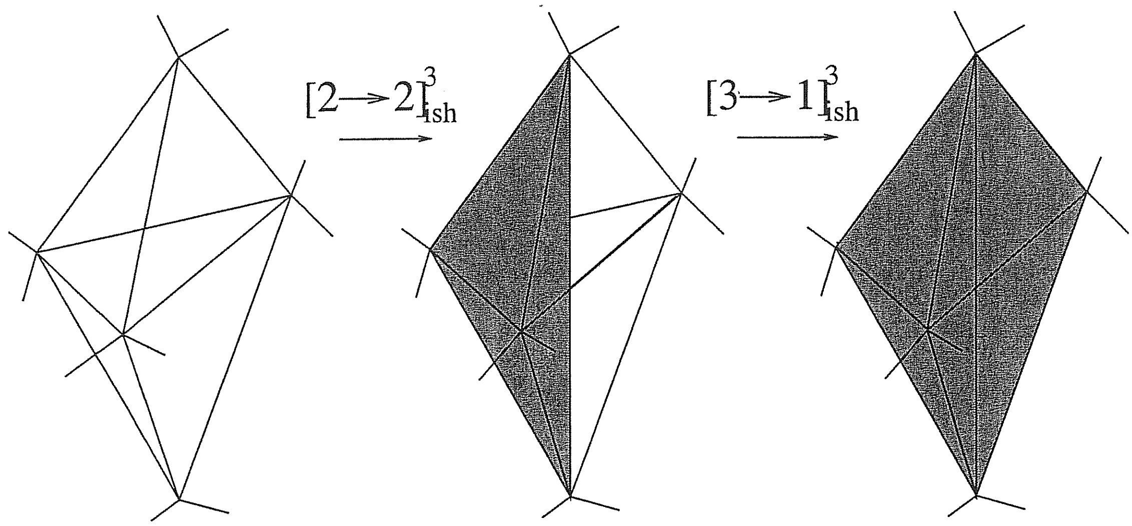

Fig. 6.2: The move $[2 \to 3]^3_{bst}$ in terms of inverse shellings performed on the removed PL-ball.

The remaining 3-dimensional bistellar moves can be explicitly worked out following a similar procedure and by employing a definite set of shellings.

Also for what concerns the 4-dimensional case we could describe step–by–step the implementation of all transformation. However, since in that case a pictorial counterpart is not so easy displayed, we turn to the general rule in dimension d. On the basis of the characterization of d-dimensional inverse shellings given in (5.26) we can reparametrize also the set of all d-bistellar moves according to

$$[k \to (d-k+1)]^{\mathbf{d}}_{bst} \;\; ; k \; = \; 1, 2, \ldots, (d-1), \tag{6.3}$$

paying attention to the fact that here k enumerates d-simplices, while in (5.26) it was referred to $(d-1)$-simplices in a given σ^d. With this reformulation, we see that the generic move $[k \to (d-k+1)]^{\mathbf{d}}_{bst}$ can be obtained with the *cut and paste* procedure following the steps:

- extract from the bulk of $(T^d, \partial T^d)$ a PL-ball $\mathcal{B}^d(\sigma_1 \cup \sigma_2 \cup \ldots \cup \sigma_k)$, where $k = 1, 2, \ldots, (d-1)$;
- implement on the ball the sequence of inverse shellings $[k \to d-k+1]^{\mathbf{d}}_{ish}$, $[k+1 \to d-k]^{\mathbf{d}}_{ish}$, ..., $[d+1 \to 1]^{\mathbf{d}}_{ish}$, by choosing in the initial configuration one $(d-1)$-simplex in each of

the components of the original ball and by involving in the subsequent moves one $(d-1)$ for each of the components generated before (including also the initial one);

- glue back the resulting modified simplicial ball along the hole left in $(T^d, \partial T^d)$ using a PL–homeomorphism.

Having shown that the extended state sum is equivalent under (a finite set of) bistellar moves performed in the bulk for any dimension d, we can conclude that the expression of $Z[M^d]$ in (6.2) share the same property. Thus, owing to [14], it is formally an invariant of the PL-structure. For what concern the q-deformed regularized $Z[M^d](q)$, we refer as usual to the notations and definitions collected in Appendix 8.1.

6.2 Derivation of associated TQFTs.

Here we are going to establish a connection between the non trivial lattice spin models defined before and the continuum approach to field theory given in particular by BF-type actions [28] [50]. We limit ourselves to present some of the results which will be collected in [38]. Such issue can be addressed essentially in two different ways. Thus we show the equivalence using both the discretization procedure of BF theory proposed by Freidel and Krasnov [37], and a generalization in d dimension of the Ooguri approach [5] which stresses the role of the associated surface and the deep geometrical meaning of the invariant. Notice also that, although the spin models proposed in this thesis can be defined irrespectively of the orientability properties of the underlying PL-manifolds, when dealing with continuum theories we are forced to consider only orientable manifolds. A further remark is about possible ambiguities arising from the *topological* character of the class of models in question. Notwithstanding the fact that in dimension greater than three it does not exists a one to one correspondence between the topological and the PL types of closed manifolds, we can always associate with each differentiable structure a *unique* PL structure in any dimension d.

Recall that a BF theory is a topological quantum field theory in dimension d characterized by a classical action

$$\int_M [TrB \wedge F + \Phi(B)] \tag{6.4}$$

where M is a d-dimensional closed manifold, B is a Lie algebra valued $(d-2)$-form field, F is the curvature 2-form of a connection A and Φ is certain polynomial function of the B field which can also depend on some Lagrangian multipliers (as happens when quantum gravity models are considered). We are interested here in pure BF theories, namely those for which Φ in (6.4) vanishes. We refer e.g. to [26] for a detail account on this subject.

6.2.1 A proof by means of the Freidel-Krasnov discretization method.

Let us fix a triangulation Δ of a d-dimensional compact oriented spacetime manifold M. According to the final remarks of Chapter 2, this triangulation defines another decomposition of M into cells called dual complex. There is one-to-one correspondence between k-simplices of the triangulation and (d–k)-cells in the dual complex. We orient each cell of the dual complex in an arbitrary fashion, which also defines an orientation for all simplices of the triangulation. The (d–2)-form B can now be integrated over the (d–2)-simplices of the triangulation, the result being a collection of the Lie algebra elements X, namely one vector $X \in$ su(2) for each 2-cell dual to a (d–2)-simplex of the triangulation. In view of our task, we would like to discretize this model by replacing in a straightforward way the continuous B-field by the collection of the Lie algebra elements X. It turns out, however, that a more convenient set of variables introduced by Reisenberger [51] exists, and we shall use this one.

Then instead of a single X for each dual face which is a 2-cells of the dual triangulation, we introduce a set of variables, denoted by X_w. To do this, we divide each dual face into what Reisenberger calls "wedges" (see Fig. 6.3). To construct wedges of the dual face one first has to find the "center" of the dual face. This is just the point on the dual face where it intersects the corresponding (d–2)-simplex of the triangulation. One then has to draw lines connecting this center with the centers of the all neighboring dual faces. The portion of the dual face that lies between two such lines is exactly the wedge. Thus, each dual face splits into wedges and we assign a Lie algebra element X_w to each wedge w. All variables X_w that correspond to a single dual

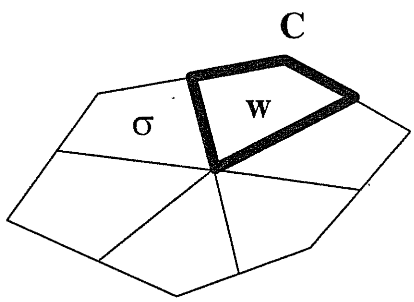

Fig. 6.3: A face σ of the dual triangulation. The portion of σ indicated by bold lines is a wedge. The point labelled by C is the center of one of the d-simplices intersected by σ.

face are required to have the same length (recall that vectors of the same length only differ by a gauge transformation). Wedges of a given dual face are in one-to-one correspondence with the d-simplices of the triangulation neighboring this dual face. Thus, we may say that each variable X_w arises from the integral of B over the (d–2) simplex of the triangulation "from the point of view" of a particular d-simplex containing this (d–2)-simplex. Note that the number of variables X_w that arises in this way for a given triangulation Δ is equal to the number of d-simplices in Δ times the number of (d–2)-simplices in each d-simplex.

Once the geometrical meaning of the wedge variables X_w is made clear, we introduce the distributional B fields. Heuristically, our procedure of replacement of a smooth B field by a distribution concentrated along the wedges amounts to a "squeezing" of the smooth B field (originally is "spread" over a (d-2) simplex of the triangulation) to a single point on this (d-2) simplex; this is just the point where the simplex intersects with the 2-cell of the dual complex. Accordingly, we define a distributional field B_w concentrated along a wedge w to be a 2-form satisfying the following relation:

$$\int_M \mathrm{Tr}(B_w \wedge J) = \mathrm{Tr}(X_w \int_w J). \tag{6.5}$$

Here J is any 2-form which takes values in the adjoint representation, and w stands for a wedge. The integral on the right-hand side is extended over the wedge w. This fact implies in particular that the Lie algebra element X_w is equal to the integral of B_w over the (d–2)-simplex of the triangulation which is dual to the 2-cell σ. The distributional field B is defined as

$$B \doteq \sum_w B_w. \tag{6.6}$$

Although the introduction of the wedge variables increases the number of independent variables in the theory, one can still argue that the physical content of the theory should be the same since the norms of all the X_w belonging to one and the same dual face are required to be equal. In the case of BF theory one can prove in a straightforward way that the introduction of the independent wedge variables does not change the theory, at least as far as the topology of dual faces σ is that of a disc (this will be taken for granted from now on).

In order to calculate the generating functional Z for a fixed triangulation Δ, we have to integrate the exponentiated action over the "discretized" dynamical fields A, B. Using (6.5),(6.6), it can be shown that the discretized action is given by

$$\sum_w \int_w \left[\mathrm{Tr}(F\, X_w) + \mathrm{Tr}(J\, X_w)\right], \tag{6.7}$$

where the sum is taken over the wedges of the dual faces introduced before, and the integral is performed over each wedge. The integrand contains the curvature of the connection A contracted with the Lie algebra element X_w living on that wedge and the current J contracted with X_w. Each integral is evaluated by using the orientation of the dual face to which the wedge belongs.

We should now substitute this discretized action into the path integral and integrate over X and A. However, we first have to discuss the meaning of the integration over A, by replacing the continuous field A by a collection of group elements. We get the following approximated expression:

$$\int_w \mathrm{Tr}(F\, X_w) \approx \mathrm{Tr}(Z_w X_w), \tag{6.8}$$

where Z_w is the Lie algebra element corresponding to the holonomy of A around the wedge (see Fig. 6.4) (the base point of the holonomy is not fixed at this stage, see below). In other words, in the generating functional there must appear terms of the form:

$$\exp Z_w = g_1 h_1 h_2 g_2, \tag{6.9}$$

where g_1, h_1, h_2, g_2 are the holonomies of A along the four edges that form the boundary of the

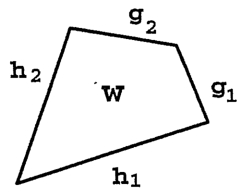

Fig. 6.4: A wedge w of the dual face and the associated group elements: the holonomies are taken along the edges of w.

wedge w (here we have tacitly assumed a local trivialization of the bundle over w so that the holonomies are group elements). The order according to which the product of group elements is taken is determined by the orientation of the dual face. Of course, $\exp Z_w$ is defined only up to its conjugacy class (anyone of the four edges can be taken to be the "first"). As a consequence, there is an ambiguity in the choice of the base point for the holonomy, and it is necessary to introduce the notion of "discretized" gauge transformation; fixing the ambiguity amounts then to require that the discrete action is gauge invariant.

Before addressing this point, let us replace the continuous current field J by a collection of Lie algebra elements J_w:

$$J_w := \int_w J. \tag{6.10}$$

Here a trivialization of the bundle over the wedge w is chosen. The discretized action now becomes

$$\sum_w (\mathrm{Tr}(Z_w\, X_w) + \mathrm{Tr}(J_w\, X_w)). \tag{6.11}$$

Coming back to the definition of discrete gauge transformations, we require that they act in the center of each d-simplex. More precisely, a gauge transformation is parameterized by a collection of group elements in such a way that a group element g turns out to be assigned to each d-simplex. Than a gauge transformation is defined for the holonomy U of the connection A along any loop that starts and ends at the center C of the d-simplex according to:

$$U \to gUg^{-1}. \tag{6.12}$$

In turn, the wedge variables X_w and the discrete current variables J_w transform as

$$X_w \to gX_wg^{-1}, \quad J_w \to gJ_wg^{-1}. \tag{6.13}$$

Given this definition, $\mathrm{Tr}(X_w Z_w)$ is gauge invariant only when $\exp Z_w$ is actually the holonomy around the wedge w whose starting and final point is the center C of the d-simplex, as in (6.9). This fixes the ambiguity in the original choice of Z_w and makes the discretized action gauge invariant.

The approximation (6.8) is good as far as Z_w is close to the identity in the Lie algebra. This is certainly the case of BF theories, where we expect only connections close to flat ones to matter. To find out a further justification of the approximation for what concerns the problem of the integration over X_w variables, we shall address later some standard field theory arguments applied to BF theory in two dimensions.

Given for granted the approximation (6.8) we turn to the expression for the generating functional Z, obtained by integrating the exponentiated discrete action (6.11) over the Lie algebra elements X_w and group elements g, h. This path integral is given by

$$Z(J, \Delta) = \prod \int_{SU(2)} dg \prod \int_{SU(2)} dh \int \prod_w dX_w \, e^{i \sum_w \mathrm{Tr}(X_w Z_w) + \mathrm{Tr}(X_w J_w)}. \qquad (6.14)$$

Here the integrals are taken over all group elements g, h, entering the integrand through Z_w, (see (6.8)). The first two sets of integrals are the discrete analog of $\int \mathcal{D}A$, and dg is the normalized Haar measure $\int dg = 1$ on $SU(2)$. The integrals over X_w variables – one for each edge – are the analog of the integral over $\mathcal{D}B$. The measure dX_w represents some measure on the Lie algebra to be specified. Recall now that the integrals over X_w are not independent: all X_w that belong to one and the same dual face should have the same norm. However, as we shall see, there is no need to impose these constraints: one can integrate over all X_w independently, and later, when one integrates over the group elements, only the contributions coming from X_w with the same norm will survive. This is the reason why we do not impose these constraints in (6.14).

Let us now investigate the structure of the path integral (6.14). To calculate Z we have to find the functional of $\exp Z_w, \exp J_w$ given by

$$\int dX_w e^{i \,\mathrm{Tr}(X_w Z_w + X_w J_w)}. \qquad (6.15)$$

In fact, it is not hard to see that this function is proportional to the δ-function of $\exp Z_w$ peaked at $\exp J_w$. The proportionality coefficient must be a gauge invariant function of J_w. The expression in (6.15) must be set to be equal to $P(J_w)$, where P is the function that relates the Lebesgue measure on the Lie algebra and the Haar measure on the group (see Appendix 8.4). Thus the result of the calculation for (6.15) is given by the expression

$$P(J_w)\,\delta(\exp Z_w \exp J_w), \tag{6.16}$$

where δ is the standard δ-function on the group. Moreover, the function of Z_w, J_w given by (6.15) can be written equivalently as

$$P(J_w)\sum_j \mathrm{dim}_j \chi_j(\exp Z_w \exp J_w), \tag{6.17}$$

where we used the well known decomposition of the δ-function on the group into the sum over the characters $\chi_j(\exp Z_w \exp J_w)$ of the irreducible representations of the group. Here the sum is taken over all irreducible representations of $SU(2)$ (labelled by spins j), and $\mathrm{dim}_j = (2j+1)$.

Thus, we find that

$$Z(J,\Delta) = \prod \int_{SU(2)} dg \prod \int_{SU(2)} dh \prod_w P(J_w) \sum_{j_w} \mathrm{dim}_{j_w} \chi_{j_w}(\exp Z_w \exp J_w). \tag{6.18}$$

The integration over the group elements can now be easily performed using the well known formulas for handling integrals of products of matrix elements. However, for the sake of completeness, let us first give a systematic derivation of the result (6.16).

The expression (6.15) is related to a more complicated integral, which can be exactly calculated in the framework of 2D BF theories. Moreover, this procedure will allow us to specify the measure in (6.15). Let us focus our attention to a particular wedge w. We can restrict the bundle $\mathcal{P}$ to w and get an $SU(2)$ bundle $\mathcal{P}_w$ over w. Let A be a connection on $\mathcal{P}_w$, and B be an $\mathrm{Ad}(\mathcal{P})$-valued 0-form. Consider the following path integral:

$$\int \mathcal{D}A\mathcal{D}B \exp\left(i\int_w [\mathrm{Tr}(F\,B) + \mathrm{Tr}(J\,B)]\right), \tag{6.19}$$

where the integration over A is performed under the condition that the connection on the boundary of w is keeped fixed, and J is given by

$$J = \delta(p) J_w, \tag{6.20}$$

where p is an arbitrary fixed point on w, and J_w is defined as in (6.15),(6.16). The path integral (6.19) is just the partition function of BF theory on the disk with the distributional source given by (6.20). This partition function can be evaluated following the procedure of [52] and the result is given by (6.16), where Z_w is the Lie algebra element that corresponds to the holonomy of A along the boundary of w. The result (6.16) can then be checked by taking the partition function on the disk (which is equal to $\delta(g)$, where g is the holonomy along the boundary of the disk), and integrating it over dg. This calculation must give the partition function on a punctured sphere, and indeed we see that it reproduces the result given in [52]. The only cautionary remark is that the calculation performed in [52] gives a gauge invariant partition function, namely an expression in which one takes $J = \delta(p)hJ_wh^{-1}$ and integrates over dh. Thus strictly speaking, the techniques developed in [52] can be used only to calculate gauge invariant quantities, and are not directly applicable to the integral (6.19). Therefore, on the basis of [52], one can only argue that (6.19) is equal to

$$P(J_w)\delta(e^{Z_w}he^{J_w}h^{-1}), \tag{6.21}$$

where h is some group element. To get rid of h in this expression recall how "discretized" gauge transformations act on the Lie algebra elements Z_w, J_w (see (6.12),(6.13)). Since the result of (6.15) must be invariant under this gauge transformations, it is not hard to see that this requirement fixes h above to be the identity, thus giving (6.16).

After this technical point concerning the evaluation of the path integral (6.19), let us show that this path integral is actually equivalent to (6.15). Indeed, the integration over B in (6.19) can be performed in two steps. First, one integrates over those $B(x)$ with $x \neq p$, and then one integrates over $B(p)$, namely

$$\int dX_w \int_{B(p)=X_w} \mathcal{D}B \int \mathcal{D}\omega \exp\left(i\int_w [\mathrm{Tr}(F\,B) + \mathrm{Tr}(J\,B)]\right). \tag{6.22}$$

Since the current is distributional and concentrated at point p, in the last integrand it does not matter when one integrates over $\mathcal{D}B, \mathcal{D}\omega$. On the other hand, using the same approximation as in (6.8), it is not hard to show that

$$\int_{B(p)=X_w} \mathcal{D}B \int \mathcal{D}A \exp\left(i\int_w \mathrm{Tr}(F\,B)\right), \tag{6.23}$$

where the integral over A (keeping A on the boundary of w fixed) is approximated by

$$e^{i\mathrm{Tr}(Z_w\, X_w)}, \tag{6.24}$$

where $\exp Z_w$ is the holonomy of A along the boundary of w. Putting this last result back into (6.22) one gets exactly (6.15). This completes our discussion on the derivation of (6.16).

Coming back to the expression (6.18) for the generating functional, we can now perform the integrals over the group elements. Integration over the group elements h that correspond to edges dividing dual faces into wedges is the same in any dimension, and we can perform it directly. The rest of the group elements corresponds to edges that form the boundary of the dual faces. The integration over these group elements g depends on the dimensions.

Each group element h is "shared" by two wedges; thus, we have to take the integral of the product of two matrix elements. By integrating over all these edges, and making a simple change of variables to eliminate trivial integrations, we find

$$\begin{aligned} Z(J,\Delta) &= \prod_\epsilon \int_{SU(2)} dg_\epsilon \prod_\sigma \sum_{j_\sigma} (\dim_{j_\sigma})^{\kappa_\sigma} P(J_1)\cdots \\ &\quad \cdots P(J_n)\chi^{j_\sigma}(\exp J_1\, g_{\epsilon_1}\, \exp J_2 \cdots \exp J_n\, g_{\epsilon_n}). \end{aligned} \tag{6.25}$$

As we said before, the remaining integrals are over the group elements g_ϵ that correspond to the edges ϵ of the dual complex (edges that connect centers of d-simplices). The second product is taken over the dual faces σ; j_σ is the spin labelling the dual face σ, χ^{j_σ} is the character of the irrep labelled by j_σ and κ_σ is the Euler characteristics of σ. Each of these last terms is equal when the dual face has the topology of a disc. In what follows we will always assume that this is the case. The order of the group elements in the argument of χ^{j_σ} is clear from Fig. 6.5.

The only terms which survive in (6.25) are those for which the spins j_σ of all wedges corresponding to one and the same dual face are equal. As one can see from the formula (8.13) for the inverse Fourier transform, the spin labelling a wedge in (6.18) has the meaning of the length of the corresponding Lie algebra element X. Thus there is no need to impose the constraint that the length of all wedge variables X_w belonging to one and the same dual face are equal: this constraint is automatically fullfilled when the integration over the group elements is performed.

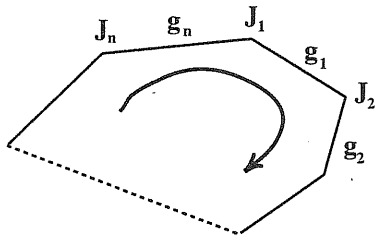

Fig. 6.5: The product of the group elements is the holonomy around the dual face σ with the insertions of the group elements $\exp J$ at each center of the corresponding d-simplex.

The generating functional is generally not invariant under a refinement of the triangulation Δ unless the theory is a topological field theory (namely unless $J = 0$). By setting now $J = 0$ in the definition of the generating functional, the integrand in (6.25) becomes

$$\prod_{\epsilon}\prod_{\sigma}\sum_{j_\sigma}(\dim_{j_\sigma})\chi^{j_\sigma}(g_{\epsilon_1}\cdots g_{\epsilon_n}). \tag{6.26}$$

using the obvious relations $\chi^j(g) = \sum_m D^j_{mm}(g)$ and $D^j_{mm}(gh) = \sum_{m'} D^j_{mm'}(g)D^j_{m'm}(h)$ we may rewrite the characters in (6.26) according to

$$\chi^j(g_{\epsilon_1}\cdots g_{\epsilon_n}) = \sum_{m,m_1,\cdots,m_{n-1}} D^j_{mm_1}(g_{\epsilon_1})D^j_{m_1m_2}(g_{\epsilon_1})\cdots D^j_{m_{n-1}m}(g_{\epsilon_n}). \tag{6.27}$$

As we said before in the d dimensional case we have d dual faces intersecting on a dual edges; then in the partition function there appears, as a contribution from each σ^{d-1} of the original triangulation, the integral

$$\int dg_{\epsilon_j} D^{j_1}_{m_1m'_1}(g_{\epsilon_j})D^{j_2}_{m_2m'_2}(g_{\epsilon_j})\cdots D^{j_d}_{m_dm'_d}(g_{\epsilon_j})$$

where $j_1,\cdots,j_d$ are the colors of the faces of a $(d-1)$-simplices bordering a d-simplex. But, as we can see comparing the result of section (5.2) and (6.1) this is exactly the basic expression which enters our spin models. More precisely, if we expand the integral above in terms of 3jm symbols we obtain

$$\sum_{\{J\}} \prod_{k=1}^{d-3} (-1)^{2J_k} (2J_k+1) \sum_{\mathcal{M},\nu} (-1)^{\mathcal{M}+\nu} \begin{pmatrix} j_1 & j_2 & J_1 \\ m_1 & m_2 & \mathcal{M}_1 \end{pmatrix} \begin{pmatrix} J_1 & j_3 & J_2 \\ -\mathcal{M}_1 & m_3 & \mathcal{M}_2 \end{pmatrix} \cdot$$

$$\begin{pmatrix} j_1 & j_2 & J_1 \\ m'_1 & m'_2 & \nu_1 \end{pmatrix} \begin{pmatrix} J_1 & j_3 & J_2 \\ -\nu_1 & m'_3 & \nu_2 \end{pmatrix} \cdots \begin{pmatrix} J_{d-4} & j_{d-2} & J_{d-3} \\ -\mathcal{M}_{d-4} & m_{d-2} & \mathcal{M}_{d-3} \end{pmatrix}$$

$$\begin{pmatrix} J_{d-3} & j_{d-1} & j_d \\ -\mathcal{M}_{d-3} & m_{d-1} & m_d \end{pmatrix} \cdot \begin{pmatrix} J_{d-4} & j_{d-2} & J_{d-3} \\ -\nu_{d-4} & m'_{d-2} & \nu_{d-3} \end{pmatrix} \begin{pmatrix} J_{d-3} & j_{d-1} & j_d \\ -\nu_{d-3} & m'_{d-1} & m'_d \end{pmatrix} . \tag{6.28}$$

Collecting together all the σ_j^{d-1} occurring in a fundamental block $\tilde{\sigma}^d$, the result amounts exactly to a $\{\frac{3}{2}(d+1)(d-2)\}j$ symbols times a product of sets of 3jm symbols. Each one of these subfactors is used to generate the contribution of another σ^d sharing σ_j^{d-1} with the previous $\tilde{\sigma}^d$. Iterating this procedure on all the d-simplices of the triangulation Δ we obtain exactly the state sum model given in Section 6.1.

6.2.2 A proof by means of a generalization of the Ooguri approach. A Correspondence between the Hilbert spaces.

Our first aim is to show that the space of physical states in the discretized model, $H(\Delta)$, is isomorphic to H_{BF}, the space of gauge-invariant functions over the moduli space of flat $SU(2)$ connections.

We start by discussing the definition of $H(\Delta)$ which is a generalization of the corresponding definition stated in the original approach of [5]. Consider a closed d-dimensional manifold M^d and decompose it into three parts, M_1^d, M_2^d and N^d (the picture in Fig. 6.6 refers to a simple example in $d=3$), where N^d has the topology of $\Sigma \times [0,1]$ with Σ a closed orientable $(d-1)$-dimensional submanifold, and each M_i^d $(i=1,2)$ has a boundary which is homeomorphic to Σ. The manifold M^d is reconstructed by glueing the boundaries of N^d with ∂M_1^d and ∂M_2^d. (From now on we omit the overscript d on M_1, M_2, N for short). Corresponding to this decomposition of M^d, the partition function $Z[M^d]$ of the manifold M^d can be expressed as a sum of products of three components, associated with M_1, M_2 and N, respectively. To explicitate such an expression, we note that, since the partition function $Z[M^d]$ is independent of the choice of the simplicial decomposition of M^d, we can place d-simplices in M^d in such a way that M_1, M_2 and N do not share any d-simplex,

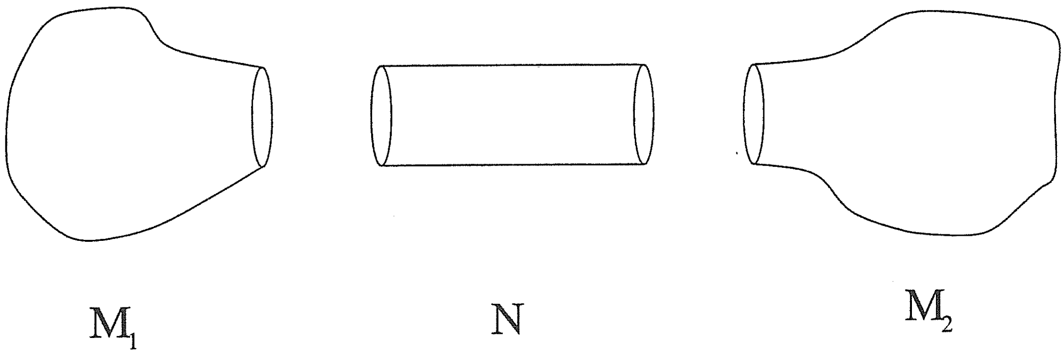

Fig. 6.6: Decomposition of a 3-manifold M into three parts.

namely their boundaries are triangulated by faces of d-simplices. Corresponding to this simplicial decomposition, we can re-express our $Z[M^d]$ in (6.2) as

$$Z[M^d] = \sum_{\substack{c_1 \in C(\Delta_1) \\ c_2 \in C(\Delta_2)}} Z[M_1, \Delta_1](c_1) w_L^{-\Xi(\Delta_1)} P_{\Delta_1,\Delta_2}(c_1, c_2) w_L^{-\Xi(\Delta_2)} Z[M_2, \Delta_2](c_2), \tag{6.29}$$

Here Δ_i $(i = 1, 2)$ denotes fixed triangulations of the boundaries ∂M_i, $C(\Delta_i)$ is the set of all possible colorings on Δ_i, and $\Xi(\Delta_i)$ agree with the definition given in Section (5.3) for Δ_i. Each factor $Z_{M_i,\Delta_i}(c_i)$ is given by the sum over all the possible colorings on the $(d-2)$-simplices in the interior of M_i, namely

$$Z[M_i, \Delta_i](c_i) == w_L^{(-1)^d \Xi^{int}} \prod_{all\ \tilde{\sigma}^{d-2} \in \Delta_i} (-1)^{2j_{\tilde{\sigma}^{d-2}}} (\sqrt{2j_{\tilde{\sigma}^{d-2}} + 1})$$

$$\sum_{coloring} \prod_{all\ \sigma^{d-2} \in M_i} (-1)^{2j_{\sigma^{d-2}}} (2j_{\sigma^{d-2}} + 1) \prod_{all\ \sigma^{d-1} \in M_i} \left(\prod_{C=1}^{d-3} (-1)^{2J_C} (2J_C + 1) \right)_{\sigma^{d-1}} \cdot$$

$$\cdot \prod_{all\ \sigma^d} \left\{ \tfrac{3}{2}(d-2)(d+1)j \right\}_{\sigma^d} (J),$$

where now we have keeped fixed the coloring c_i on σ^{d-2} lying in ∂M_i and $\Xi^{int} = N_0^{int} - N_1^{int} + N_2^{in} + \cdots + (-1)^d - 2N_{d-2}^{int}$. Similarly, $P_{\Delta_1,\Delta_2}(c_1, c_2)$ is given by a sum over all the possible colorings on the internal σ^{d-2} of N with fixed colorings c_1 and c_2 on $\partial N \cong \Sigma + \Sigma$.

Since also the operator P_{Δ_1,Δ_2} is obviously independent of the simplicial decomposition of the interior of N, it satisfies the following property with respect to compositions

$$\sum_{c_2 \in C(\Delta_2)} P_{\Delta_1,\Delta_2}(c_1, c_2) w_L^{-\Xi(\Delta_2)} P_{\Delta_2,\Delta_3}(c_2, c_3) = P_{\Delta_1,\Delta_3}(c_1, c_3), \tag{6.30}$$

where Δ_2 is a triangulation of a copy of Σ which lies between Δ_1 and Δ_3. Therefore we can define an operator $\mathcal{P}$

$$\mathcal{P}[\phi_\Delta](c) = \sum_{c' \in C(\Delta)} P_{\Delta,\Delta}(c,c') w_L^{-\Xi(\Delta)} \phi_\Delta(c'),$$

which acts as a projection operator ($\mathcal{P} \cdot \mathcal{P} = \mathcal{P}$) on the space of complex (piecewise-linear) functions ϕ_Δ on $C(\Delta)$. By using (6.30), we can rewrite (6.29) as

$$Z[M^d] = \sum_{c_1,c_2} \mathcal{P}[Z[M_1,\Delta_1]](c_1') w_L^{-\Xi(\Delta_1)} P_{\Delta_1,\Delta_2}(c_1,c_2) w_L^{-\Xi(\Delta_2)} \mathcal{P}[Z[M_2,\Delta_2]](c_2').$$

Then we see that "states" propagating from M_1 to M_2 through N are projected out by $\mathcal{P}$. Thus it is natural to define a physical Hilbert space $H(\Delta)$ for the triangulated surface Σ as a subspace projected out by $\mathcal{P}$, i.e.

$$\phi_\Delta(c) \in H(\Delta) \qquad \Longleftrightarrow \qquad \phi_\Delta = \mathcal{P}[\phi_\Delta] \tag{6.31}$$

We define an inner product in $H(\Delta)$ by setting

$$(\phi_\Delta, \phi'_\Delta) = \sum_{c,c' \in C(\Delta)} \phi_\Delta(c) w_L^{-\Xi(\Delta)} P_{\Delta,\Delta}(c,c') w_L^{-\Xi(\Delta)} \phi'_\Delta(c'). \tag{6.32}$$

It can be proved that $Z[M_1,\Delta](c)$ and $Z[M_2,\Delta](c)$ are real solutions of the Wheeler-DeWitt equation (6.31) and the partition function $Z[M^d]$ is given by their inner product according to

$$Z[M^d] = (Z[M_1,\Delta], Z[M_2,\Delta]). \tag{6.33}$$

On the other hand, in order to investigate the structure of the physical Hilbert space H_{BF} of a pure BF theory in dimension d we consider the topology $N = \Sigma \times [0,1]$ again, and we note that, performing the integration over the B field, we obtain that a wave-function of the theory can be represented by a function $\Phi(A)$, where A is a $SU(2)$ connection on Σ. The constraint $F_{ij} = 0$ implies that $\Phi(A)$ must vanish unless A is flat. The natural inner product in H_{BF} is given by the integral

$$(\Phi_1, \Phi_2)_{BF} = \int [dA] \delta(F_{ij}) \Phi_1^*(A) \Phi_2(A). \tag{6.34}$$

Thus a physical wave-function is a half-density on the moduli space of flat $SU(2)$ connections.

Before analyzing the structure of H_{BF}, we focus our attention on the state space H containing the gauge-invariant functions on the space of all $SU(2)$ connections. An element of H is built up by means of Wilson-line operators $U_j(x,y)$ (x,y are point in Σ, $j=0,\frac{1}{2},1,...$), defined as

$$U_j(x,y) = P\exp(\int_x^y A^a t_j^a),$$

where $P\exp$ denotes the path ordered exponential and t_j^a ($a=1,2,3$) is the spin-j generator of $SU(2)$. Under a gauge transformation, $A \to \Omega^{-1}A\Omega + \Omega^{-1}d\Omega$, and the Wilson-line operator behaves as $U(x,y) \to \Omega(x)^{-1}U(x,y)\Omega(y)$. Consider now a finite number of Wilson operators and take their tensor product $\otimes_{i=1}^n U_{j_i}(x_i,y_i)$. To make this quantity gauge-invariant, we need to contract the group indices of U_i's in such a way that the gauge factors Ω cancel out. Invariant tensors we can use to play this role are:

1) the Generalized Clebsch-Gordan (GCG) coefficient $\langle (j_1 \cdots j_{n-1})^A a j_n m_n | j_1 m_1 \cdots j_{n-1} m_{n-1} \rangle$, (defined in Section 3.2);

2) the metric $g_{mm'}^{(j)} := \sqrt{2j+1}\langle jmm'|00\rangle = (-1)^{j-m}\delta_{m+m',0}$.

It can be shown that a gauge-invariant function which arises in this way corresponds to a colored multivalent graph Y on Σ. Such a graph can be decomposed into three-valent graphs by expanding the GCG in terms of Clebsch-Gordan: a path from x to y in Y corresponds to a Wilson-line $U(x,y)$ or an identity (if associated to intermediate angular momenta of GCG) and a three-valent vertice in Y represents the CG-coefficients.

The case of Wilson-lines intersections must be handled with care. We cut the Wilson-lines at the intersecting point and we use the identity

$$g_{m_1 n_1}^{(j_1)} g_{m_2 n_2}^{(j_2)} = \sum_{j,m,n} g_{mn}^{(j)} \langle j_1 j_2 m_1 m_2 | jm\rangle \langle j_1 j_2 n_1 n_2 | jn\rangle$$

to replace the intersection with a pair of vertices and one infinitesimal Wilson-line connecting them. Actually, it is more convenient to use the cyclic-symmetric $3jm$-symbols rather than the Clebsch-Gordan coefficients. By regarding the m_i's in the $3jm$-symbol as lower indices which can be raised by the metric $g_{j_i}^{m_i m_i'}$, when three Wilson-lines meet together at the same point on Σ we can use the $3jm$-symbols and the metric $g_{mm'}^j$ to contract their group indices. We can also connect two Wilson-lines by the metric if they carry the same spin.

Summing up, we have shown so far that with each colored trivalent graph Y we can associate a function $\Psi_Y \in H$. In general, a gauge-invariant function of A is a linear combination of such

Ψ_Y's. Thus the space state H is isomorphic to a vector space $\tilde{C}(\Sigma)$ which is freely generated by colored trivalent graphs on Σ. The isomorphism is defined by $\sum_i a_i Y_i \in \tilde{C}(\Sigma) \leftrightarrow \sum_i a_i \Psi_{Y_i} \in H$, where Y_i's are colored trivalent graphs.

Each function $\Psi_Y(A)$ can be regarded as an element of H_{BF} simply by restricting its domain to the space of flat connections. However, the map $Y \to \Psi_Y \in H_{BF}$ is not injective (i.e. two different graphs Y and Y' may give the same function $\Psi_Y = \Psi_{Y'}$). In general, if two graphs Y and Y' are homotopic, the corresponding functions Ψ_Y and $\Psi_{Y'}$ have the same value on flat connections. On the other hand, with each colored trivalent graph Y one can always associate a colored triangulation and if two graphs Y and Y' are homotopically inequivalent, they correspond to distinct colored triangulations. The isomorphism between $\tilde{C}(\Sigma)$ and H then induces a homomorphism $\varphi : C(\Sigma) \to H_{BF}$, where $C(\Sigma) = \oplus_\Delta C(\Sigma, \Delta)$ is a vector space freely generated by colored triangulations.

As a consequence of these remarks, with each colored triangulation Δ we can associate a physical wave-function $\Psi_{\Delta,c}$ of the BF theory. The arbitrary wave-function $\Phi(A)$ is expanded in terms of such functions:

$$\Phi(A) = \sum_{\Delta} \sum_{c \in \Delta} \varphi_\Delta(c) w_L^{-\Xi(\Delta)} \Psi_{\Delta,c}(A). \tag{6.35}$$

Notice that the $\Psi_{\Delta,c}(A)$ are not linearly independent; rather, they obey just the following set of relations:

$$\Psi_{\Delta,c}(A) = \sum_{c' \in C(\Delta')} P_{\Delta,\Delta'}(c,c') w_L^{-\Xi(\Delta')} \Psi_{\Delta',c'}(A). \tag{6.36}$$

Owing to the flatness of A, we can now make the Wilson-line length to be arbitrarily small without changing the value of $\Psi_{\Delta,c}(A)$. Namely, the Wilson-line can be replace by an identity and the function $\Psi_{\Delta,c}$ should contain only a sum of products of the $3jm$-symbols used to obtain a gauge invariant function. In this way we get an expression which is formally identical to the corresponding expression in the spin model.

One can show that the relations among the $\Psi_{\Delta,c}$ on a flat connection A due to the change of the boundary triangulation are generated from the identity proving the invariance under elementary shellings of the discretized spin model [38]. Therefore (6.36) is proved and the uniquely comes out by the fundamental character of the relations.

By substituting (6.36) into (6.35), we obtain

$$\Phi(A) = \sum_{c \in C(\Delta)} \phi_\Delta(c) w_L^{-\Xi(\Delta)} \Psi_{\Delta,c}(A), \tag{6.37}$$

where $\phi_\Delta(c)$ is defined by

$$\phi_\Delta(c) = \sum_{\Delta'} \sum_{c' \in C(\Delta')} P_{\Delta,\Delta'}(c,c') w_L^{-\Xi(\Delta')} \varphi_{\Delta'}(c')$$

for an arbitrary *fixed* triangulation Δ of Σ. Then it follows from (6.30) that $\phi_\Delta(c)$ solves the Wheeler-DeWitt equation (6.31) of the spin model, namely it satisfies: .

$$\phi_\Delta = \mathcal{P}[\phi_\Delta].$$

Summing up, for each solution $\phi_\Delta(c)$ of the Wheeler-DeWitt equation, there exists a physical state $\Phi(A)$ of the BF theory given by (6.37). Since (6.36) are the only relations among $\Psi_{\Delta,c}$'s, this correspondence between ϕ_Δ and Φ is one-to-one.

We will show in the following point C that the inner product of Wilson-line networks

$$(\Psi_{\Delta_1,c_1}, \Psi_{\Delta_2,c_2})_{BF}$$

in the BF theory is equal to $P_{\Delta_1,\Delta_2}(c_1,c_2)$ for the discretized spin model, up to a constant factor. Therefore the map from $H(\Delta)$ to H_{BF} defined by (6.37) preserves the inner products in the two spaces and provides the isomorphism between the physical Hilbert spaces of our spin network model and the pure BF theory in any dimension d.

B Correspondence between wave-functions.

In the following we are going to show that the isomorphism between the Hilbert spaces discussed before identifies in both models wave-functions associated with the same underlying d-dimensional geometry.

Recall that in a pure BF theory, the physical wave-function Φ_{M^d} for M^d may be defined as

$$\Phi_{M^d}(A_{|\Sigma})\delta(F_{ij|\Sigma}) = \int_{A_{|\Sigma}:fixed} [dB, dA] \exp(i \int_M B \wedge (dA + A \wedge A)), \tag{6.38}$$

where we perform the functional integral over B and flat A in the interior of M with a fixed boundary condition for A on $\partial M^d = \Sigma$. The integration over $B_{|\Sigma}$ gives rise to the delta function $\delta(F_{ij|\Sigma})$. This ensures that the functional integrals in the right-hand side gives a physical state of the BF theory.

In order to analyze the structure of $\Phi_{M^d}(A)_\sigma$ we start by considering the exact sequence of homotopy groups for the pair $(M^d, \partial M^d)$, namely:

$$\begin{gathered}\cdots \to \pi_2(\partial M^d) \to \pi_2(M^d) \to \pi_2(M^d, \partial M^d) \to \pi_1(\partial M^d) \to \\ \to \pi_1(M^d) \to \pi_1(M^d, \partial M^d) \to \pi_0(\partial M^d) \to \pi_0(M^d).\end{gathered} \tag{6.39}$$

If G is a compact Lie group we may also apply the controvariant functor $Hom(\cdot, G)$ to obtain another long exact sequence which reads:

$$\cdots \to Hom(\pi_1(M^d), G) \to Hom(\pi_1(\partial M^d), G) \to Hom(\pi_2(M^d, \partial M^d), G) \to \cdots \tag{6.40}$$

From the exactness of this last sequence we get that $\mu : Hom(\pi_1(\partial M^d), G) \to Hom(\pi_2(M^d, \partial M^d), G)$, $\varphi : Hom(\pi_1(M), G) \to Hom(\pi_1(\partial M^d), G)$, than $Ker\mu = Im\varphi$. On the other hand, there exists an isomorphism between $Hom(\pi_1(N), G)$ and the set of flat connections on some N.

We fix now the condition that the *Holonomy* around any element of $\pi_2(M^d, \partial M^d)$ for a connection $A \in Hom(\pi_1(\partial M^d), G)$ on ∂M is equal to zero (namely, A is an element of the Kernel of μ). Thus we obtain that A is the image under φ of a flat connection τ over M^d, namely τ is the preimage of A. In other words, the condition $Hol(A) = 0$ over the group $\pi_2(M^d, \partial M^d)$ turns out to be sufficient to extend A to a flat connection on M^d. But it is also a necessary condition, since the holonomy of a flat connection around a contractible loop is zero.

Thus the group $\pi_2(M^d, \partial M^d)$, representing the cycles on ∂M^d that are contractible on M^d, encodes the information on the flat connections on ∂M^d, giving rise to flat connections on the whole manifold.

In the previous point we have found that for each physical state $\phi_\Delta(c)$ of the spin model, there is a corresponding state in the BF theory defined by (6.37). Therefore it is natural to expect that the wave-functions $\Phi_M(A_{|\Sigma})$ and $Z[M, \Delta](c)$ associated with the same d-dimensional manifold M

are related through

$$\Phi_M(A_{|\Sigma}) = D_b \sum_{c \in C(\Delta)} Z[M,\Delta](c) w_L^{-\Xi(\Delta)} \Psi_{\Delta,c}(A_{|\Sigma}), \tag{6.41}$$

when $A_{|\Sigma}$ is a flat connection and D_b is a constant depending on $rank(\pi_2(M, \partial M)) \equiv b$. This is indeed the case, as we shall show below.

Since the necessary and sufficient condition for $A_{|\Sigma}$ to have a flat extension in M is that its holonomies $U_{(a)}$ $(a = 1, ..., b)$ around the contractible cycles are trivial, we get

$$\Phi_M(A_{|\Sigma}) = D'_b \prod_{a=1}^{b} \delta(U_{(a)} - \mathbf{1}), \tag{6.42}$$

where D'_b is a constant independent of $A_{|\Sigma}$, and $\delta(U - \mathbf{1})$ is a δ-function with respect to the Haar measure of $G = SU(2)$.

In order to check (6.41), we need to show first that the sum over colorings in the right hand side of equation (6.42) imposes the constraint $U_{(a)} = \mathbf{1}$ on $A_{|\Sigma}$. Namely, we should prove that, by recombining the Wilson-lines, the expression reduces to sums over the colorings of the contractible cycles according to

$$\sum_{c \in C(\Delta)} Z[M,\Delta](c) w_L^{-\Xi(\Delta)} \Psi_{\Delta,c}(A_{|\Sigma}) = \prod_{a=1}^{b} \left[\sum_{j=0}^{\infty} (2j+1)\ Tr(U_{(a)} j) \right]. \tag{6.43}$$

The orthonormality and the completeness properties of the irreducible $SU(2)$ characters imply that the right hand side of this equation gives the product of δ-functions as in (6.42).

To prove the equality in (6.43), suppose we have used a collection of n d-simplices in computing the wave-function $Z[M,\Delta](c)$ for the discretized manifold M. The d-simplices have been placed in such a way that the boundary Σ of M is triangulated by(Δ, c). Choose one of the d-simplices which has some of its boundary in (Δ, c). Since $A_{|\Sigma}$ is flat, we can use (6.36) to remove this particular d-simplex, namely

$$\sum_{c \in C(\Delta)} Z[M,\Delta](c) w_L^{-\Xi(\Delta)} \Psi_{\Delta,c}(A_{|\Sigma}) = \sum_{c' \in C(\Delta')} Z[M,\Delta'](c) w_L^{-\Xi(\Delta')} \Psi_{\Delta',c'}(A_{|\Sigma}),$$

where Δ is the original triangulation of Σ, and Δ' is obtained by removing that d-simplex. Obviously, in computing $Z[M,\Delta'](c)$, the number of d-simplices we use is $(n-1)$. By implementing this procedure we obtain a triangulation with a tree structure, in which each d-simplex is glued to the complementary triangulation through at most one $(d-1)$-subsimplices and/or some $(d-r)$-subsimplices, with $r \geq 2$. The state sum reduces to contain only a boundary contribution, if we recall that the graphical relation given in Fig. 5.10 eliminates the contributions of the internal $(d-1)$-subsimplices of this new triangulation.

In order to show how this procedure works, we have to restrict our analysis to the d-torus topology, while other cases will be addressed elsewhere [38]. The study of the contribution to (6.43) associated with such kind of configurations in $d = 4, 5$ (refer to Appendix 8.5) can be exploited in order to show that in any dimension there exists an auxiliary 2-torus encoding the combinatorial structure of the state sum. Thus such a 2-torus T^2 is the fundamental object associated with the discretized theory. In particular, by cutting it into an upper and a lower part (topologically we get an annulus) we can decompose them into two triangles as shown in Fig. 6.7. Corresponding

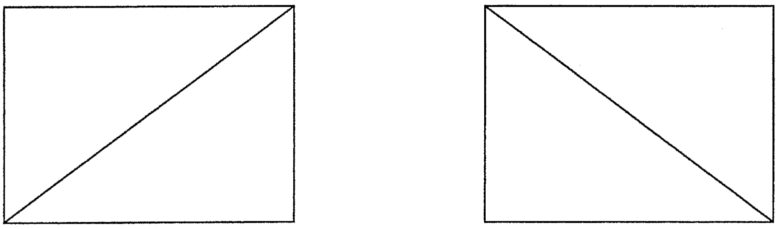

Fig. 6.7: Triangulation of the surface S.

to the above triangulations there are six Wilson-lines on Σ which are connected by four vertices (Fig. 6.7). We can choose now one of the Wilson-lines, say j_2 in Fig. 6.8, and remove a pair of

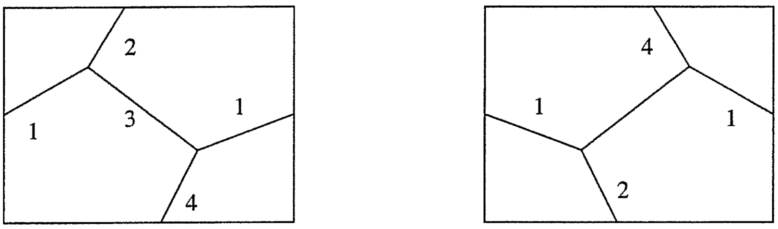

Fig. 6.8: Graph of Wilson-lines.

vertices at its end-points by using the orthogonality condition of the $3jm$ symbols. The resulting diagram is shown in Fig. 6.9. Owing to the flatness of $A_{|\Sigma}$, we can move around the Wilson-line j_1

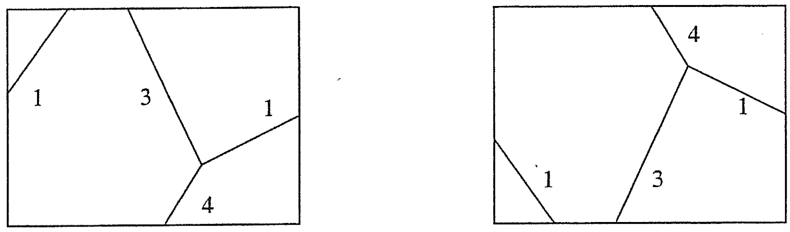

Fig. 6.9: Removing of a couple of vertices.

homotopically, and the network in Fig. 6.9 can be brought into the configuration depicted in Fig. 6.10. Since the Wilson-loop consisting of j_1 and j_3 is contractible on Σ, we end up with the final

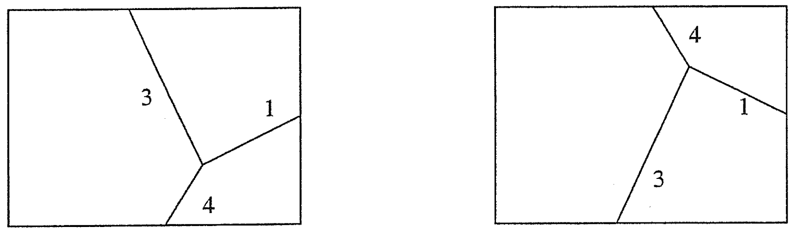

Fig. 6.10: Removing of a Wilson-line.

configuration shown in Fig. 6.11. Summing up, the Wilson-line network on the auxiliary torus

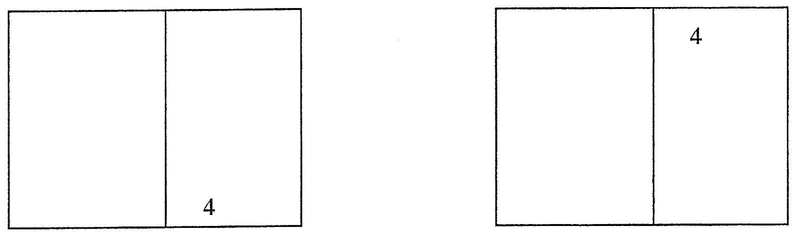

Fig. 6.11: Final configuration of the triangulation on S.

is deformed into a single Wilson-loop around its homology cycle contractible in M^d. Moreover, taking into account the weight in $Z[M,\Delta](c)$, we have checked that the resulting summation over j_4 reproduces the right hand side of (6.43) for the d-torus case.

This proves the identity (6.41), and the equivalence between D_b and D'_b.

C Correspondence between the partition functions.

We show here that the partition functions of the two theories considered above coincide, as long as the d dimensional manifolds involved are obtained by glueing together d-tori and spheres S^d.

As we have shown in item B, the wave-functions of the BF theory and of the spin model are related by (6.41). $Z^{(BF)}_{M^d} = (\Phi_{M_1}, \Phi_{M_2})_{BF}$ and $Z[M^d]$, given in (6.33), are the same since the isomorphism (6.35) preserves the inner products in the two Hilbert spaces, H_{BF} and $H(\Delta)$. Thus, in order to establish the equivalence $Z^{(BF)}_{M^d} = Z[M^d]$, we have just to show that

$$(\Psi_{\Delta_1,c_1}, \Psi_{\Delta_2,c_2})_{BF} = D_b^2 \cdot P_{\Delta_1,\Delta_2}(c_1, c_2) \tag{6.44}$$

or equivalently that

$$\sum_{\substack{c_1 \in C(\Delta_1) \\ c_2 \in C(\Delta_2)}} \Psi_{\Delta_1,c_1}(A_1) w_L^{-\Xi(\Delta_1)} P_{\Delta_1,\Delta_2}(c_1, c_2) w_L^{-\Xi(\Delta_2)} \Psi_{\Delta_2,c_2}(A_2) = D_b^{-2} \cdot K(A_1, A_2), \tag{6.45}$$

where $K(A_1, A_2)$ is a kernel for the inner product, namely

$$(\Phi, \Phi')_{BF} = \int [dA_1]\delta(F_{1,ij}) \int [dA_2]\delta(F_{2,ij}) \Phi(A_1) K(A_1, A_2) \Phi(A_2),$$

and it is given in terms of the functional integral

$$K(A_1, A_2)\delta(F_{1,ij})\delta(F_{2,ij}) = \int_{\substack{A(t=0)=A_1 \\ A(t=1)=A_2}} [dB, dA] \exp(iS_{BF}(B, A)) \tag{6.46}$$

for the topology $N = \Sigma \times [0, 1]$.

Firstly, we show that the left-hand side of (6.45) is proportional to the right-hand side. The factor D_b^{-2} will be fixed later. Since Ψ_{Δ_i,c_i} is evaluated on a flat connection A_i, we may use (6.36) to rewrite the left hand side of (6.45) as

$$\sum_{c \in C(\Delta)} w_L^{-\Xi(\Delta)} \Psi_{\Delta,c}(A_1) \Psi_{\Delta,c}(A_2). \tag{6.47}$$

On the other hand, it follows from the functional integral expression (6.46) that the kernel $K(A_1, A_2)$ vanishes unless A_1 and A_2 have both flat extensions in N. For $N = \Sigma \times [0, 1]$, the flat extension exists if and only if A_1 and A_2 are gauge-equivalent. Thus we need to show that the sum over colorings in (6.47) imposes the constraint $A_1 \simeq A_2$

Let us examine the case when M_i are tori. As we have seen in item B, the auxiliary surface S associated to ∂M_i is a 2-torus. It can be decomposed into two triangles and the corresponding network of Wilson-lines is shown in Fig. 6.12. A flat connection A on the torus can be specified

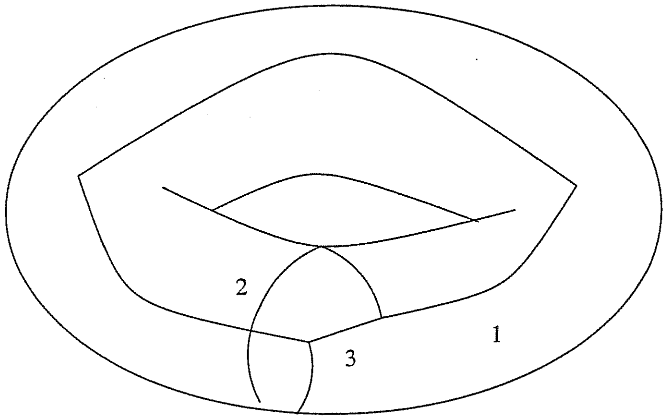

Fig. 6.12: Wilson-line on torus.

by the holonomies U and V around the two homology cycles on Σ. The wave-function $\Psi_{\Delta,c}$ for the network can then be regarded as a function of U and V. In the network in Fig. 6.12, the Wilson-line j_3 can be made arbitrarily short (using the flatness of A) and replaced by an identity. In this case, the wave-function $\Psi_{\Delta,c}$ is expressed as a function of U and V according to

$$\begin{aligned} \Psi_{\Delta;c}(U,V) = \textstyle\sum_{m_i,m_i',m_i''} U_{j_1 m_1'}^{\ m_1} V_{j_2 m_2'}^{\ m_2} g_{j_1}^{m_1' m_1''} g_{j_2}^{m_2' m_2''} g_{j_3}^{m_3 m_3''} \\ \begin{pmatrix} j_1 & j_2 & j_3 \\ m_1 & m_2 & m_3 \end{pmatrix} \begin{pmatrix} j_1 & j_2 & j_3 \\ m_1'' & m_2'' & m_3'' \end{pmatrix}. \end{aligned} \tag{6.48}$$

Here we marked the homology cycles on S in such a way that the Wilson-lines j_1 and j_2 wind around cycles corresponding to the holonomies U and V. The holonomies U and V commute with each other, so they can be diagonalized simultaneously. Since the wave-function $\Psi_{\Delta,c}$ is invariant under the simultaneous conjugation, $U \to \Omega^{-1}U\Omega$, $V \to \Omega^{-1}V\Omega$, we can substitute diagonal matrices $U_{jm'}^{\ m} = e^{im\theta}\delta_{m'}^{m}$ and $V_{jm'}^{\ m} = e^{im\varphi}\delta_{m'}^{m}$ into U and V in (6.48).

Consider now the following summation

$$\sum_{j_1,j_2,j_3} \Lambda^{-1}\Psi_{\Delta,c}(\theta_1,\varphi_1)\Psi_{\Delta,c}(\theta_2,\varphi_2), \tag{6.49}$$

where (θ_1,φ_1) and (θ_2,φ_2) are phases of the holonomies (U_1,V_1) and (U_2,V_2) for A_1 and A_2, respectively. Although it is possible to do the summation for generic values of the phases, it is more instructive to study the cases when two, among the four phases, vanish. (Actually it is enough, as we shall see below)

Let us consider the case when $V_1 = V_2 = \mathbf{1}$. In this case, the wave-function $\Psi_{\Delta,c}(U_i, V_i)$ is simplified as

$$\Psi_{\Delta,c}(U_i, V_i = \mathbf{1}) = \sqrt{\frac{(2j_1+1)(2j_2+1)(2j_3+1)}{2j_1+1}}\, Tr(U_{ij_1}).$$

The result of the summation (6.49) gives

$$\begin{aligned} &\textstyle\sum_{j_1,j_2,j_3} \Psi_{\Delta,c}(U_1, V_1 = \mathbf{1})\Psi_{\Delta,c}(U_2, V_2 = \mathbf{1}) \\ &= \textstyle\sum_{j_1} Tr(U_{1j_1})Tr(U_{2j_1}) \cdot w_L^{-1} \cdot \frac{1}{2j_1+1} \sum_{|j_2-j_3|\le j_1 \le j_2+j_3} (2j_2+1)(2j_3+1) \\ &= \textstyle\sum_{j_1} Tr(U_{1j_1})Tr(U_{2j_1}) = \delta(U_1 - U_2). \end{aligned}$$

Here we have used the definition of w_L and the orthonormality of the irreducible characters $Tr(U_{j_1})$. Thus the sum over colorings in the left-hand side of (6.45) indeed imposes the constraint $U_1 = U_2$ when $V_1 = V_2$. It is straightforward to do the computations in other cases, namely when $U_2 = V_2 = \mathbf{1}$ or $V_1 = U_2 = \mathbf{1}$. The sum in (6.49) imposes $U_1 = U_2$ and $V_1 = V_2$ in both of these cases.

We have seen that the left hand side of (6.45) is proportional to $K(A_1, A_2)$ as far as two among the four phases are equal to zero. Let us relax now this condition and suppose that they are not necessarily zero, but their ratios θ_i/φ_i $(i = 1, 2)$ are rational numbers. Since (6.49) is invariant under the modular transformations of S, we can change the basis of the homology cycles in such a way that two among the four phases around the cycles become equal to zero. The summation in (6.49) then reduces to the computation made above, and we see that the constraints $A_1 \simeq A_2$ arises owing to the presence of the summation. In general, when the ratios are not rational, we can find a series of rational numbers which converges to θ_i/φ_i. At each step in the series, the sum over the colorings in (6.49) gives the constraints $A_1 \simeq A_2$. Thus it will also be the case in the limit of the series.

So far we have found that the left hand side of (6.45) is equal to $K(A_1, A_2)$ up to a constant factor E_b, namely

$$\sum_{\substack{c_1 \in C(\Delta_1) \\ c_2 \in C(\Delta_2)}} \Psi_{\Delta_1,c_1}(A_1) w_L^{-\Xi(\Delta_1)} P_{\Delta_1,\Delta_2}(c_1,c_2) w_L^{-\Xi(\Delta_2)} \Psi_{\Delta_2,c_2}(A_2) = E_b \cdot K(A_1,A_2).$$

Equivalently we can write:

$$(\Psi_{\Delta_1,c_1}, \Psi_{\Delta_2,c_2})_{CS} = E_b^{-1} \cdot P_{\Delta_1,\Delta_2}(c_1,c_2).$$

By combining this last relation with (6.41) and by using the expressions of $Z_{M^d}^{(BF)}$ and $Z[M^d]$ in terms of pairings, we obtain

$$Z_M^{(BF)} = D_b^2 E_b^{-1} Z^d[M^d] \tag{6.50}$$

for b=1 (the d-torus has only one contractible homology). If we consider now the topology $M = S^d$ and normalize the invariants to be equal on it, by noticing that S^d can be constructed by glueing two tori, we obtain $D_b^2 E_b^{-1} = 1$, which completes the proof.

Chapter 7

Observables in Turaev-Viro model and explicit computation of $Z_{TV}[M^3]$.

In this chapter we introduce observables associated to link invariant in the context of the Turaev-Viro model and we show how this extension, which is based on a presentation of the manifolds in terms of Dehn surgery operations, allows the explictly computation of the invariant $Z_{TV}[M^3]$ (equivalent, in its explicit realization, to $Z[M^3](q)$) for lens space. The content of this chapter is based on [40].

7.1 Observable and link invariants.

In the original formulation given by Turaev and Viro in [3] links were absent, a gap filled only later on by Turaev himself in [53]. Our starting point is the notion of fat graph in a compact 3–manifold N. By this we mean a finite graph whose vertices and edges are extended to small 2–disks and *narrow* bands respectively. We will consider here only 3–valent fat graphs equipped with colors given by the assignment to edges of non negative integer or half–integer lying between 0 and $(k-2)/2$, where k is related to the deformation parameter of the quantum group associated to the theory. In our case we consider $SL_q(2,C)$ with $q = \exp \frac{2\pi i}{k}$ [53]. Note that the model without links will turn out to reproduce the usual form of the Turaev–Viro invariant (cfr. Section 6.1 and Appendix 8.1).

The set of the initial data of Turaev-Viro model are defined as follows. Fix a commutative ring

K, let $K^\star$ be the subgroup of invertible element of K. If I is a given finite set, let us consider the functions $i \to \omega_i$, $I \to K^\star$ and a given element w of $K^\star$. A G-tuple will be admissible if his triples are admissible, *adm*, and a triple is admissible if, in the explicitly realization of this context using a quantum group, its elements satisfy the triangular inequality. To every 6-tuple we associate the symbol $\begin{vmatrix} j_1 & j_2 & j_3 \\ j_4 & j_5 & j_6 \end{vmatrix} \in K$.

The initial data satisfy the conditions:

a) $\forall j_1, j_2, \ldots, j_6 \in I$ such that $(j_1 j_3 j_4)$, $(j_2 j_4 j_5)$, $(j_1 j_3 j_6)$ and $(j_2 j_5 j_6)$ are admissible triples, we have

$$\sum_j \omega_j^2 \begin{vmatrix} j_2 & j_1 & j \\ j_3 & j_5 & j_4 \end{vmatrix} \begin{vmatrix} j_3 & j_4 & j_6 \\ j_2 & j_5 & j \end{vmatrix} = \delta_{j_4 j_6}; \tag{7.1}$$

b) $\forall a, b, c, e, f, j_1, j_2, j_3, j_{23} \in I$, such that $(j_{23} a e j_1 f b)$ e $(j_3 j_2 j_{23} b f c)$ are admissible, we have

$$\sum_j \omega_j^2 \begin{vmatrix} j_2 & a & j \\ j_1 & c & b \end{vmatrix} \begin{vmatrix} j_3 & j & e \\ j_1 & f & c \end{vmatrix} \begin{vmatrix} j_3 & j_2 & j_{23} \\ a & e & j \end{vmatrix} = \begin{vmatrix} j_{23} & a & e \\ j_1 & f & b \end{vmatrix} \begin{vmatrix} j_3 & j_2 & j_{23} \\ b & f & c \end{vmatrix}; \tag{7.2}$$

c) $\forall j \in I$ we have

$$\omega^2 = \omega_j^{-2} \sum_{k,l:(jkl) \in amm.} \omega_k^2 \omega_l^2; \tag{7.3}$$

To this set we add another function $q_i \in K^*$, which satisfies the relation

$$\sum_{j_{13} \in I} \omega_{j_{13}}^2 q_{j_{13}} \begin{vmatrix} j_3 & j_1 & j_{13} \\ j_2 & j & j_{12} \end{vmatrix} \begin{vmatrix} j_2 & j_3 & j_{23} \\ j_1 & j & j_{13} \end{vmatrix} = q_j q_{j_1} q_{j_2} q_{j_3} q_{j_{12}}^{-1} q_{j_{23}}^{-1} \begin{vmatrix} j_3 & j_2 & j_{23} \\ j_1 & j & j_{123} \end{vmatrix}. \tag{7.4}$$

From this latter, the following basic relations are obtained

$$\begin{vmatrix} j_3 & g & e \\ j_1 & d & c \end{vmatrix} = \begin{vmatrix} j_1 & c & g \\ j_3 & e & d \end{vmatrix} = \sum_{j_{13} \in I} \omega_{j_{13}}^2 q_e q_c q_{j_1} q_{j_3} q_b^{-1} q_g^{-1} q_{j_{13}}^{-1} \begin{vmatrix} j_1 & j_3 & j_{13} \\ c & e & d \end{vmatrix} \begin{vmatrix} c & j_1 & g \\ j_3 & e & j_{13} \end{vmatrix}, \tag{7.5}$$

$$\sum_{j \in I} \omega_j^2 (q_a q_j q_b^{-2})^\varepsilon \begin{vmatrix} i & b & j \\ i & b & a \end{vmatrix} = q_i^{2\varepsilon} \tag{7.6}$$

where $\varepsilon = \pm 1$, and

$$\sum_{\substack{k \\ (i,j,k) \in adm}} \omega_k^2 = \omega_i^2 \omega_j^2. \tag{7.7}$$

If we consider the quantum initial data [53], namely if we explicitly realize the model using a quantum group, we obtain:

$$\begin{aligned}
\omega^2 &= -2r/(q^{1/2} - q^{-1/2})^2 \equiv w_q^2 \\
\omega_j &= (-1)^{2i}[2j+1]_q^{1/2} \equiv w_{(q)j} \\
\left| \begin{matrix} j_1 & j_2 & j_3 \\ j_4 & j_5 & j_6 \end{matrix} \right| &= (\sqrt{-1})^{-2(\sum j_i)} \left\{ \begin{matrix} j_1 & j_2 & j_3 \\ j_4 & j_5 & j_6 \end{matrix} \right\}_q \\
q_i &= \exp(\pi\sqrt{-1}(i - i(i+1)r^{-1})).
\end{aligned} \tag{7.8}$$

where $[k] = \frac{q^{k/2}-q^{-k/2}}{q^{1/2}-q^{-1/2}}$ and $\left\{ \begin{matrix} j_1 & j_2 & j_3 \\ j_4 & j_5 & j_6 \end{matrix} \right\}_q$ is the quantum Racah-Wigner symbols.

The Turaev–Viro invariants can be generalized to get invariant of the form $|M^3, F|_\mu$, with F a certain union of components of fixed ∂M^3,

$$|M^3, F|_\mu = \omega^{-2\alpha+\beta'} \prod_{e''} \omega_\mu(e'') \prod_e \omega^2_{\mu(e)} \prod_T |T|_\mu \tag{7.9}$$

where α is the number of vertices of M^3, β' the number of vertices of $\partial M^3 \backslash F$, e runs over the edges of M^3, which do not lie in ∂M^3, e'' runs over the edges of $\partial M^3 \backslash F$ and T runs over all 3–simplices of M^3.

A coloring of a 3–valent graph φ is a function which associates an element of the set I with each edge of φ. This assignement is such that, for any vertex of φ incident to 3 (resp. 2) edges of φ, the colors of these edges form an admissible triple (resp. are equal to each other). Each fat graph Γ has a core $c(\Gamma)$ which is an ordinary graph consisting of edges and vertices.

If F is any compact surface, a fat graph in the cylinder $F \times [-1, 1]$ may be represented by graph diagrams on F containing only double transversal crossings of edges (provided with an additional structure showing the undercrossings and overcrossings). Let now F be an oriented compact surface and let φ and ψ two colored 3–valent graphs embedded in F. Let Γ be an oriented colored fat graph in $F \times [-1, 1]$ and D its graph diagram on F. We may assume that φ, ψ and D lie in general position so that all crossings of $\varphi \cup \psi \cup D$ are double transversal crossings of edges. We derive a graph diagram from $\varphi \cup \psi \cup D$ assuming that φ lies everywhere over $\psi \cup D$, and ψ lies everywhere under $\varphi \cup D$. Denote the resulting graph diagram on F by σ and denote by Σ the graph in F obtained from σ ignoring the over/under crossing information. The set of vertices of

Σ may be split into five subsets (Fig. 7.1):

1) the 2–valent vertices of φ, ψ, D;

2) the 3–valent vertices of φ, ψ, D;

3) crossings of φ with ψ;

4) crossings of D with φ or ψ;

5) self–crossings of D.

A *region* of D with respect to φ and ψ is a connected component of $F\backslash\Sigma$ and an *area–coloring* of D is an arbitrary mapping from the set of the regions of D into the set I. An *area–coloring* η of D is called admissible if for each edge e of Σ, the color of e together with the η–colors of the two regions of D adjacent to e form an admissible triple. Denote the set of admissible area–colorings by $adm(D)$. With each $\eta \in adm(D)$ we will associate an element $|D|_\eta$ of the ring K. For a region y of D we set

$$|y|_\eta = \omega_{\eta(y)}^{2\chi(y)} \tag{7.10}$$

where $\eta(y)$ and $\chi(y)$ are respectively the η–color and the Euler characteristic of y.

With respect to the previous classification we have five possible ways of characterizing a vertex $a \in \Sigma$, namely:

1) $|a|_\eta = 1$;

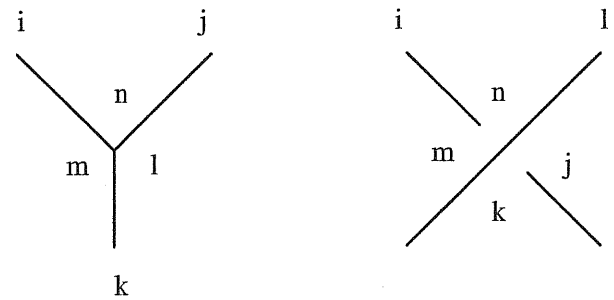

Fig. 7.1: Vertices configurations in Σ.

2)

$$|a|_\eta = \begin{vmatrix} i & j & k \\ l & m & n \end{vmatrix} \tag{7.11}$$

where i, j, k denote the colors of the three edges of Σ incident in a and l, m, n are the η–colors of the opposite regions;

3) the same expression used as in 2) where l is the color of the upper branch and i that of lower branch; moreover j, k, m, n are the η–colors of the four regions of D incident in a;

4)

$$|a|_\eta = q_k^{1/2} q_n^{1/2} q_j^{-1/2} q_m^{-1/2} \begin{vmatrix} i & j & k \\ l & m & n \end{vmatrix}. \tag{7.12}$$

5)

$$|a|_\eta = q_k q_n q_j^{-1} q_m^{-1} \begin{vmatrix} i & j & k \\ l & m & n \end{vmatrix}. \tag{7.13}$$

Finally, let us define the following quantity:

$$\langle \varphi | D | \Psi \rangle_\eta = \prod_y |y|_\eta \prod_a |a|_\eta \tag{7.14}$$

where y runs over all regions of D and a runs over all vertices of Σ. The state sum

$$\langle \varphi | \Gamma | \Psi \rangle = \sum_{\eta \in am(D)} \langle \varphi | D | \Psi \rangle_\eta \ \in K \tag{7.15}$$

turns out to be an invariant both under ambient isotopies of φ and ψ in F, and under isotopies of Γ in $F \times [-1, 1]$ [53]. If F is a disjoint union of n surfaces $F_1, \ldots, F_n$ then we can extend (7.14) and (7.15) according to:

$$\langle \varphi | \Gamma | \Psi \rangle = \prod_{k=1}^{n} \langle \varphi_k | \Gamma_k | \Psi_k \rangle \tag{7.16}$$

where φ_k, ψ_k are the components of φ, ψ lying on F_k, and Γ_k is the part of Γ lying in $F_k \times [-1, 1]$, $(\forall k = 1, 2, \ldots n)$ [53].

We can define now the invariants of links on a generic manifold. Let M^3 be a compact 3–manifold with a triangulated boundary ∂M^3 and let Γ be a 3–valent colored fat graph lying in $intM^3$. We set $F = \partial U$, where U is an oriented closed regular neighborhood of Γ in M^3. Consider a non–singular normal vector field on the surface of Γ which, together with the fixed orientation of this surface, determines uniquely the orientation of U. Shifting Γ along this vector field we get a parallel copy Γ' of Γ lying on F. U is an handle-body consisting of 3–balls and solid cylinders. Choose in each of these cylinders a meridian disk which lies transversal with respect to the corresponding band of Γ. Let $\psi_1, \ldots, \psi_m$ be the boundaries of discs obtained in this way, where m is the number of edges of Γ. The former loops can be considered as graphs with one vertex and one edge. We color them with a sequence $J = (j_1, \ldots, j_m) \in I^m$ and set $\omega_J = \prod_{k=1}^{m} \omega_{j_k}^2$. Let N be the compact

3–manifold $M^3 \backslash U$ bounded by $\partial N = F \cup \partial M^3$. We provide M^3 with an arbitrary triangulation, which extends the given triangulation of ∂M^3; also F is equipped with the induced triangulation and let s be the number of vertices of Γ. Then for each $\lambda \in col(\partial M^3)$ we define a relative invariant of the pair M^3, Γ,with respect to λ:

$$Z_{TV}[M^3, \Gamma, \lambda] = \omega^{2-2s} \sum_{\mu \in col(K), \mu|_{\partial M^3} = \lambda, J \in I^m} \omega_j |N, F|_\mu \langle \gamma_F^{\mu_F} | \Gamma' | \Psi_j \rangle \tag{7.17}$$

where γ_F is the dual graph of the 1–skeleton of the triangulation of F and $\mu_F = \mu|_F$. We introduce invariants on Heegaard diagrams of a closed 3–manifolds [53]. Recall that an Heegaard surface in a closed 3–manifold M^3 is a closed connected oriented surface $F \subset N$ which splits M^3 into the union of two handle-bodies U and V, bounded by F. We distinguish these handle-bodies assuming that the orientation of F, together with the normal vector field on F directed outwards U, defines uniquely the orientation of M^3. Let $\varphi_1, \ldots, \varphi_g$ (resp. $\psi_1, \ldots \psi_g$) be the boundaries of a system of meridian disks of V (resp. of U), where g is the genus of F. The surface F, together with these sets of loops, is a Heegaard diagram of N. We will treat the loops $\varphi_1, \ldots, \psi_g$ as graphs on F, each one of them having just one vertex and one edge. Denote by ψ_J the colored graph on F obtained from $\psi_1 \cup \ldots \cup \psi_g$ by assigning the coloring $j_1, \ldots, j_g$ to the edges of $\psi_1, \ldots, \psi_g$ respectively; a similar definition holds true for φ_H. Therefore if Γ is a colored 3–valent fat graph lying in $F \times [-1, 1] \subset N$ we obtain the invariant

$$Z_{TV}[M^3, \Gamma] = \omega^{-2} \sum_{\substack{J = (j_1 \ldots j_g) \in I^g \\ H = (h_1 \ldots h_g) \in I^g}} \prod_{i=1}^{r} \omega_{j_i}^2 \prod_{k=1}^{g} \omega_{h_k}^2 \langle \varphi_k | \Gamma' | \psi_j \rangle . \tag{7.18}$$

where Γ' is defined as before.

7.2 Dehn surgery.

A manifold M^3 can be understood as the union of several components glued together by some given identification of the points on their boundaries. If these components are glued in a different way, one may find a new manifold $M^{3\prime}$. In this case, we say that $M^{3\prime}$ can be obtained from M^3 by means of surgery. As is well known, any closed, orientable and connected 3-manifold can be obtained by surgery from the 3-sphere S^3 [54]. In this section we give a brief review of the surgery operations in S^3. In particular, we concentrate on Dehn surgery performed along knots or links in S^3. In order to describe Dehn surgery operations, we need to consider solid tori. A solid torus is a 3-dimensional space V homeomorphic to $S^1 \times D^2$. A given homeomorphism $h : S^1 \times D^2 \to V$ is called a framing of V. Given a tubular neighborhood N of a knot C and a framing h of N, the longitude $h(S^1 \times 1)$ of N defines a framing C_f of C, which is a preferred framing if the linking number of C and C_f is equal to zero. The longitude $\lambda = h(S^1 \times 1)$, defined by a preferred framing h of N, is oriented in the same way as C, and the meridian $\mu = h(1 \times \partial D^2)$ is oriented in such a way that its linking number with C is equal to $+1$. We say that the longitude λ and the meridian μ of N are the homotopy generators of a Rolfsen basis in ∂N and any class $[f] \in \pi_1(\partial N)$ is expressed in this basis as

$$[f] = a \cdot [\lambda] + b \cdot [\mu] = (a, b).$$

A Dehn surgery performed along a knot Z in S^3 can be described in the following way

1) first remove the interior $\dot{N}$, of a tubular neighborhood N of the knot Z, from S^3;

2) consider $S^3 \setminus \dot{N}$ and N as distinct spaces whose boundary $\partial(S^3 - \dot{N})$ and ∂N are tori;

3) glue back N and $S^3 - \dot{N}$ by identifying the points on their boundaries with a given homeomorphism $h : \partial N \to \partial(S^3 - \dot{N})$.

The knot Z and the glueing homeomorphism h completely specify the surgery operation and the resulting manifold is denoted by

$$M^3 = (S^3 - \dot{N}) \bigcup_h N. \tag{7.19}$$

Actually, the manifold (7.19) depends (up to homeomorphism) only upon the homotopy class of $h(\mu)$ in $\partial(S^3 - \dot{N})$, where μ is a meridian of N. The surgery is characterized then by the knot Z and by a closed curve $Y \in \partial N$ representing $h(\mu)$. The convention introduced by Rolfsen in order to codify the surgery instruction consist in choosing:

$$Y = a \cdot [\lambda] + b \cdot [\mu] := (a, b),$$

where the generators λ and μ are the longitude and the meridian of a Rolfsen basis in ∂N. The ratio $r = b/a$ is called the surgery coefficient. In conclusion, the surgery instructions are specified simply by the knot Z in S^3 and by the rational surgery coefficient r. Clearly, the surgery operation of removing and gluing back a solid torus can be iterated. Therefore, a general surgery instruction consists in the assignment of an unoriented link L in S^3 with given surgery coefficients $\{r_i\}$ associated with its components $\{L_i\}$. For example, when L is a circle with surgery coefficient $r = b/a$, the resulting space is homeomorphic with the lens space $L(a, b)$.

Two manifolds associated with different surgery instructions are homeomorphic if and only if the two surgery instruction are related by a finite sequence of Rolfsen moves [54] [55]. A Rolfsen move of the first type state amounts to add or delete a component of the surgery link L with surgery coefficient $r = \infty$. A Rolfsen move of the second type describes the effects of an appropriate twist homeomorphism $\tau_\pm$ on the surgery instruction.

Let L be a surgery link such that one of its components, say L_1, is a circle with surgery coefficient r_1. This means that all the remaining components L_j, with $j \neq 1$, belong to the complement solid torus V_1 of L_1 in S^3. Under a twist homeomorphism $\tau_\pm$ of V_1, the component L_1 is not modified, whereas L_j are changed according to $\tau_\pm : L_j \to L'_j$. Moreover the surgery coefficients become:

$$r'_1 = \frac{1}{1/r_1 \pm 1} \tag{7.20}$$

$$r'_j = r_j \pm [\theta(L_j, L_1)]^2 \quad for\, j \neq 1, \tag{7.21}$$

where $\theta(L_j, L_1)$ is the linking number of L_j and L_1.

When the surgery coefficient r is an integer, one can take $a = 1$ and $b = r$; in this case, the curve Y is a longitude of N and can be interpreted as a framing of the surgery knot Z.

7.3 Reformulation of the Turaev–Viro invariant.

The main purpose of this section is to rewrite the surgery construction in terms of the Turaev formalism. We start from the T–V invariant expression in the Heegaard splitting framework

$$Z[M^3](q) = w_q^{-2} \sum_{\substack{J = (j_1 \dots j_g) \in I^g \\ H = (h_1 \dots h_g) \in I^g}} \prod_{i=1}^{g} \omega^2_{(q)j_i} \prod_{k=1}^{g} \omega^2_{(q)h_k} \langle \varphi_k | 0 | \psi_j \rangle, \tag{7.22}$$

where φ_k and ψ_j are the meridians of the two handlebodies generating the manifolds. Let us consider the case in which the surgery link consists of many distinct loops with generic framings.

This is a sufficiently general situation which can be used to represents a great number of manifolds by explaiting the Kirby relations. In this situation $\langle\varphi_k|0|\psi_j\rangle$ becomes $\prod_i\langle\varphi_{k_i}|0|\psi_{j_i}\rangle$ where each term lives on a single torus, the regular neighborhood of each link component. It is necessary now to consider what happens to the torus in the Heegaard–splitting configuration as a consequence of the surgery operation. In the following we shall consider several distinct cases.

7.3.1 $S^2 \times S^1$.

We start with the case $r = 0$, where the surgery operation sends a meridian into a longitude on the surface; the curves that realize the quantity $\langle\varphi_k|0|\psi_j\rangle$ are a meridian of the torus (transformed) and a meridian of the complement respectively. The starting graph is showed in Fig. 7.2 where

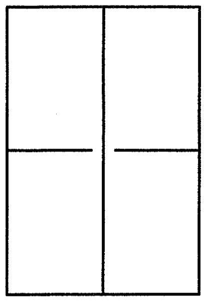

Fig. 7.2: Graph associated to the surgery operation with $r = 0$, in which we consider the transformed torus as a handle-body.

we consider the transformed torus. If we had considered the initial torus instead, the meridian of the complement would have been the curve that sticks to the meridian of the torus under surgery operation. Since the stick operation forces us to associate longitude to meridian, the graph that we must consider is shown in Fig. 7.3: it represents the torus meridian and the meridian of the complement after the action of the surgery operation. The value of the invariant associated with this graph is simply

$$w_q^{-2}\sum w_{(q)i}^2 w_{(q)j}^2 \sum_{\substack{ab\\(iab)\\(jab)}} 1, \tag{7.23}$$

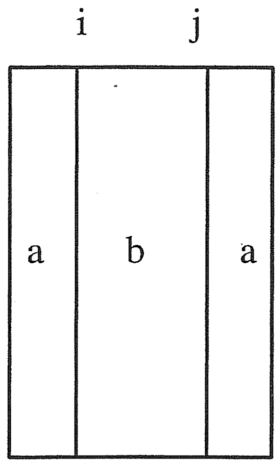

Fig. 7.3: Graph associated to the surgery operation with $r = 0$, in which we consider the torus before the transformation, namely the object associated to the S^3 splitting.

since the surfaces that the two links bound on the torus surface have Euler numbers equal to zero. We rewrite the two sums in (7.23) according to:

$$\sum_{ij} w^2_{(q)i} w^2_{(q)j} \sum_{\substack{ab \\ (iab) \in adm \\ (jab) \in adm}} 1 = \sum_{ab} \sum_{\substack{ij \\ (iab) \in adm \\ (jba) \in adm}} w^2_{(q)i} w^2_{(q)j} = \tag{7.24}$$

$$= \sum_{ab} \sum_{\substack{i \\ (iab) \in adm}} w^2_{(q)i} \sum_{\substack{j \\ (jab) \in adm}} w^2_{(q)j} = \sum_{ab} (\sum_{\substack{i \\ (iab) \in adm}} w^2_{(q)i})^2 .$$

Using the relation (7.7) we obtain:

$$w_q^{-2} \sum_{ab} w^4_{(q)a} w^4_{(q)b} = w_q^2$$

which is exactly the T-V invariant for $S^2 \times S^1$ [3].

7.3.2 S^3.

As is well known S^3 can be obtained with a surgery operation along a link with framing equal to one: the meridian of the torus is sent into a longitude that becomes knotted once along the surface. The graph associated to this situation is depicted in Fig. 7.4, where we can see the curve that goes trough one meridian and one longitude before closing. The corresponding expression for

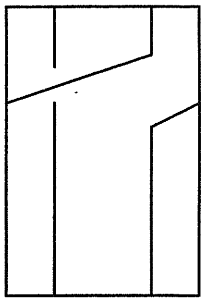

Fig. 7.4: Graph associated to the surgery operation with $r = 1$.

the invariants reads:

$$w_q^{-2} \sum w_{(q)i}^2 w_{(q)j}^2 \sum_a w_{(q)a}^2 \begin{vmatrix} i & a & a \\ j & a & a \end{vmatrix}. \tag{7.25}$$

Now we consider $Z[S^3](q)$ in its expression coming from (7.17):

$$\sum_{\mu j} w_{(q)j}^2 |M, F|_\mu \langle \gamma_F^\mu | 0 | \psi_j \rangle = Z[S^3](q), \tag{7.26}$$

where the term $\langle \gamma_F^\mu | 0 | \psi_j \rangle$ of $Z[S^3](q)$ corresponds exactly to:

$$\sum_a \omega_{(q)a}^2 \begin{vmatrix} j & a & a \\ \mu & a & a \end{vmatrix}. \tag{7.27}$$

Thus, by using the expression of $|M, F|_\mu$ in (7.9), we get:

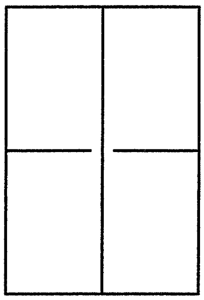

Fig. 7.5: Graph associated to S^3 in definition of the invariant.

$$Z[S^3](q) = \omega_q^{-2} \sum_{\mu j} \omega_{(q)j}^2 \omega_{(q)\mu}^2 \sum_a \omega_{(q)a}^2 \begin{vmatrix} j & a & a \\ \mu & a & a \end{vmatrix} \tag{7.28}$$

which represents the desired result.

7.3.3 The lens space $L(2,1)$

In the $L(2,1)$ case the associated graph is depicted in Fig. 7.6, where we can see the curve that goes trough one meridian and two longitudes before closing. To this graph we associate the

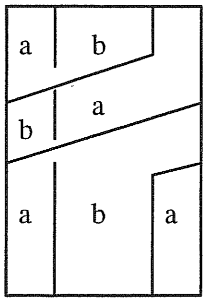

Fig. 7.6: Graph associated to $L(2,1)$

quantity

$$w_q^{-2} \sum w_{(q)a}^2 w_{(q)b}^2 \left| \begin{matrix} i & a & b \\ j & a & b \end{matrix} \right| \left| \begin{matrix} i & b & a \\ j & b & a \end{matrix} \right| \tag{7.29}$$

Carrying out the sum on i and using the first axiom on the structure of the initial data, we obtain that the invariant, expressed in the Heegaard–splitting framework, is equal to:

$$w_q^{-2} \sum w_{(q)a}^2 w_{(q)b}^2 \sum_{\substack{i \\ (iab)}} = w_q^{-2} \sum_i \sum_a w_{(q)a}^2 \sum_{\substack{b \\ (iab)}} w_{(q)b}^2 . \tag{7.30}$$

According to relation (7.7), we eventually obtain the formula

$$w_q^{-2} \sum_i w_{(q)i}^2 \sum_a w_{(q)a}^4 , \tag{7.31}$$

which gives exactly the T-V invariant for $L(2,1)$ [3].

7.3.4 The lens space $L(3,1)$

Let us consider now $L(3,1)$. In this case, the surgery link has a framing $r = 3$, so that the meridian of the complement is sent into a curve which goes trough one meridian and tree longitudes before closing. We obtain the graph of Fig. 7.7, and the associated invariant is expressed by the quantity:

$$w_q^{-2} \sum w_{(q)a}^2 w_{(q)b}^2 w_{(q)c}^2 \left| \begin{matrix} i & a & b \\ j & c & b \end{matrix} \right| \left| \begin{matrix} i & c & b \\ j & c & a \end{matrix} \right| \left| \begin{matrix} i & c & a \\ j & b & a \end{matrix} \right| . \tag{7.32}$$

Carrying out the sum on i and by using the second axiom we obtain

$$w_q^{-2} \sum w_{(q)j}^2 w_{(q)a}^2 w_{(q)b}^2 w_{(q)c}^2 \left| \begin{matrix} j & j & j \\ c & a & b \end{matrix} \right| \left| \begin{matrix} j & j & j \\ a & b & c \end{matrix} \right| . \tag{7.33}$$

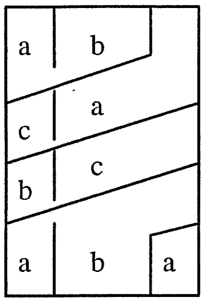

Fig. 7.7: Graph associated with $L(3,1)$.

Finally, upon summation over b and using the relation (7.1), we get as in [3]

$$w_q^{-2} \sum_{\substack{j \\ (jjj)}} \sum_{\substack{ac \\ (jac)}} w^2_{(q)a} w^2_{(q)c} = \sum_{\substack{j \\ (jjj)}} w^2_{(q)j}. \tag{7.34}$$

7.3.5 The lens space $L(n,1)$

$L(n,1)$ is obtained by a surgery along a link with framing $r = n$; the meridian of the complement solid torus is sent into a curve that goes trough one meridian and n longitudes of the torus surface before closing, the associated graph is given by Fig. 7.8. The expression of the invariant becomes

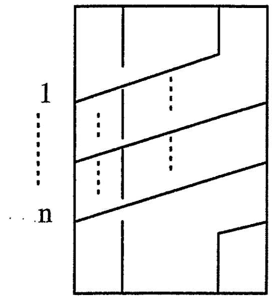

Fig. 7.8: Graph associated to the surgery operation with $r = n$.

$$Z[L(n,1)](q) = w_q^{-2} \sum w^2_{(q)i} w^2_{(q)j} \prod_i w^2_{(q)j_i} \left| \begin{array}{ccc} i & j_1 & j_2 \\ j & j_1 & j_n \end{array} \right| \cdots \left| \begin{array}{ccc} i & j_n & j_{n-1} \\ j & j_n & j_1 \end{array} \right| \tag{7.35}$$

Using the relation defining the 3nj symbols (see (3.5) and [56]) we get

$$\left[\begin{array}{ccccccccc} a_1 & & a_2 & & \cdots & & a_n & \\ & b_1 & & b_2 & & \cdots & & b_n \\ c_1 & & c_2 & & \cdots & & c_n & \end{array} \right]_q = \sum_z (-1)^{S+nz} [2z+1]_q \left\{ \begin{array}{ccc} a_1 & c_1 & z \\ c_2 & a_2 & b_1 \end{array} \right\}_q \times$$
$$\times \left\{ \begin{array}{ccc} a_2 & c_2 & z \\ c_3 & a_3 & b_2 \end{array} \right\}_q \cdots \left\{ \begin{array}{ccc} a_n & c_n & z \\ c_1 & a_1 & b_n \end{array} \right\}_q \tag{7.36}$$

where S denotes the sum over all the 3n arguments and

$$\left\{ \begin{array}{ccc} a_1 & c_1 & z \\ c_2 & a_2 & b_1 \end{array} \right\}_q = (-1)^{(a_1+a_2+b_1+c_1+c_2+z)} \left| \begin{array}{ccc} a_1 & c_1 & z \\ c_2 & a_2 & b_1 \end{array} \right| .$$

We can rewrite the expression of the invariant in terms of 3nj-symbols

$$Z[L(n,1)](q) = w_q^{-2} \sum [2j+1]_q \prod_i [2j_i+1]_q \left[\begin{array}{ccccccccc} j_1 & & j_2 & & \cdots & & j_n & & \\ & j & & j & & \cdots & & j & \\ j_n & & j_1 & & \cdots & & j_{n-1} & & \end{array} \right]_q . \quad (7.37)$$

7.3.6 Explicit computation of the invariant for the lens space $L(p,h)$

We generalize now the procedure, introduced in the previous section, to the generic 3-dimensional lens space $L(p,h)$ where p,h are relatively prime, $(p,h) = 1$. We can denote them collectively $L(nh+f,h)$, with n integer and $(f,h) = 1$ with $h > f$. We have seen in section (7.2) that, in the surgery representation, the meridian of the tubular neighborhood of a surgery link is sent into a curve which goes trough p meridians and h longitudes before closing. The graphs associated to these configurations are quite more complicated than the ones considered before. Let us consider first the graphs and the invariants in some particular cases.

A. The lens space $L(2n+1,2)$

Put $h = 2$ and consider as an example of this class $L(5,2)$, with the associated graph shown in Fig. 7.9. In order to construct this graph we put three points on each horizontal line and five

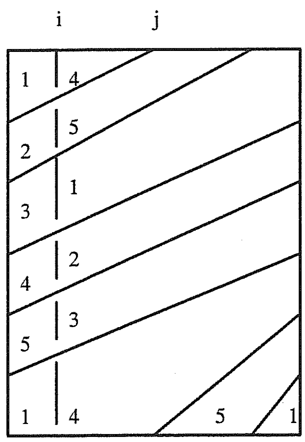

Fig. 7.9: Graph associated with $L(5,2)$.

points on each vertical one at the same distance from each other, connect among themselves the first point of the horizontal lines, the second point of bottom horizontal line with the first point of vertical left line and the other in pairs with lines "parallel" to this one. It is easy to see that the graph represents the intersection of two links, one of them going trough two meridians and five longitudes before closing. Using the rules described above, the expression of the invariant is

$$Z[L(5,2)](q) = w_q^{-2} \sum w^2_{(q)i} w^2_{(q)j} \prod_i w^2_{(q)j_i} \begin{vmatrix} i & j_4 & j_5 \\ j & j_2 & j_1 \end{vmatrix} \begin{vmatrix} i & j_5 & j_1 \\ j & j_3 & j_2 \end{vmatrix} \times$$
$$\times \begin{vmatrix} i & j_1 & j_2 \\ j & j_4 & j_3 \end{vmatrix} \begin{vmatrix} i & j_2 & j_3 \\ j & j_5 & j_4 \end{vmatrix} \begin{vmatrix} i & j_3 & j_4 \\ j & j_1 & j_5 \end{vmatrix}, \tag{7.38}$$

which, using (7.36), can be rewritten in term of a 15j symbol

$$Z[L(5,2)](q) = w_q^{-2} \sum [2j+1]_q \prod_i [2j_i+1]_q \begin{bmatrix} j_4 & & j_5 & & j_1 & & j_2 & & j_3 & \\ & j & & j & & j & & j & & j \\ j_1 & & j_2 & & j_3 & & j_4 & & j_5 & \end{bmatrix}_q . \tag{7.39}$$

Starting from expression (7.38) and using some basic relations involving 6j symbols [47], it is possible to recover easily the value given in [57]. We will give, in Appendix 8.6, the explicitly computation for this example and for a similar one. From this analysis we can recover the following expression of the invariant for the class $L(2n+1,2)$, (see Fig. 7.10),

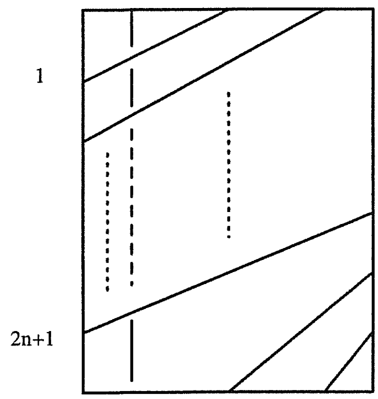

Fig. 7.10: Graph associated with $L(2n+1,2)$.

$$Z[L(2+1n,1)](q) = w_q^{-2} \sum [2j+1]_q \prod_i [2j_i+1]_q \times$$
$$\times \begin{bmatrix} j_{2n} & & j_{2n+1} & & j_1 & & \cdots & & j_{2n-1} & \\ & j & & j & & j & & \cdots & & j \\ j_1 & & j_2 & & j_3 & & \cdots & & j_{2n+1} & \end{bmatrix}_q . \tag{7.40}$$

B. The lens spaces $L(3n+1,3)$ and $L(3n+2,3)$

For $h=3$, we have two classes $L(3n+1,3)$ and $L(3n+2,3)$. As an example of the first case we consider $L(7,3)$, and for the second case $L(8,3)$. The graph associated to $L(7,3)$ is shown in Fig. 7.11. The link goes trough tree meridians and seven longitudes before closing. The associated

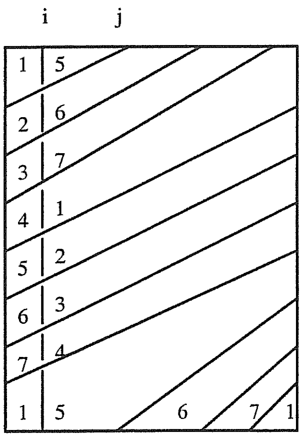

Fig. 7.11: Graph associated with $L(7.3)$.

expression for the invariant is

$$Z[L(7,3)](q) = w_q^{-2}\sum w^2_{(q)i}w^2_{(q)j}\prod_i w^2_{(q)j_i}\begin{vmatrix} i & j_5 & j_6 \\ j & j_2 & j_1 \end{vmatrix}\times$$
$$\times\begin{vmatrix} i & j_6 & j_7 \\ j & j_3 & j_2 \end{vmatrix}\begin{vmatrix} i & j_7 & j_1 \\ j & j_4 & j_2 \end{vmatrix}\cdots\begin{vmatrix} i & j_4 & j_5 \\ j & j_1 & j_7 \end{vmatrix}. \tag{7.41}$$

Note that, by using the relation (7.36), it can be rewritten in terms of a 21j symbol

$$Z[L(7,3)](q) = w_q^{-2}\sum[2j+1]_q\prod_i[2j_i+1]_q\times$$
$$\times\begin{bmatrix} j_5 & & j_6 & & j_7 & & j_1 & & \cdots & & j_4 & \\ & j & & j & & j & & j & & \cdots & & j \\ j_1 & & j_2 & & j_3 & & j_4 & & \cdots & & j_7 & \end{bmatrix}_q. \tag{7.42}$$

It is also possible to obtain the value given in [57], using a sequence of relation described in [47]. We are now in condition of constructing, for $L(3n+1,3)$, the associated graph, (see Fig. 7.12). The corresponding invariant is given explicitly by the formula

$$Z[L(3n+1,3)](q) = w_q^{-2}\sum[2j+1]_q\prod_i[2j_i+1]_q\times$$
$$\times\begin{bmatrix} j_{3n-1} & & j_{3n} & & j_{3n+1} & & j_1 & & \cdots & & j_{3n-2} & \\ & j & & j & & j & & j & & \cdots & & j \\ j_1 & & j_2 & & j_3 & & j_4 & & \cdots & & j_{3n+1} & \end{bmatrix}_q. \tag{7.43}$$

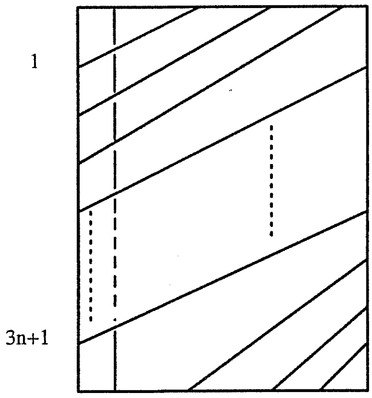

Fig. 7.12: Graph associated with $L(3n+1,3)$.

Let us now consider $L(8,3)$: the associated graph is shown in Fig. 7.13 and it is generated by

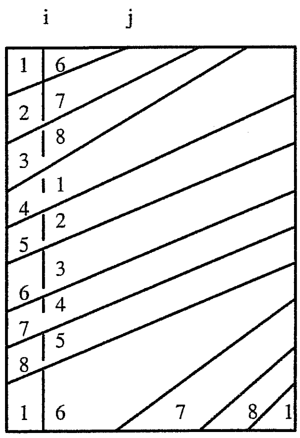

Fig. 7.13: Graph associated with $L(8,3)$.

using the usual procedure.

The corresponding expression of the T-V invariant, can be written, by exploiting (7.36), in term of a 24j symbols, namely

$$Z[L(8,3)](q) = w^{-2} \sum [2j+1]_q \prod_i [2j_i+1]_q \times$$

$$\times \begin{bmatrix} j_6 & & j_6 & & j_8 & & j_1 & & \cdots & & j_5 & \\ & j & & j & & j & & j & & \cdots & & j \\ j_1 & & j_2 & & j_3 & & j_4 & & \cdots & & j_8 & \end{bmatrix}_q . \tag{7.44}$$

Also in this case it is possible to obtain the value given in [57].

Finally we can associate with the lens space $L(3n+2,3)$ the graph shown in Fig. 7.14. The

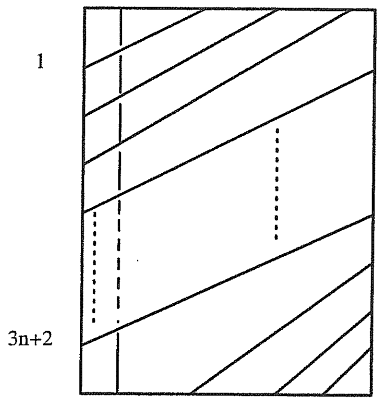

Fig. 7.14: Graph associated with $L(3n+2,3)$.

invariant expression is given by

$$Z[L(3n+2,3)](q) = w_q^{-2} \sum [2j+1]_q \prod_i [2j_i+1]_q \times$$

$$\times \begin{bmatrix} j_{3n} & & j_{3n+1} & & j_{3n+2} & & j_1 & & \cdots & & j_{3n-1} & \\ & j & & j & & j & & j & & \cdots & & j \\ j_1 & & j_2 & & j_3 & & j_4 & & \cdots & & j_{3n+2} & \end{bmatrix}_q . \qquad (7.45)$$

C. The lens space $L(nh+f,h)$

On the basis of the above examples we are now able to construct the graph associated to a generic 3 dimensional lens space and its related invariant. The strategy is to put $hn+f$ point on each vertical line (at the same distance from each other) $h+1$ points on each horizon line and then connect among themselves the first point of the horizontal lines, the first point of the vertical left line with the second one of the bottom horizontal line and the other in pairs with "parallel" lines. Such kind of graph is shown in Fig. 7.15 where $\bar{f}$ is the value of f for which $(h,f)=1$, and the expression of the invariant can be written, in terms of a $3(nh+\bar{f})$j symbols with entries positions depending from h, in the form

$$Z[L(nh+\bar{f},h)](q) = w_q^{-2} \sum [2j+1]_q \prod_i [2j_i+1]_q \times$$

$$\times \begin{bmatrix} j_{nh+\bar{f}-h+1} & & j_{nh+\bar{f}-h+2} & & \cdots & & j_{nh+\bar{f}} & & j_1 & & \cdots & & j_{nh+\bar{f}-h} & \\ & j & & j & & \cdots & & j & & j & & \cdots & & j \\ j_1 & & j_2 & & \cdots & & j_h & & j_{h+1} & & \cdots & & j_{nh+\bar{f}} & \end{bmatrix}_q \qquad (7.46)$$

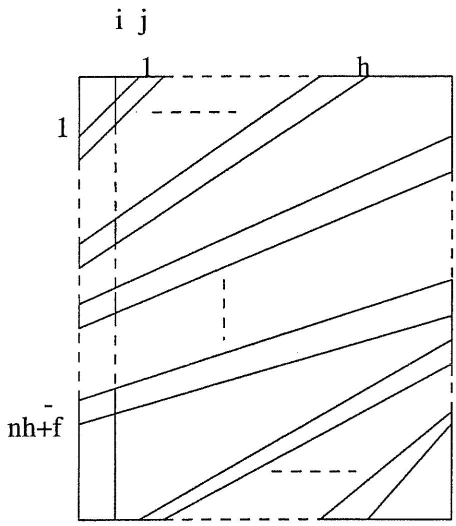

Fig. 7.15: Graph associated with $L(nh + \bar{f}, h)$.

Chapter 8

Appendices.

8.1 Quantum extension.

Let us consider the quantum group $U_q(G)$. This is the quantum universal covering space of the Lie algebra G and is an associative algebra over the ring of formal power series generated by the elements H_i, X_i^+, X_I^- with $i = 1, \ldots, r = rankG$, satisfying the relations:

$$[H_i, H_j] = 0, \ [H_i, X_j^{\pm}] \pm (\alpha_i \alpha_j) X_j^{\pm},$$
$$[X_i^+, X_j^-] = \delta_{ij} \frac{sinh(\frac{h}{2} H_i)}{sinh(\frac{h}{2})}, \ \sum_{k=0}^{n} (-1)^n \left[\begin{array}{c} n \\ k \end{array} \right] (X_i^{\pm})^k X_j^{\pm} (X_i^{\pm})^{n-k} = 0, \ i \neq j \tag{8.1}$$

$\{\alpha_i\}_{i=1}^r$ are the simple roots of G, ($\alpha_i \alpha_j$ is the value of the canonical bilinear form in the root space and

$$\left[\begin{array}{c} n \\ k \end{array} \right] = \frac{sinh(\frac{nh}{2}) \cdots sinh(\frac{(k+1)h}{2})}{sinh(\frac{(n-k)h}{2}) \cdots sinh(\frac{h}{2})}$$

The spin variables $\{j\}$ take their values in a finite set $I = (0, 1/2, 1, \ldots, k)$ where $exp(\pi i/k) = q$. For each $j \in I$ a function $w_{(q)j}^2 \doteq (-1)^{2x_j} [2x_j + 1]_q \in K^*$ is defined, where $K^* \equiv K \setminus \{0\}$ (K a commutative ring with unity). Recall that the notation $[.]_q$ stands for a q-integer, namely $[n]_q = (q^n - q^{-n})/(q - q^{-1})$ and that, for each admissible triple (j, k, l), we have: $w_{(q)j}^{-2} \sum_{k,l} w_{(q)k}^2 w_{(q)l}^2 = w_q^2$, with $w_q^2 = -2k/(q - q^{-1})^2$.

We just notice that the basic receipt to transform the classical state sums into the quantum ones can be summarized as follows

- the classical weights $(-1)^{2j}(2j+1)$ are replaced by $w_{(q)j}^2$, while each of the factors $\Lambda(L)^{-1}$ becomes w_q^{-2};

- each Wigner symbol of $SU(2)$ is replaced by its q-analog $q-3jm$, normalized as explained below;

- each classical recoupling coefficient (or $3nj$ symbol) of a given type has its q-deformed counterpart, obtained by summing over magnetic numbers products of $q-3jm$ symbols, apart from suitable phase factors

Recall from [58] and [59] that the relation between the quantum Clebsh–Gordan coefficient $(j_1m_1j_2m_2|j_3m_3)_q$ and the $q-3jm$ symbol is given by

$$(j_1m_1j_2m_2|j_3m_3)_q = (-1)^{j_1-j_2+m_3}([2j_3+1]_q)^{1/2}\begin{pmatrix} j_1 & j_2 & j_3 \\ m_1 & m_2 & -m_3 \end{pmatrix}_q, \tag{8.2}$$

where, as usual, an m variable runs in integer steps between $-j$ and $+j$, and the classical expression is recovered when $q=1$. The symmetry properties of the $q-3jm$ symbol read

$$\begin{aligned}
\begin{pmatrix} j_1 & j_2 & j_3 \\ m_1 & m_2 & -m_3 \end{pmatrix}_q &= (-1)^{j_1+j_2+j_3} \begin{pmatrix} j_2 & j_1 & j_3 \\ m_2 & m_1 & -m_3 \end{pmatrix}_{1/q}, \\
\begin{pmatrix} j_1 & j_2 & j_3 \\ m_1 & m_2 & -m_3 \end{pmatrix}_q &= (-1)^{j_1+j_2+j_3}q^{-m_1/2} \begin{pmatrix} j_1 & j_3 & j_2 \\ m_1 & m_3 & -m_2 \end{pmatrix}_{1/q}, \\
\begin{pmatrix} j_1 & j_2 & j_3 \\ m_1 & m_2 & -m_3 \end{pmatrix}_q &= (-1)^{j_1+j_2+j_3} \begin{pmatrix} j_1 & j_2 & j_3 \\ -m_1 & -m_2 & m_3 \end{pmatrix}_q.
\end{aligned} \tag{8.3}$$

Thus we define the *normalized* $q-3jm$ symbols, for deformation parameters q and $1/q$ respectively, according to

$$\begin{aligned}
\begin{bmatrix} j_1 & j_2 & j_3 \\ m_1 & m_2 & -m_3 \end{bmatrix}_q &\doteq q^{(m_1-m_2)/6}\begin{pmatrix} j_1 & j_2 & j_3 \\ m_1 & m_2 & -m_3 \end{pmatrix}_q \\
\begin{bmatrix} j_1 & j_2 & j_3 \\ m_1 & m_2 & -m_3 \end{bmatrix}_{1/q} &\doteq q^{(m_2-m_1)/6}\begin{pmatrix} j_1 & j_2 & j_3 \\ m_1 & m_2 & -m_3 \end{pmatrix}_{1/q}
\end{aligned} \tag{8.4}$$

The orthogonality relation involving the normalized symbols (which are used for instance in order to handle identities representing elementary shellings and inverse shellings) reads

$$\sum_{jm} w^2_{(q)j}(-1)^{\Theta}q^{(m_2-m_1)/3}\begin{bmatrix} j_1 & j_2 & j \\ m_1 & m_2 & -m \end{bmatrix}_q \begin{bmatrix} j_2 & j_1 & j \\ -m'_2 & -m'_1 & -m \end{bmatrix}_q = \delta_{m_1m'_1}\delta_{m_2m'_2}, \tag{8.5}$$

where $\Theta = m_1 + m_2 + m_3$. As an example, we just give here the q-counterpart of the state sum (5.24)

$$Z[(T^d(j_{\sigma^{d-2}}, J_{\sigma^{d-1}}), \partial T^d(j'_{\sigma^{d-2}}, J'_{\sigma^{d-1}}; m, \mathcal{M})] \to (M^d, \partial M^d)](q) =$$
$$= w_q^{(-1)^d \Xi} \prod_{all\, \sigma^{d-2}} (-1)^{2j_{\sigma^{d-2}}}[2j_{\sigma^{d-2}}+1]_q \prod_{all\, \sigma^{d-1}} \left(\prod_{C=1}^{d-3} (-1)^{2J_C}[2J_C+1]_q \right)_{\sigma^{d-1}} \cdot$$
$$\cdot \prod_{all\, \sigma^d} \left\{ \frac{3}{2}(d-2)(d+1)j \right\}_q^{\sigma^d} (J, J') \prod_{\sigma^{d-1} \in \partial T^d} \sum_{\mathcal{M}} (-1)^{\sum m/2 + \sum \mathcal{M}} q^{m/2+M/2} \, .$$
$$\cdot \begin{bmatrix} j'_1 & j'_2 & J'_1 \\ m_1 & m_2 & \mathcal{M}_1 \end{bmatrix}_q \cdots \begin{bmatrix} J'_{d-3} & j'_{d-1} & j'_d \\ -\mathcal{M}_{d-3} & m_{d-1} & m_d \end{bmatrix}_q . \qquad (8.6)$$

where $\Xi = 2(N_0 - N_1 + \ldots + (-1)^{d-3}N_{d-3})$, $(N_0, N_1, N_2, \ldots)$ is the total number of $(0, 1, 2, \ldots)$-dimensional simplices, the $\{\frac{3}{2}(d - 2(d + 1)j\}_q$ symbols are defined substituting in the classical expression the q-3jm symbols (for each m the factor $q^{m/2}$ must be added).

8.2 Explicit calculus of $Z_\chi[M^2]$.

To obtain the exact value of the invariant Z_χ^2 we may act in this way: we start by considering triangulations of the 2-sphere S^2 and of the torus T^2, and then we look what happens adding other holes. In Fig. 8.1 part (1) we can see the triangulation of S^2 with, in evidence, the structure of the invariant namely of the graph Γ. Using fundamental relations from the angular momentum theory, the invariant can be rewrite as $w_q^{-N_0} \sum_{abc} w^4_{(q)a} w^4_{(q)b} w^4_{(q)c}$, with $w^2_{(q)a} w^2_{(q)b} w^2_{(q)c}$ coming out by the loop obtained after graphical operations. The final result give us w_q^{-2}, that can be also written as $w_q^{2-2\chi}$.

Let us consider the case of the torus, the triangulation of which is given in Fig. 8.2 (with the boundary of the hole and the rest depicted separately) where the loops represent the $w^2_{(q)i}$ contributions obtained after graphical operations. The result is $w_q^{2(6+4)}$ which by introducing the normalization factor $w_q^{-2N_0}$ (where N_0 is equal to 9 for this particular triangulation) gives $Z_\chi^2 = w_q^2 = w_q^{2-2\chi}$.

To increase the genus of the surface we analyze which is the contribution generated by the triangulation of an additional hole: the corresponding picture is given in Fig. 8.3 where it is also put in evidence the loop contribution. We notice how the triangulation of this "new" hole adds

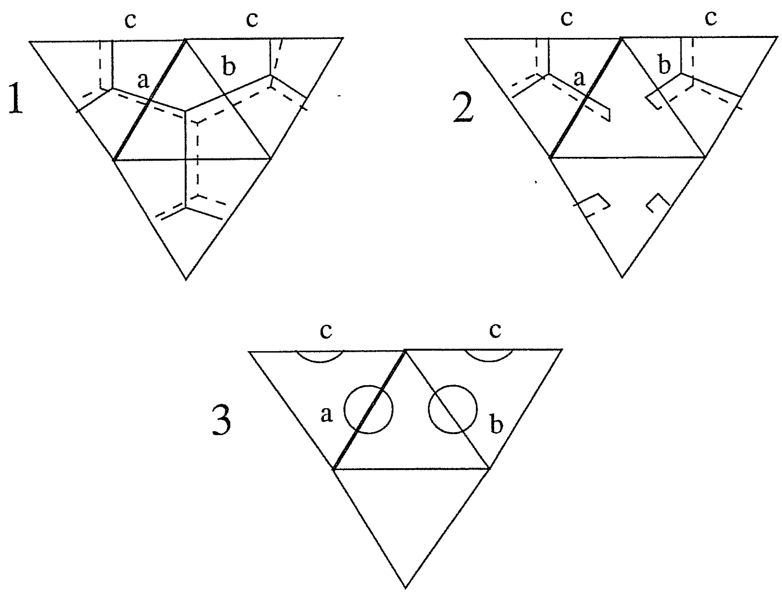

Fig. 8.1: (1) Triangulation of S^2 whit the structure of the invariant, (2) after the application of the relation given in Fig. 5.9, (3) after the twice application of the orthogonal condition of 3jm symbols.

to the triangulations of the previous surface (and to the invariant), 5 new vertices and a diagram contribution consisting of 5+2 loops. Thus the final result is, denoting by h the number of the hole

$$w_q^{-2(4+5h)+2(7h+3)} = w_q^{-2+4h} = w_q^{2-2\chi}.$$

8.3 Relations proving the invariance of $Z[(M^4, \partial M^4)]$ under shellings.

Recall from (5.18) and (5.20) that there we made use of primed spin variables $\{j', J'\}$ in order to label those components which lie in ∂T^4 in some configuration, while plain $\{j, J\}$ denoted components in $int(T^4)$. Since here almost all variables are indeed in ∂T^4, we agree to change our previous notation according to

$$j'_1, j'_2, \ldots, j'_{10} \longrightarrow j_1, j_2, \ldots, j_{10},$$

$$J'_a(\subset \partial T^4) \longrightarrow J_a,$$

$$J_a(\subset int(T^4)) \longrightarrow \mathbf{J_a}.$$

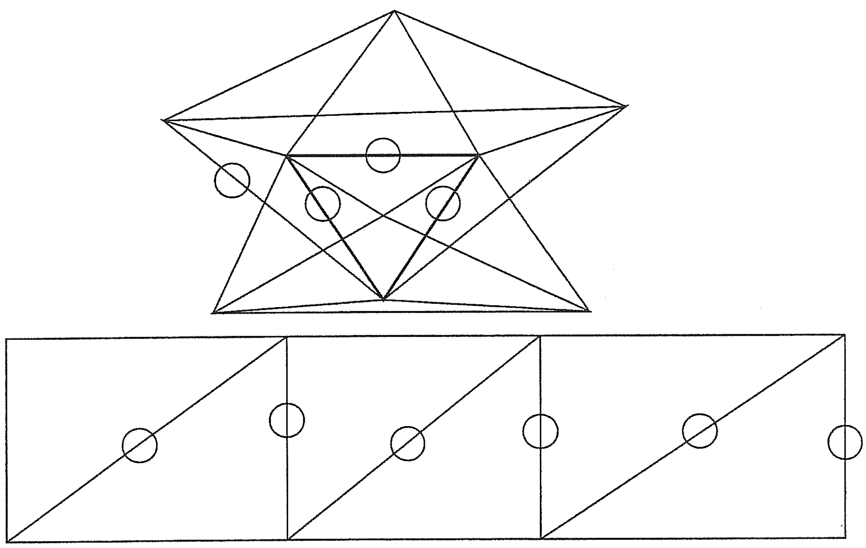

Fig. 8.2: Triangulation of T^2 with the structure of the invariant after several application of the relation given in Fig. 5.9.

For the corresponding m variables we keep on denoting them by plain $m_1, m_2, \ldots, m_{10}; m_a, \ldots, m_e$, since no ambiguity can arise. We set also $w_j^2 \equiv (2j+1)$, and the summation labels and arguments are shortened as far as possible.

$[\mathbf{1} \to \mathbf{4}]^{\mathbf{4}}_{\mathbf{sh}}$ (see Fig. 5.5)

$$\sum_{J_a, m_a} w_{J_a}^2 (-1)^{m_a} \begin{pmatrix} j_1 & j_2 & J_a \\ m_1 & m_2 & m_a \end{pmatrix} \begin{pmatrix} j_3 & j_4 & J_a \\ m_3 & m_4 & -m_a \end{pmatrix} [J_a, \mathbf{J_b}, \mathbf{J_c}, \mathbf{J_d}, \mathbf{J_e}] =$$

$$\cdot \sum_{m_i} (-1)^{\sum_i m_i} \sum_{m_A} (-1)^{\sum_A m_A} \begin{pmatrix} j_5 & j_6 & J_b \\ m_5 & m_6 & m_b \end{pmatrix} \begin{pmatrix} j_3 & j_7 & J_b \\ -m_3 & m_7 & -m_b \end{pmatrix} \cdot$$

$$\cdot \begin{pmatrix} j_5 & j_8 & J_c \\ -m_5 & m_8 & m_c \end{pmatrix} \begin{pmatrix} j_1 & j_9 & J_c \\ -m_1 & m_9 & -m_c \end{pmatrix} \begin{pmatrix} j_6 & j_{10} & J_d \\ -m_6 & m_{10} & m_d \end{pmatrix} \cdot$$

$$\cdot \begin{pmatrix} j_2 & j_8 & J_d \\ -m_2 & -m_8 & -m_d \end{pmatrix} \begin{pmatrix} j_7 & j_{10} & J_e \\ -m_7 & -m_{10} & m_e \end{pmatrix} \begin{pmatrix} j_4 & j_9 & J_e \\ -m_4 & -m_9 & -m_e \end{pmatrix}$$

$\{m_i\} = (m_5, m_6, m_7, m_8, m_9, m_{10})$

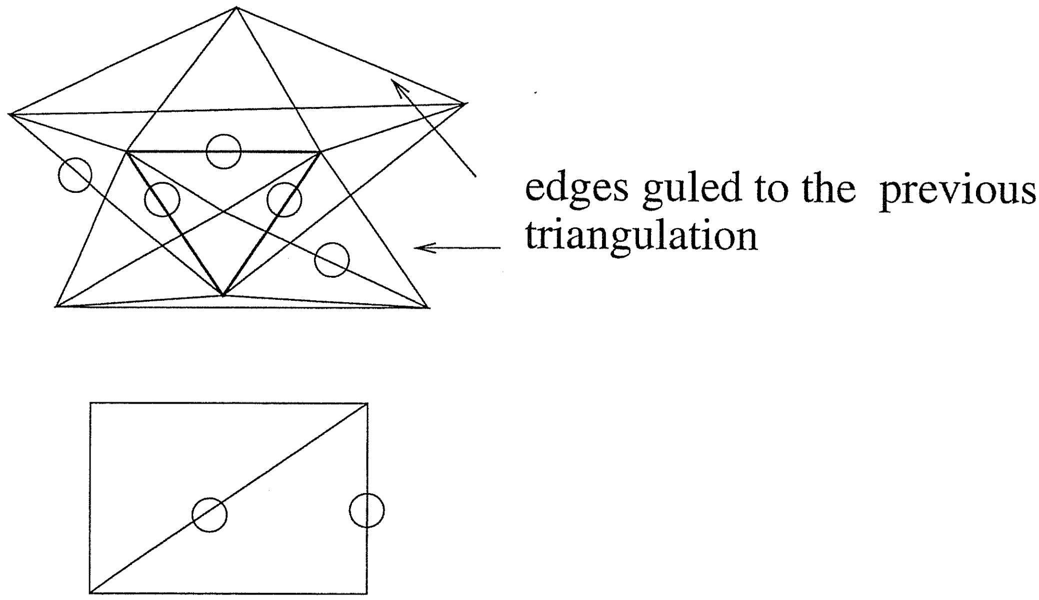

Fig. 8.3: Triangulation of an additional hole with its contribution to the invariant after several application of the relation given in Fig. 5.9.

$$\{m_A\} = (m_b, m_c, m_d, m_e).$$

$[\mathbf{2} \to \mathbf{3}]^4_{\mathbf{sh}}$ (see Fig. 5.6)

$$\sum_{j_3,m_3} w^2_{j_3}(-1)^{m_3} \sum_{J_A,m_A} (\prod_A w^2_{J_A})(-1)^{\sum_A m_A} \begin{pmatrix} j_1 & j_2 & J_a \\ m_1 & m_2 & m_a \end{pmatrix} \begin{pmatrix} j_3 & j_4 & J_a \\ m_3 & m_4 & -m_a \end{pmatrix} \cdot$$
$$\cdot \begin{pmatrix} j_5 & j_6 & J_b \\ m_5 & m_6 & m_b \end{pmatrix} \begin{pmatrix} j_3 & j_7 & J_b \\ -m_3 & m_7 & -m_b \end{pmatrix} [J_a, J_b, \mathbf{J_c}, \mathbf{J_d}, \mathbf{J_e}] =$$
$$= \sum_{m_i} (-1)^{\sum_i m_i} \sum_{m_A} (-1)^{\sum_A m_A} \begin{pmatrix} j_5 & j_8 & J_c \\ -m_5 & m_8 & m_c \end{pmatrix} \begin{pmatrix} j_1 & j_9 & J_c \\ -m_1 & m_9 & -m_c \end{pmatrix} \cdot$$
$$\cdot \begin{pmatrix} j_6 & j_{10} & J_d \\ -m_6 & m_{10} & m_d \end{pmatrix} \begin{pmatrix} j_2 & j_8 & J_d \\ -m_2 & -m_8 & -m_d \end{pmatrix} \begin{pmatrix} j_7 & j_{10} & J_e \\ -m_7 & -m_{10} & m_e \end{pmatrix} \cdot$$
$$\cdot \begin{pmatrix} j_4 & j_9 & J_e \\ -m_4 & -m_9 & -m_e \end{pmatrix}$$

$$\{J_A\} = (J_a, J_b)$$

$\{m_A\} = (m_a, m_b)$

$\{m_i\} = (m_8, m_9, m_{10})$

$\{m_B\} = (m_c, m_d, m_e).$

$[\mathbf{3} \to \mathbf{2}]^{\mathbf{4}}_{\mathbf{sh}}$ (see Fig. 5.7)

$$\sum_{j_i,m_i} (\prod_i w_{j_i}^2)(-1)^{\sum_i m_i} \sum_{J_A,m_A} (\prod_A w_{J_A}^2)(-1)^{\sum_A m_A} \begin{pmatrix} j_1 & j_2 & J_a \\ m_1 & m_2 & m_a \end{pmatrix} \cdot$$
$$\cdot \begin{pmatrix} j_3 & j_4 & J_a \\ m_3 & m_4 & -m_a \end{pmatrix} \begin{pmatrix} j_5 & j_6 & J_b \\ m_5 & m_6 & m_b \end{pmatrix} \begin{pmatrix} j_3 & j_7 & J_b \\ -m_3 & -m_7 & -m_b \end{pmatrix} \cdot$$
$$\cdot \begin{pmatrix} j_5 & j_8 & J_c \\ -m_5 & m_8 & m_c \end{pmatrix} \begin{pmatrix} j_1 & j_9 & J_c \\ -m_1 & m_9 & -m_c \end{pmatrix} [J_a, J_b, J_c, \mathbf{J_d}, \mathbf{J_e}] =$$
$$= w_L^2 \sum_{m_{10}} (-1)^{m_{10}} \sum_{m_B} (-1)^{\sum_B m_B} \begin{pmatrix} j_6 & j_{10} & J_d \\ -m_6 & m_{10} & m_d \end{pmatrix} \begin{pmatrix} j_2 & j_8 & J_d \\ -m_2 & -m_8 & -m_d \end{pmatrix} \cdot$$
$$\cdot \begin{pmatrix} j_7 & j_{10} & J_e \\ -m_7 & -m_{10} & m_e \end{pmatrix} \begin{pmatrix} j_4 & j_9 & J_e \\ -m_4 & -m_9 & -m_e \end{pmatrix}$$

$\{j_i\} = (j_1, j_3, j_5)$

$\{m_i\} = (m_1, m_2, m_5)$

$\{J_A\} = (J_a, J_b, J_c)$

$\{m_A\} = (m_a, m_b, m_c)$

$\{m_B\} = (m_d, m_e)$

$w_L^2 = \Lambda(L).$

$[\mathbf{4} \to \mathbf{1}]^{\mathbf{4}}_{\mathbf{sh}}$ (see Fig. 5.8)

$$\sum_{j_i,m_i} (\prod_i w_{j_i}^2)(-1)^{\sum_i m_i} \sum_{J_A,m_A} (\prod_A w_{J_A}^2)(-1)^{\sum_A m_A} \begin{pmatrix} j_1 & j_2 & J_a \\ m_1 & m_2 & m_a \end{pmatrix} \cdot$$
$$\cdot \begin{pmatrix} j_3 & j_4 & J_a \\ m_3 & m_4 & -m_a \end{pmatrix} \begin{pmatrix} j_5 & j_6 & J_b \\ m_5 & m_6 & m_b \end{pmatrix} \begin{pmatrix} j_3 & j_7 & J_b \\ -m_3 & m_7 & -m_b \end{pmatrix} \cdot$$
$$\cdot \begin{pmatrix} j_5 & j_8 & J_c \\ -m_5 & m_8 & m_c \end{pmatrix} \begin{pmatrix} j_1 & j_9 & J_c \\ -m_1 & m_9 & -m_c \end{pmatrix} \begin{pmatrix} j_6 & j_{10} & J_d \\ -m_6 & m_{10} & m_d \end{pmatrix} \cdot$$
$$\cdot \begin{pmatrix} j_2 & j_8 & J_d \\ -m_2 & -m_8 & -m_d \end{pmatrix} [J_a, J_b, J_c, J_d, \mathbf{J_e}] =$$

$$= w_L^6 \sum_{m_e} (-1)^{m_e} \begin{pmatrix} j_7 & j_{10} & J_e \\ -m_7 & -m_{10} & m_e \end{pmatrix} \begin{pmatrix} j_4 & j_9 & J_e \\ -m_4 & -m_9 & -m_e \end{pmatrix}$$

$$\{j_i\} = (j_1, j_2, j_3, j_5, j_6, j_8)$$

$$\{m_i\} = (m_1, m_2, m_3, m_5, m_6, m_8)$$

$$\{J_A\} = (J_a, J_b, J_c, J_d)$$

$$\{m_A\} = (m_a, m_b, m_c, m_d)$$

$$w_L^6 = \Lambda(L)^3.$$

The full set of identities can be obtained, up to regularization, from anyone of them, on applying both orthogonality/completeness conditions for $3jm$ symbols

8.4 Some remarks on $SU(2)$.

Here we give a short summary of some standard facts about the group $SU(2)$. One can parameterize an element g of $SU(2)$ which are used in section (6.2) by vectors Z from its Lie algebra. The corresponding relation is given by the exponential map:

$$g = e^Z = e^{i\psi n^i \sigma^i/2}, \tag{8.7}$$

where n^i is a unit vector, $n^i n_i = 1$, ψ is a real positive parameter, the σ^i are the usual Pauli matrices:

$$(\sigma^i \cdot \sigma^j) = i\epsilon^{ijk}\sigma^k + \delta^{ij}, \tag{8.8}$$

and ψn^i is an element of $R^3 \cong$ su(2) the Lie algebra of $SU(2)$. Since

$$g = \cos(\psi/2) + in^i\sigma^i \sin(\psi/2), \tag{8.9}$$

to cover the whole $SU(2)$ the parameter ψ should takes values in the range $[0, 4\pi]$.

The Haar measure on the group can be related to the usual Lebesgue measure in R^3 by introducing a function $P(Z)$ on the Lie algebra:

$$P(Z) = \left(\frac{\sin(\psi/2)}{\psi/2}\right). \tag{8.10}$$

Then $P^2(Z)dZ/32\pi^2$ gives the normalized Haar measure on $SU(2)$ in terms of the Lebesgue measure dZ.

The characters of irreducible representations of $su(2)$ are given by:

$$\chi^j(e^Z) = \frac{\sin(\psi(j+1/2))}{\sin(\psi/2)}, \tag{8.11}$$

where j are half-integers (spins).

The Fourier transform on $SU(2)$ maps any function on the group into a function on the space dual to the Lie algebra. Let f be a coordinate on the space su(2)*. Then the Fourier transform is given by:

$$\tilde{\phi}(f) := \int \frac{dZ}{V} P(Z) e^{-i\,f(Z)} \phi(\exp Z). \tag{8.12}$$

The inverse Fourier transform is given by:

$$\phi(\exp Z) = \sum_j \dim_j \frac{1}{P(Z)} \int_j d\Omega_f e^{i\,f(Z)} \tilde{\phi}(f), \tag{8.13}$$

where the integrals are taken over the co-adjoint orbits – spheres of radius $j+1/2$ and the measure $d\Omega_f$ on each orbit is normalized so that

$$\int_j d\Omega_f = \dim_j = 2j+1. \tag{8.14}$$

A particular case of (8.13) is the following simple formula for the characters due to Kirillov [60]

$$\chi^j(e^Z) = \frac{1}{P(Z)} \int_j d\Omega_f e^{i\,f(Z)}. \tag{8.15}$$

8.5 Construction of the auxiliary 2-torus surface.

To compute the right–hand side of (6.43) for d-dimensional tori, it is necessary to consider explicitly the triangulations involved, as well as the auxiliary surfaces.

We start with the $d = 4$ case.

Consider the solid torus $S^1 \times D^2 \times S^1$, the boundary of which is $T^3 = S^1 \times S^1 \times S^1$. From what we said in Section 6.2.2 item B, we can focus our attention on the boundary T^3 that can be obtained identifying in pairs the faces of a cube. We can triangulate a cube by starting from a triangulation of a solid cylinder made up by three tetrahedra, as shown in Fig. 8.4, Recalling which kind of

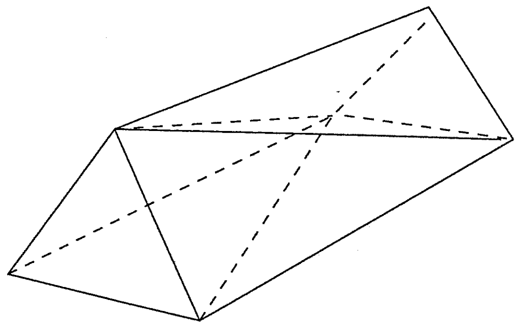

Fig. 8.4: Triangulation of a solid cylinder.

symbol turns out to be associated in d=4 with a tetrahedron (cfr. (5.12)), the auxiliary surface of the cylinder triangulation is depicted in Fig. 8.5. The cube is realized by glueing together two

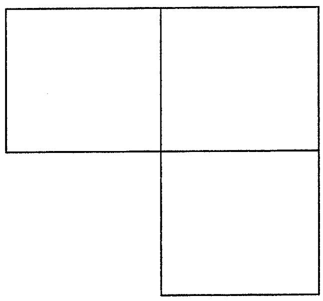

Fig. 8.5: Associated surface of a solid cylinder.

cylinders along one face (as indicated in Fig. 8.6) and the resulting auxiliary surface $S = D^2$ is depicted in Fig. 8.6. The identification procedure needed to obtain T^3 acts on the auxiliary surface giving a T^2.

Let us consider now the case $d = 5$.

The "solid" 5-torus boundary T^4 can be obtained identifying in pairs the faces of an ipercube D^4. The construction of D^4 is as follows. Collect together six 4-simplices, in such a way that each of them provide one of its tetrahedra to construct a cube (a face of D^4). There are 24 "free" tetrahedra. Now we glue the 4-simplices among themselves, leaving 12 tetrahedra "free". One of the two "free" tetrahedra of each 4-simplices is used to realize one of the other face of the ipercube and the remaining 6 "free" tetrahedra are used to glue together the 7 block of six 4-simplices necessary to construct the ipercube D^4. In total we have used 42 4-simplices. Also in

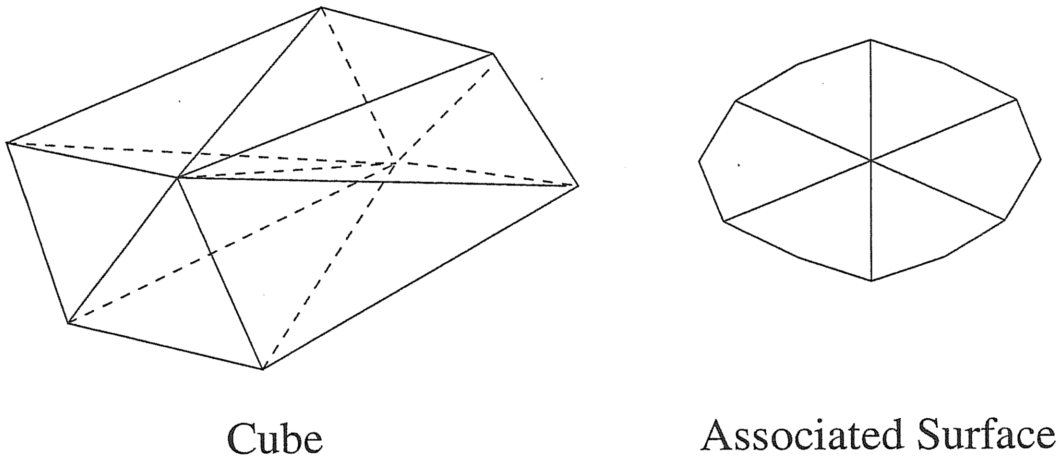

Fig. 8.6: Triangulation of a cube an its associated surface.

this case the auxiliary surface is topologically equivalent to a disc and the identification procedure to obtain T^4 give us an auxiliary T^2. This fact can be generalized in any dimension and it is a consequence of the topological equivalence between a $(d-1)$ dimensional ipercube and the standard simplex σ^{d-1}, the auxiliary surface of which is a disc.

8.6 $Z^3[L(4,1)]$ and $Z^3[L(5,2)]$ reduction.

In this appendix we want to show how it is possible to recover from our approach the Ionicioiu–Williams results [57]. We discuss only the simplest examples: $L(4,1)$ and $L(5,2)$. Recall that the T-V invariant is given by a sum, over a coloring, of a particular configuration of 3nj symbols of type II; to perform the calculus we use the diagrammatic method (see Section 3.5 and [47]). The diagrammatic representation of this symbol is given in Fig. 8.7 and for the examples we are

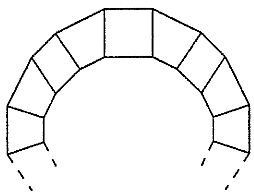

Fig. 8.7: Diagrammatic representation of 3nj symbol of type II.

considering, the diagrams as in Fig. 8.8. For $L(4,1)$ we can start using relation (10), p. 455 in [47], which gives the sum in terms of three diagrams, refer to Fig. 8.9. On the first of them we can

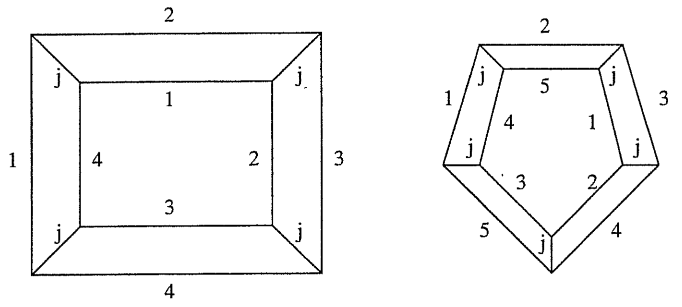

Fig. 8.8: Diagrammatic representation of $L(4,1)$ and $L(5,2)$.

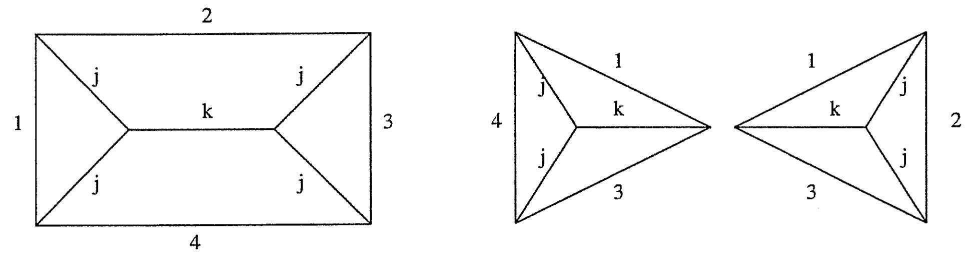

Fig. 8.9: First step in $L(4,1)$ calculation.

use relation (6), p. 454 in [47], obtaining the expression of the invariant in term of four 6j symbols. We then perform the sum over j_3, involving only three 6j-symbols, using the B-E identity. We get, in this way, three 6j symbols, one involving only j,k, $\begin{vmatrix} j & j & k \\ j & j & k \end{vmatrix}$ and the other a square of $\begin{vmatrix} j & j & k \\ j_2 & j_4 & j_1 \end{vmatrix}$. Summing over j_i and using the orthogonal relation between 6j symbols and the definition of ω^2, we obtain the value given in [57].

For $L(5,2)$ we can use the relation (15), p. 457 in [47] to obtain the invariant expressed in terms of four diagram (Fig. 8.10). We use, for the first diagram, the relation (6), p. 454 in [47]; we get

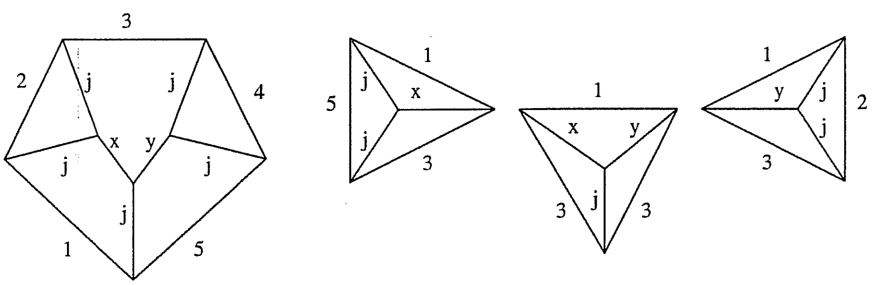

Fig. 8.10: First step in $L(5,2)$ calculation.

in this way a decomposition of the invariant in terms of six 6j symbols. Now we can perform the sum over j_5, involving three 6j symbols, and, using the B-E identity, we obtain $\begin{vmatrix} j & x & x \\ j & j & y \end{vmatrix}$ and $\begin{vmatrix} j & x & x \\ j_1 & j_3 & j_4 \end{vmatrix}$. Carrying out the sum over j_2, (which implies, using the orthogonality condition, $x = y$) and then summing over j_i, we obtain the value provided by Ionicioiu-Williams in [57].

References

[1] Regge, T., Nuovo Cimento **19** (1961) 558.

[2] Ponzano, G., Regge, T.: *Semiclassical limit of Racah coefficients.* In: Bloch, F. et al (eds.) Spectroscopic and Group Theoretical Methods in Physics, Amsterdam: North-Holland (1968) 1.

[3] Turaev, V.,Viro, O.Ya., Topology **31** (1992) 865.

[4] Mizoguchi S., Tada, T., Phys. Rev. Lett. **68** (1992) 1795.

[5] Ooguri, H., Nucl. Phys. **B 382** (1992) 276.

[6] Ooguri, H., Mod. Phys. Lett. **A 7** (1992) 2799.

[7] Carter, J.S., Flath, D.E., Saito, M.: *The Classical and Quantum 6j-symbols.* Math. Notes **43**. Princeton, NJ, Princeton University Press 1995.

[8] Carter J.S., Kauffman L.H., Saito M. (1998): *Structure and diagrammatics of four dimensional topological lattice field theories*, preprint math.GT/9806023

[9] Rovelli, C., Smolin, L., Phys. Rev. **D 52** (1995) 5743.

[10] De Pietri, R., Rovelli, C., Phys. Rev. **D 54** (1996) 2664.

[11] Pachner, U., Discr. Math. **81** (1990) 37.

[12] Carbone, G., Carfora, M., Marzuoli, A., Comm. Math. Phys. **212** (2000) 571.

[13] Carbone, G., Carfora, M., Marzuoli, A., *Invariants of spin networks with boundary in Quantum Gravity and TQFTs*, in Recent developments in general relativity, Casciaro B. at al. (Eds), Springer-Verlag, Milano (2000) 419.

[14] Pachner, U., Result. Math. **12**, (1987) 386.

[15] Crane, L., Kauffman, L.H., Yetter, D.N., *State sum invariants of four manifolds*, preprint hep–th/9409167.

[16] Roberts, J., Topology **34** (1995) 771.

[17] Turaev, V., *Quantum invariants of knots and 3–manifold,* Expodsitions in Math. **186**, W. de Gruyter, Berlino 1994.

[18] Turaev, V., *Topology of shadows, preprint* (1992).

[19] Roberts, J., *Refined state sum invariants of 3- and 4-manifolds*, in Geometric topology, Athens, GA (1993) 217.

[20] Benedetti, R., Petronio, C., J. Knoth Theory Ramif. **5** (1996) 427.

[21] Beliakova, A., Durhuus, B., Commu. Math. Phys. **167** (1995) 395.

[22] Kauffman, L., Lins, S.: *Temperley Lieb Recoupling Theory and Invariants of Three-Manifolds.* Princenton University Press 1994.

[23] Broda, B., *A gauge-field approach to 3- and 4-manifold invariants*, in Symplectic singularities and geometry of gauge field, Warsaw (1995) 201.

[24] Broda, B., *A note on the four-dimensional Kirby calculus*, preprint hep-th/9305101

[25] Broda, B., *A surgical invariants of 4-manifolds*, in Proceedings of the conference on quantum topology, Manhattan, KS (1993) 45.

[26] Cattaneo, A.S., Cotta-Ramusino, P., Frohlich, J., Martellini, M., Jour. Math. Phys. **36** (1995) 6137.

[27] Broda, B., Phys. Lett. **B 280** (1992) 47.

[28] Birmingham, D., Blau, M., Rakowski, M., Thomson, G., Phys. Rep. **209** (1991) 129.

[29] Baez, J.C., Lett. Math. Phys. **38** (1996) 129.

[30] Freidel, L., Krasnov, K., Class. Quant. Grav. **16** (1999) 351.

[31] Freidel, L., Krasnov, K., Puzio, R., *BF description of higher-dimensional gravity theories*, preprint hep-th/9901069.

[32] Cattaneo, A.S., Cotta-Ramusino, P., Martellini, M., Nucl. Phys. **B 436** (1995) 355.

[33] Cotta-Ramusino, P., Martellini, M., *BF theory and 2-knots*, in Knots and Quantum Gravity, Riverside, CA (1993) 169.

[34] Cattaneo, A.S., Comm. Math. Phys. **189** (1997) 795.

[35] Cattaneo, A.S., Cotta-Ramusino, P., Fucito, F., Martellini, M., Rinaldi, M., Tanzini, A., Zeni, M., Comm. Math. Phys. **197** (1998) 571.

[36] Fucito, F., Martellini, M., Zeni, M., Nucl. Phys. **B 496** (1997) 259.

[37] Freidel, L., Krasnov, K., Adv. Theor. Math. Phys. **2** (1999) 1183.

[38] Carbone, G., Carfora, M., Marzuoli, A., in preparation.

[39] Carbone, G., Carfora, M., Marzuoli, A., *Hierarchies of spin models*, preprint gr–qc/0008011.

[40] Carbone, G., Jour. Math. Phys. **41** (2000) 3068.

[41] Glaser, L.C.: *Geometric Combinatorial Topology*, Vol. 1. New York: van Nostrand Reinhold 1970.

[42] Rourke, C., Sanderson, B.: *Introduction to Piecewise Linear Topology*. New York: Springer-Verlag 1982.

[43] Pachner, U., Europ. J. Combinatorics **12** (1991) 129.

[44] Thurston, W.P.: *Three-dimensional Geometry and Topology.* Vol. 1, Levy, S. (Ed.), Princeton, NJ, Princeton University Press 1997.

[45] Alexander, J.W., Ann. of Math. **31** (1930) 292.

[46] Ambjørn, J., Carfora, M., Marzuoli, A.: *The Geometry of Dynamical Triangulations.* Lect. Notes in Physics **m50**. Berlin, Springer 1997

[47] Varshalovich, D.A., Moskalev, A.N., Khersonskii, V.K.: *Quantum Theory of Angular Momentum*, Singapore, World Scientific 1988.

[48] Yutsis, A.P., Levinson, I.B., Vanagas, V.V.: *The Mathematical Apparatus of the Theory of Angular Momentum*, Jerusalem, Israel Program for Sci. Transl. Ltd. 1962.

[49] R.M. Williams, J.Math.Phys. **36** (1995) 6276.

[50] Maggiore, M., Sorella, S.P., Nucl. Phys. **B377** (1992) 236.

[51] Reisenberger, M., Class. Quant. Grav. **14** (1997) 1753.

[52] Blau, M., Thompson, G., *Lectures on 2d Gauge Theories, Topological aspects and Path Integral Techniques*, preprint hep-th/9310144.

[53] Turaev, V., Inst. Hautes Études Sci. Publ. Math. **77** (1992) 121.

[54] Rolfsen, D.: *Knots and links*, Publisch or Perish 1976.

[55] Kirby, R., Invent. Math. **45** (1978) 35.

[56] Nomura, N., J. Phy. Soc. Jap. **59** (1990) 3851.

[57] Ionicioiu, R., Williams, R.M., *Lens space and handlebodies in 3d quantum gravity,* preprint gr-qc/9806027.

[58] Kirillov, A.N., Reshetikhin, N.Y., *Representations of the algebra* $U_q(sl(2))$*-othogonal polynomials and invariants of links*, in V.G.Kac (ed.) Infinite dimensional Lie algebras and groups, Adv. Ser. in Math. Phys. **7**, World Scientific, Singapore (1988) 285.

[59] Nomura, N., J.Math. Phys. **30** (1989) 2397.

[60] Kirillov, A.A.: *Elements of the theory of representations*, New-York, Springer-Verlag 1976.